NOAA Technical Memorandum ERL NSSL-78

OBJECTIVES AND ACCOMPLISHMENTS OF THE NSSL 1975 SPRING PROGRAM

PART I: OBSERVATIONAL PROGRAM

K. Wilk
K. Gray
C. Clark

PART II: RADAR QUALITY CONTROL PROGRAM

D. Sirmans
J. Dooley
J. Carter
W. Bumgarner

Property of
NWC Library
University of Oklahoma

National Severe Storms Laboratory
Norman, Oklahoma
July 1976

UNITED STATES DEPARTMENT OF COMMERCE
Elliot L. Richardson, Secretary

NATIONAL OCEANIC AND ATMOSPHERIC ADMINISTRATION
Robert M. White, Administrator

Environmental Research Laboratories
Wilmot N. Hess, Director

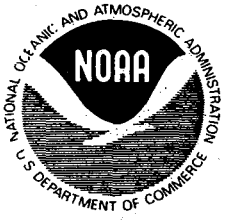

NSSL

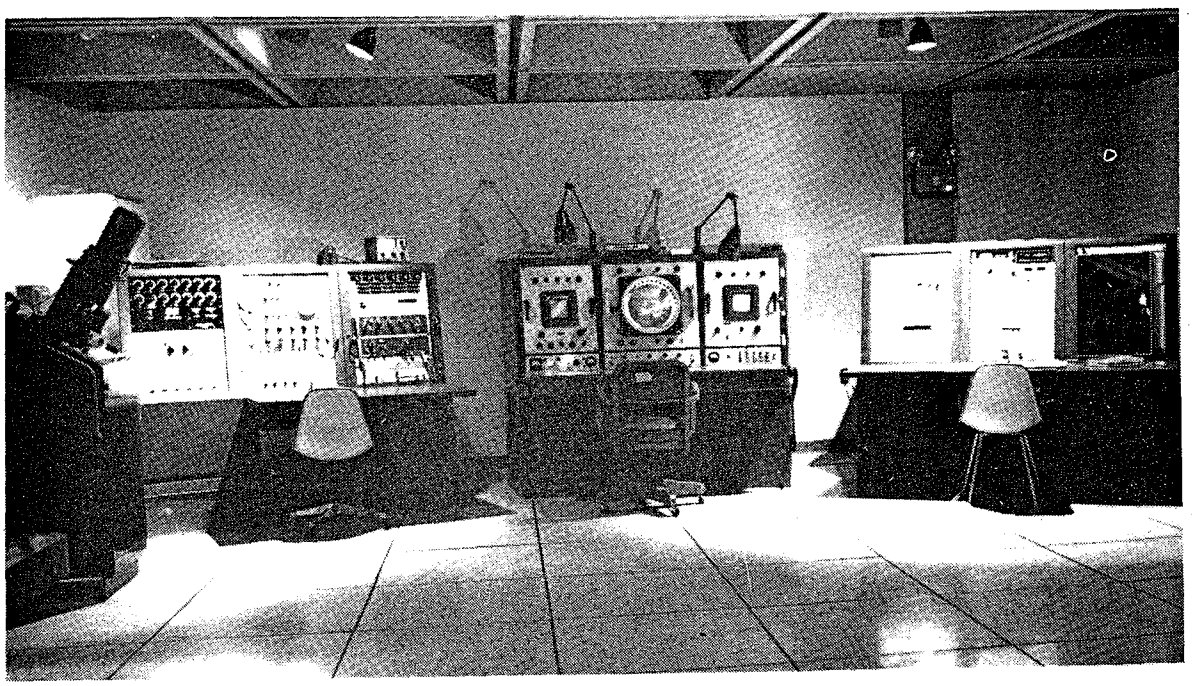

WSR-57 RADAR

OBJECTIVES AND ACCOMPLISHMENTS OF THE NSSL 1975 SPRING PROGRAM

PART I

OBSERVATIONAL PROGRAM

K. Wilk, K. Gray, and C. Clark

National Severe Storms Laboratory
Norman, Oklahoma
July 1976

PREFACE

The National Severe Storms Laboratory seeks to understand processes that create and sustain thunderstorms and their manifestations, including hail, heavy rain, lightning, and tornadoes, and to develop improved techniques for storm observation and prediction. Toward these ends NSSL has a severe storm observational program conducted annually during spring when storm activity tends to be most frequent and intense. Several kinds of standard measurements are used for surface and upper air measurements that provide support for meteorological sampling by Doppler radars, an instrumented tower, aircraft, and mobile photographic teams. While thunderstorm and slightly larger scales are emphasized, the NSSL data also provide knowledge of the synoptic setting that leads to severe storm formation. Within the customary fiscal and personnel constraints, configuration and method of operation are determined by research requirements of investigating scientists. A description of each year's Spring Program is summarized as an internal NSSL report.

The WSR-57 surveillance radar and the meteorological networks operate almost continuously for 30 to 90 days and their data are archived for later study. The other data sources mentioned operate for various intervals within the main observing period. There are usually about ten severe storm days and one or two tornadic storms during data collection. Although major NSSL interest focuses on the tornadic thunderstorm, less intense storms are also studied by a wide community of scientists both within and without the Laboratory. There are usually four to eight cases of interesting storms that cannot be reviewed in depth prior to the next annual data collection program. After a decade of operation, we have data sets from many severe storm cases archived. Therefore, future investigations will emphasize new probes to enhance synthesis of data on kinematic and dynamic processes inferred from the multiple Doppler and aircraft measurements. Consideration of new concepts and observing techniques may benefit from the perspective provided by the data sets illustrated here.

Most of the line illustrations in this report were computer-plotted as part of routine data processing by NSSL's CDP section. The radar photographs are available on 35 mm roll film, and the digital data on seven track, 556 bpi tapes. Subsynoptic data from the sixteen NSSL surface stations can be obtained from the National Space Science Data Center.

Ken Wilk
Kathryn Gray
Charles Clark

TABLE OF CONTENTS

		Page
INTRODUCTION		1
SECTION 1	Modus Operandi	3
SECTION 2	Synopsis of the Major Storms	5
	Case I May 26, 1975	7
	Case II June 6, 1975	15
	Case III June 13, 1975	23
SECTION 3	Auxiliary Information	29
REFERENCES		60

INTRODUCTION

The severe storm observational program in 1975 was reduced substantially from that of 1974. The next extensive program is planned for 1976. The reduction in 1975 was due in part to scheduling of major engineering changes in the Doppler signal processing, and in part to limitations of funds and staff. However, within these restrictions, the scope of the program was broad, with participation of scientists from NCAR, University of Wyoming, University of Oklahoma, and the Air Force Research and Development Command.

The program began with an intense 30-day quality control test, primarily concerned with the Doppler radars. The results are summarized in Part II. The routine severe storm surveillance program conducted between May 15 and June 15 is summarized in the following sections.

There were four clusters of observational activities (fig. 1). The Dual-Doppler Program (I) was given highest priority--to widen and test quality control procedures, and further develop hardware and software for improved real time displays. Program II sought to extend Doppler and aircraft measurements of turbulence and severe storm circulations. Program III mixed subprograms in storm surveillance and documentation (WSR-57 radar, rawinsonde, and cloud photography) with first attempts at "nowcasting" using hourly surface, 30-minute satellite, and continuous radar observations to make 1-2 hour predictions. Program IV provided benchmark data to describe boundary layer conditions during severe storms.

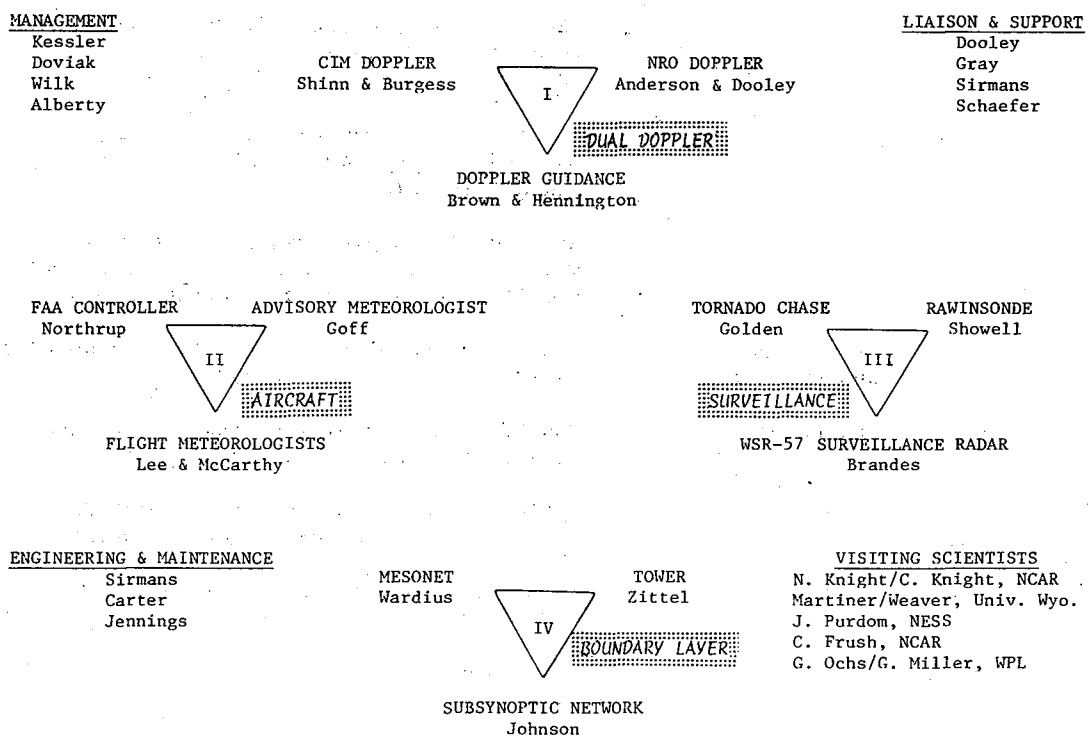

Figure 1. Observational activities.

Most of the project scientists participated in data collection with Operations staff and helped define operating procedures. Unless severe weather was evident, operations were restricted to normal working hours, with evening and weekend storms covered on a catch-as-catch-can basis.

Individual project goals (fig. 2) determined sampling rates and radar control configurations, including choice of high or low pulse repetition frequency, dual-Doppler scanning, scope photography, and digital recording.

PROJECT GOALS

	INVESTIGATORS	EXPERIMENTS
1.	Brandes and Sirmans	WSR-57 radar: *Wet radome effect on rainfall measurements.*
2.	Brandes and Sirmans	WSR-57 radar: *Effect of sampling interval on precipitation measurements.*
3.	Brandes and Sirmans	NRO and CIM Doppler radar data: *Effect of velocity variance on precipitation measurements.*
4.	Ray	NRO Doppler radar: *High PRF and tornado detection.*
5.	Brown, Davies-Jones McCarthy, and Ray	NRO and CIM Doppler radars, WSR-57 radar, chase teams, aircraft and radiosonde: *3-D modeling.*
6.	Burgess	NRO and CIM Dopplers: *Study of vortex signatures as shown on reflectivity and PPP displays.*
7.	Kessler	WSR-57 radar: *Demonstration of immediate analysis of raingage and radar data using the Brandes technique.*
8.	Lee	NRO and CIM Doppler radars: *Correlation of aircraft wind and measured turbulence with Doppler wind and variance measurements.*
9.	Golden, Davies-Jones, Purcell, and Doswell	WSR-57 and Doppler radars: *Film documentation of tornadoes and damage surveys.*
10.	Schaefer and Lemon	WSR-57 radar, satellite, rawinsonde, and Service A data: *Severe storm prediction.*
11.	Dooley, Showell and Zittel	Optical anemometers and mesonetwork data: *Direct measurement of surface convergence.*
12.	Walker and Ray	Acoustic radar and WKY tower data: *Quantitative measurements with the acoustic radar.*
13.	Nelson	Radar and Volunteer Observers network: *Hail Studies*
14.	WPL; NCAR; Wyoming [Ochs, Young, Frush, C. Knight, N. Knight, and Martener	WSR-57 and Doppler radars; *Optical anemometer; Project Dustorm; Storm Chase.*

Figure 2. Project goals.

SECTION 1

Modus Operandi

A Central Control Facility was established in 1974 in the Norman Doppler Building (Barnes et al., 1974). During 1975, controllers for chase and rawinsonde projects were returned to the WSR-57 radar room in the main building to relieve congestion in the Doppler building and to separate communications. This year, "real time" discussions to coordinate dual-Doppler and aircraft probing were not mixed with "delayed time" operations involving guidance messages to chase teams and rawinsonde flights. By reducing cross talk and clustering the projects, it was hoped that fewer staff would be required and the operation would be more efficient.

This was only partially successful. While several of the experiments completed data collection independently, the chase teams were not always adequately supported in their statewide pursuit of severe storms.

For example, some data were lost on major storms on June 6 and June 13, because of cessation of operations between 1700 and 1900 CST. Also, ad hoc arrangements did not provide satisfactory radar coverage during the evenings and on weekends. Improvements in short range prediction are needed to keep the operational teams on site when new storm development is eminent.

The deploying of radar, rawinsonde, and chase teams requires prediction of the likelihood of thunderstorms and prediction of generally when and where (i.e., occurrence in the dual-Doppler area, within driving distance of the chase vehicles, and occurrence before sunset for aircraft probing). Each morning, a "convective outlook" was prepared to indicate presence and motion of the fronts and upper level short waves and to specify "standby" status for the day. The sequence of activities which followed on storm days is illustrated in Figure 3. On "no-standby" days, the radar crews returned to work on the new Pulse-Pair processors or to run quality control checks and fine tune the radar systems. On "standby" days, all radars were calibrated and made ready for data collection. Beginning at noon, the "nowcaster" used 30 min satellite and continuous radar observations to supplement hourly surface analysis. During the afternoon and early evening, he prepared frequent advisories for dissemination to the project teams.

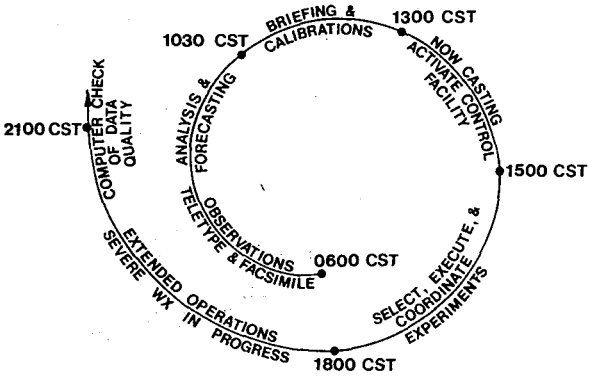

Figure 3. 1975 Operations Clock.

The three radar sites were linked by lease-line telephone for voice communication. A telewriter system was used as back-up and for leaving messages. A radio communication system, using a repeater transceiver on the WKY tower, linked the Central Control Facility, chase cars, rawinsonde sites, and WSR-57 radar room.

The 1975 upper air network was limited to two rawinsonde stations at Tinker AFB and Fort Sill, Oklahoma. A subsynoptic network of 16 surface stations (fig. 4) was operated to supplement the hourly NWS observations. Examples of these data with streamline analysis are shown later in the discussions of the major storms.

Closed circuit television was used to relay satellite pictures, surface analysis and nowcasts from the main building to the Central Control Facility. A tower-mounted television sky camera, remotely controlled from the radar room, provided real time (and video taped) data on distant cloud tops visible from the Laboratory.

Digital data sets were scanned and archived by the Laboratory's Computer Processing Group. The Operations Group screened and archived analog and film data from the surface networks, WSR-57 radar, and the WKY tower. Section 3 contains lists of data now available for study, and material relative to the format of the data.

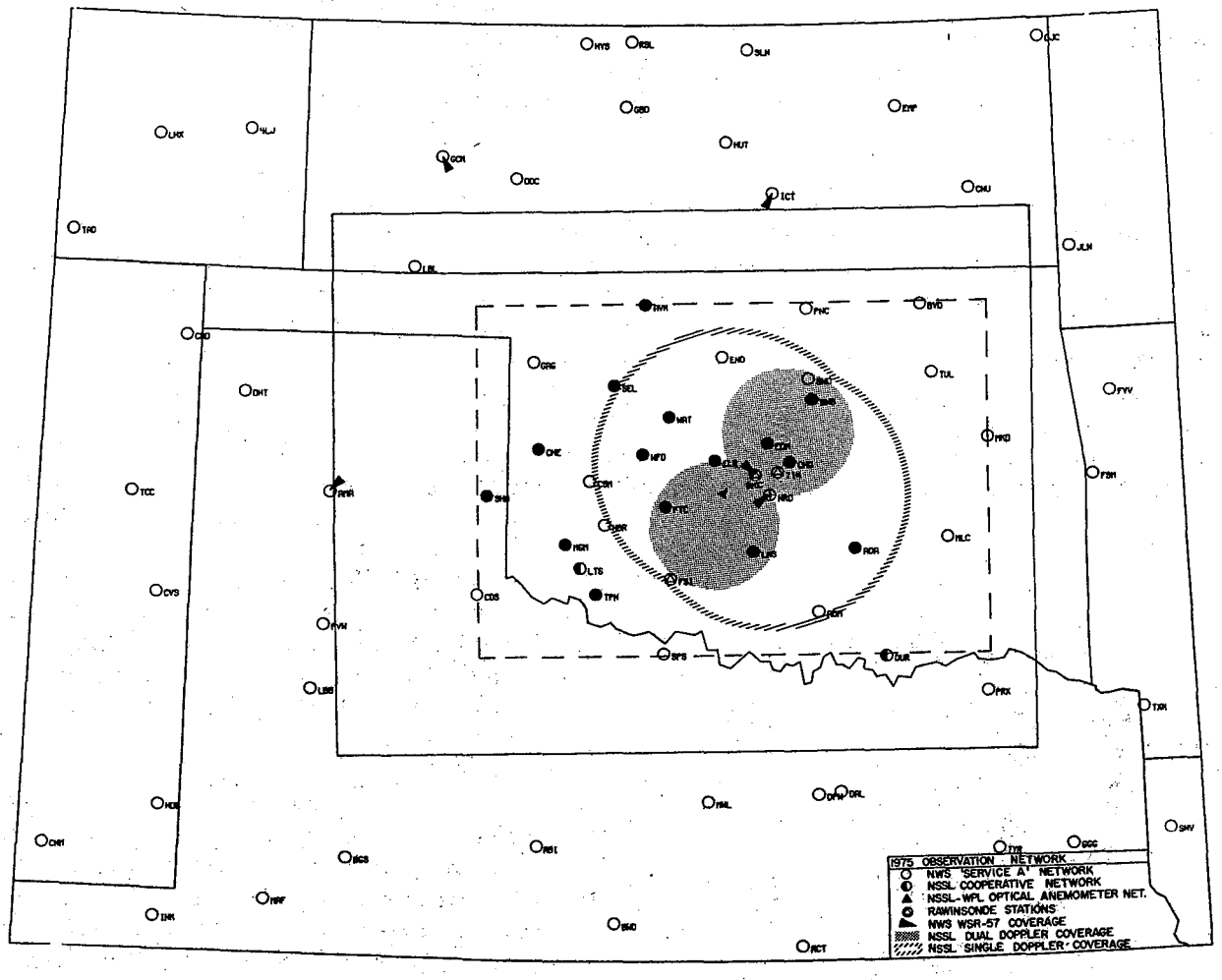

Figure 4. 1975 Observational Network

SECTION 2

Synopsis of the Major Storms

In documenting activities of the 1974 program, Barnes (op cit) showed daily synoptic analyses and WSR-57 scope displays. In addition to these, there are numerous other cases documented in detail (Barnes, 1970; Vlcek, 1973; Lemon, 1976; Brown, 1973) and little new information could be added by showing similar records for 1975. Instead, three cases are illustrated in this report to exemplify situations with varying degrees of difficulty to "nowcast". Similar situations occur each year, sometimes resulting in excessive overtime, loss of data, and "household" hardships. Fortunately, the most severe situations are usually predicted by forecasters at NSSFC, and handled very well by NSSL forecasters on an hour-by-hour basis.

The three cases chosen for graphic review in this report are May 26, June 6, and June 13. On May 26, the first NSSL computerized display of mean velocity was recorded showing a mesocyclone signature in real time (Burgess, 1976). The Doppler data were supplemented with measurements from the University of Wyoming mobile weather station (Martner, 1975) and the NCAR aircraft. As shown in the following illustrations, the storm was an isolated cell, developing in an area of weak cyclogenesis at the time of maximum surface heating.

The second storm, June 6, was a "typical" evening mid-western squall line which produced a classical gust front (Goff, 1975). Surface wind speeds reached 46 m s^{-1} at Edmond, Oklahoma, a few km north of the NSSL tall tower facility. No Doppler data were collected because of the extensive multiple trip return, and because the development of the line occurred in late evening after the cessation of normal operations.

The final case illustrated was a major tornado occurrence at Stillwater, Oklahoma, about 110 km northeast of NSSL. Dual-Doppler radar, aircraft, and WSR-57 three-dimensional data were obtained while several people in Stillwater were photographing the funnel cloud.

Data inquiries and requests should be submitted in writing to:

Mrs. Kathryn C. Gray
Computer and Data Processing
National Severe Storms Laboratory
1313 Halley Circle
Norman, Oklahoma 73069

Date: 26 May 1975

. . . . Forecast (1100 - Sunset) . . . . [X] Standby [ ] No Standby

Discussion:

Yesterday - Went as forecast with even less clouds than called for.

Today - 9:00 a.m. front Harrison - Altus - Clovis. Wave formed by 10:00 a.m. at Altus with front to south past Mineral Wells - Midland. Air mass south of front quite unstable. 500 mb trying to go zonal with weak "wiggles" present. Expect early afternoon show in south and southeast Oklahoma.

. . . . Outlook for Tomorrow . . . . [ ] Standby [X] No Standby

Discussion:

Indications are that front to settle south of Red River during night leaving unseasonable cool stable air mass.

Joseph T. Schaefer

Figure 5. NSSL Operational Forecast, issued at 1100 CST each day.

CASE I

May 26, 1975

The storm developed on a frontal wave crest 120 km southeast of NSSL. As indicated in the Forecast and Nowcast, activity was anticipated and WSR-57 radar data collection began prior to time of first echo. The satellite picture at 1545 CST shows the storm developing southwest of NSSL, just beyond the range of the Doppler radar at Cimarron. The Norman Doppler radar was within sampling range for a brief period and recorded the first real time display of the mean velocity and spectral width values at 1538 CST.

The reflectivity and Doppler velocity fields indicate the storm contained hail and cyclonic circulation aloft. The University of Wyoming Chase Team observed heavy rain and hail and a weakly developed wall cloud, however, a telephone survey of the 100 km^{-2} area failed to locate wind damage or observations of funnel clouds. A "fly-by" probe to the southwest of the storm was made by the NCAR aircraft during the period of rapid growth, and the University of Wyoming staff later collected drop size data at 1600 CST further south in the same storm (Martner, op cit).

Some significant aspects of the data sets are mentioned in the figure captions.

NOWCAST FOR 26 MAY 1975

Based on 1124 CST data. Appears that wave is around Rush Springs, Lindsey area with front extending to SW and discontinuity or front (unclear which) to ESE. Warm unstable air mass to south with convergence along discontinuities should give rise to TRW. Lack of upper air support is only significant--but serious--drawback. No short waves evident on satellite pictures except one to east in Arkansas. Possible first echo experiment (outside dual-Doppler network) but will have to result from surface forcing (not upper level lift).

1200 CST data. Actual front is difficult to differentiate. May be radar detectable thin line (dashed on map analysis) or wave discontinuity system to south. (Line of cumulus along ESE portion of discontinuity is quite evident on 1123 CST satellite photo.) Greatest chance for TCU and TRW growth will occur when thin line overtakes wave in 3-4 hours near or north of ADM.

1300 CST data. Now appears that thin line is front and early morning TRW outflow produced discontinuity (along which TCU are presently seen in satellite pictures) extends ESE from wave. Best TRW chance will be near wave-front-outflow intersection in about 2 hours with additional surface heating since synoptic surface forcing is weak and upper support is lacking.

1400 CST data. Satellite and radar development have begun to occur rapidly on outflow boundary. This should persist and juncture between front and boundary looks favorable for further development. With strong instability these cells look good for large hail.

1500 CST data. Satellite data shows some weakening or "breaking up" of boundary W of strong cell S of ADH. However, front still in that area and generation of another meso system to provide forcing must be considered possible. Satellite pictures provided excellent information on overall situation and high potential region but neither satellite nor surface data indicated TCU enhancement before radar detected first echo.

Leslie R. Lemon

Figure 6. NSSL Operational Nowcast, issued hourly beginning at 1100 CST on standby days.

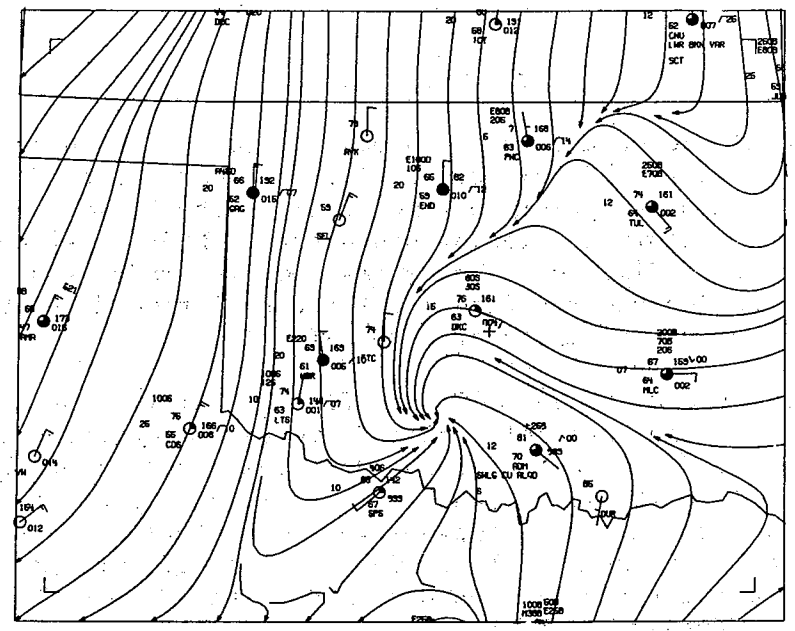

Figure 7. Surface map time 1200 CST. Boundary layer convergence over south-central Oklahoma three hours prior to development of severe thunderstorm. Line of convergence extending northwest marks a southward moving cold front, which was "seeded" with chaff at 1300 CST.

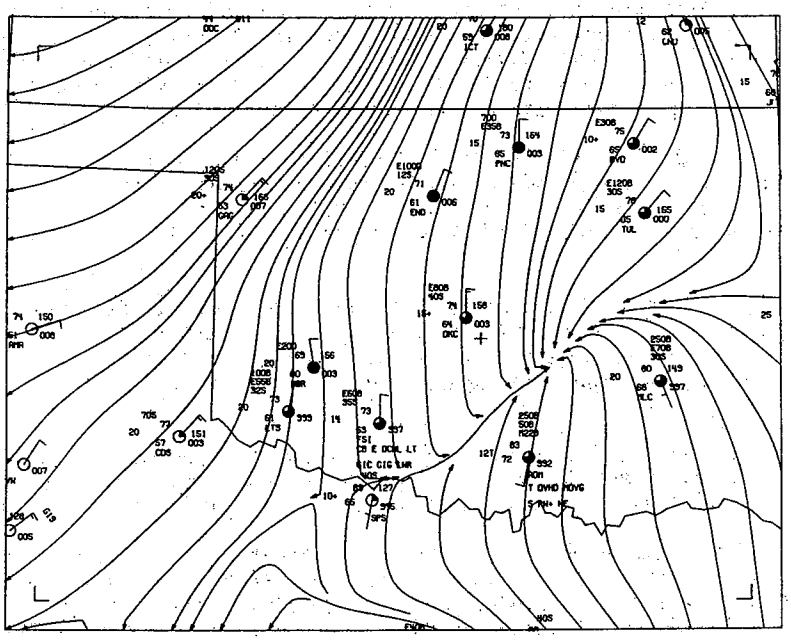

Figure 8. Surface map time 1600 CST. Boundary layer convergence during severe storm. The line of convergence with the cold front apparently merged with the subsynoptic scale cyclone (or is no longer resolvable), which has moved northeast.

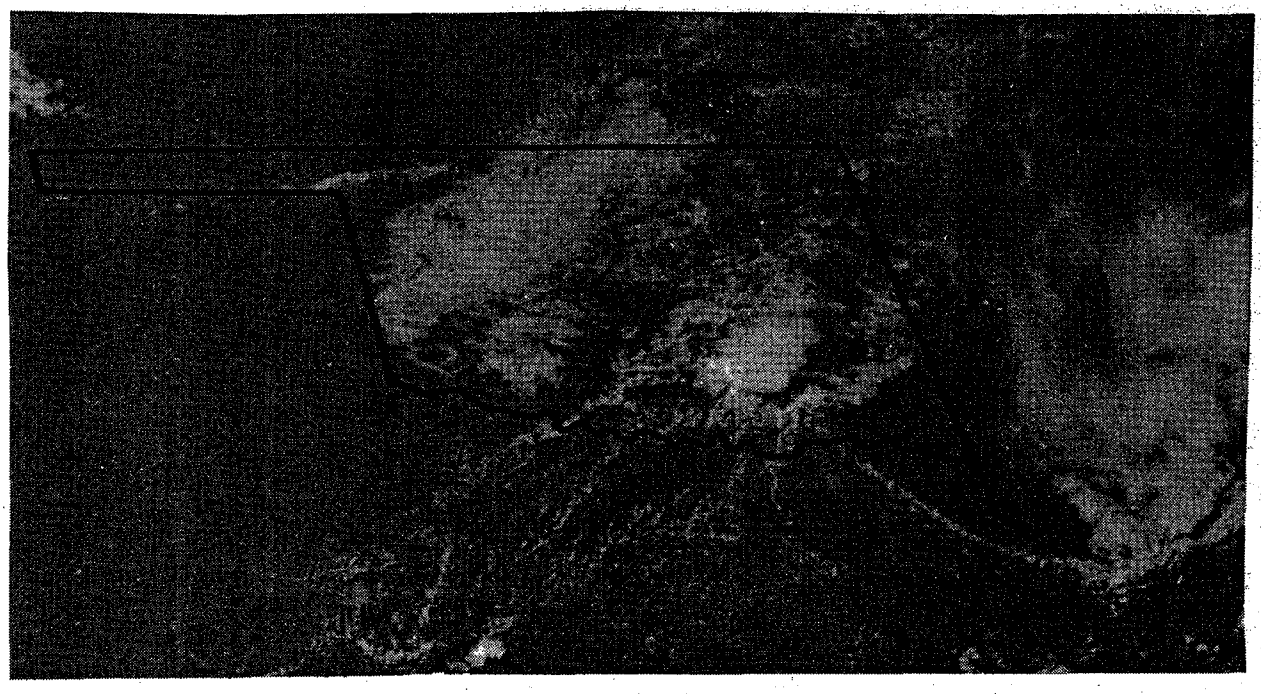

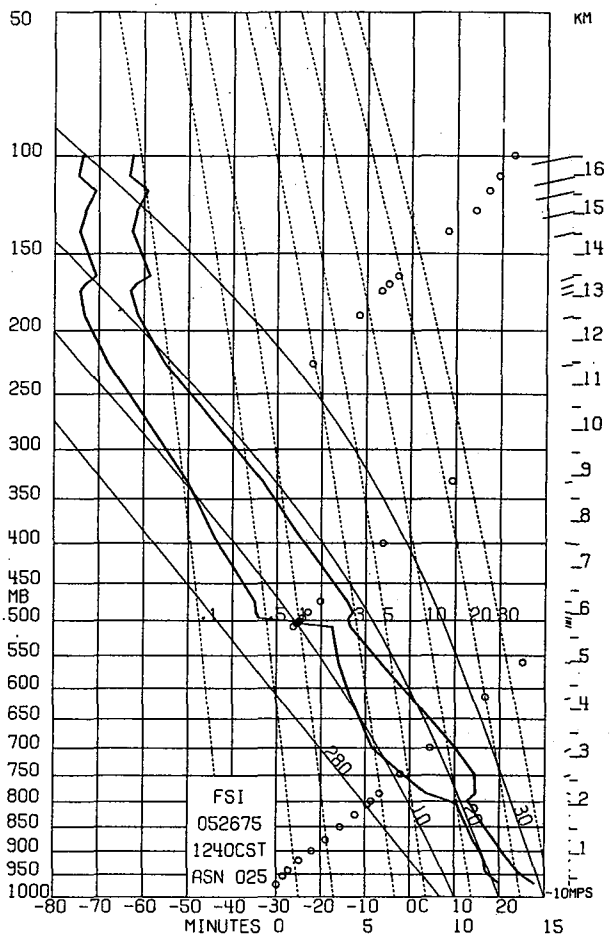

Figure 9. (above) Satellite photograph taken at 1545 CST, 26 May 1975, showing thunderstorm development on wave crest in south-central Oklahoma. The warm air boundary extending into east Texas was created by the southward moving nighttime squall line now dissipating over western Louisiana.

Figure 10. (left) Sounding taken at Fort Sill, Oklahoma, 130 km west, and approximately one hour before the development of the storm.

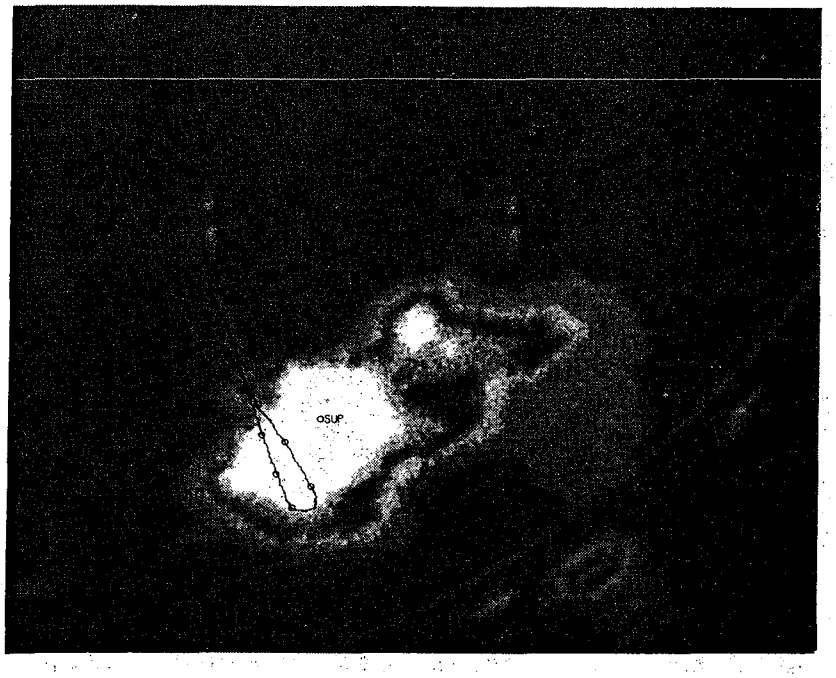

Figure 11. Track of NCAR aircraft taken to record data shown below. The University of Wyoming mobile weather station was southeast of Sulphur (SUP) at the time. The small cancellation north of SUP is coincident with reports of marble size hail.

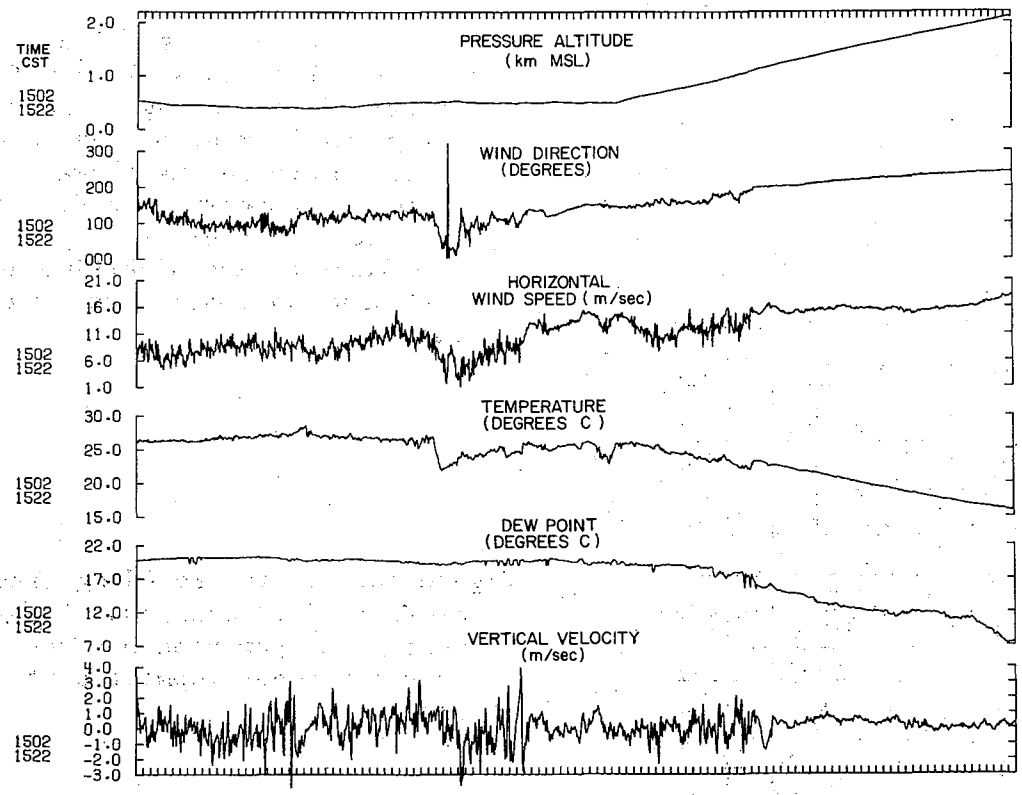

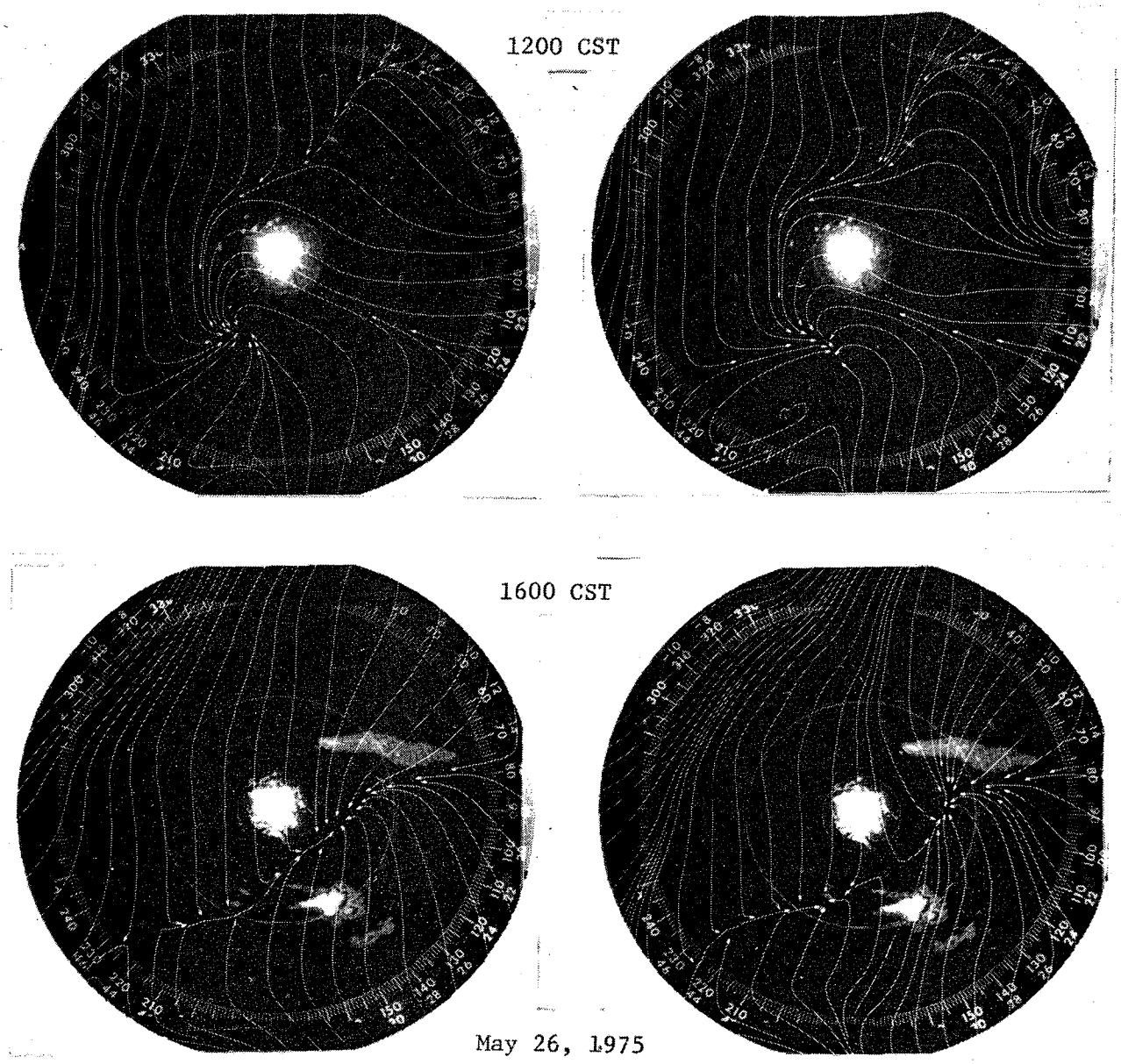

Figure 12. The subsynoptic trajectory analyses are shown superimposed on the WSR-57 radar displays. In each case, the left photograph is the wind pattern derived using the technique developed by Barnes (1974), and the right photograph shows the Barnes output analyzed with a pressure constraint developed by Sasaki (1973). In most of these cases the differences in the convergence patterns are second order. However, the effect on magnitudes of moisture convergence may be more significant.

Figure 13. (right) Comparison between WSR-57 and NRO Doppler radar intensity measurements made simultaneously in the Storm of May 26, at 1535 CST, at 4° antenna tilt.

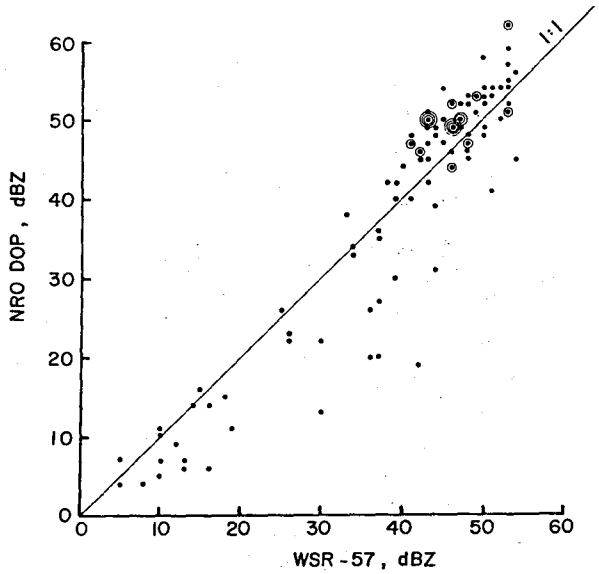

Figure 14. (below) WSR-57 radar tilt sequences showing vertical profile of storm reflectivity patterns at 1515 CST and 1540 CST.

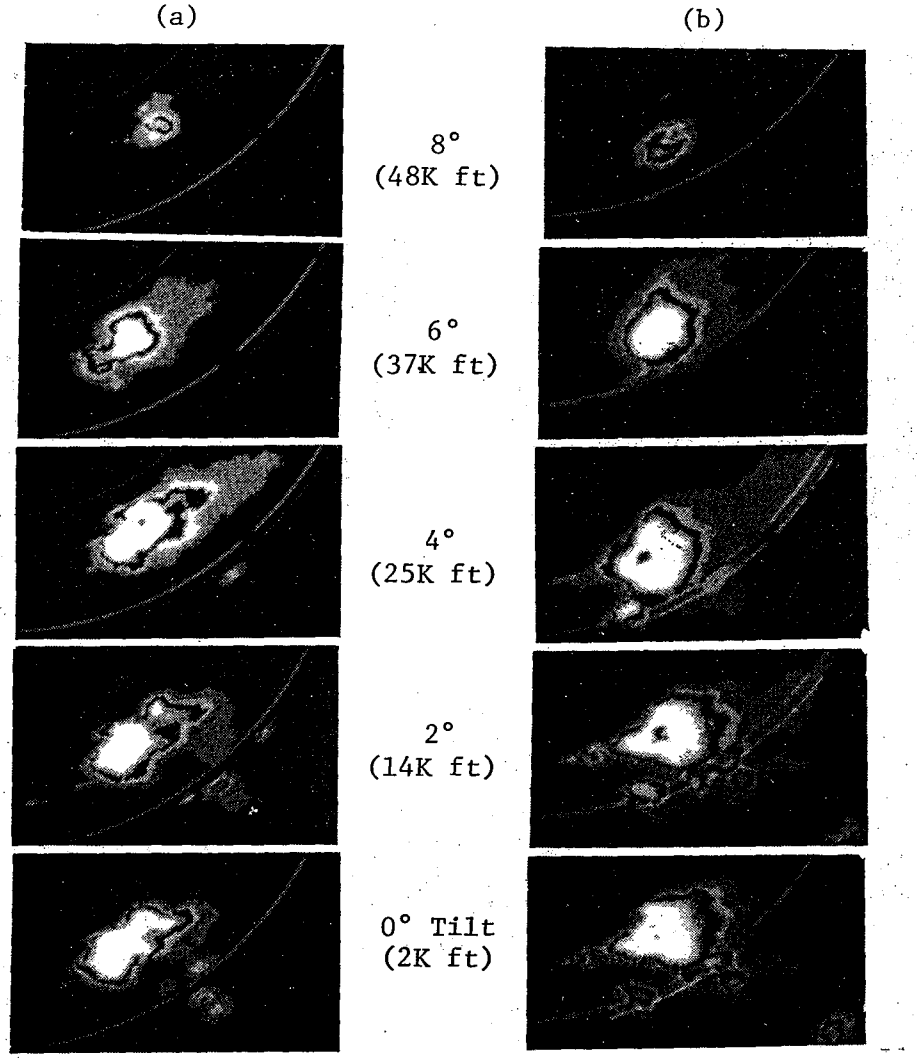

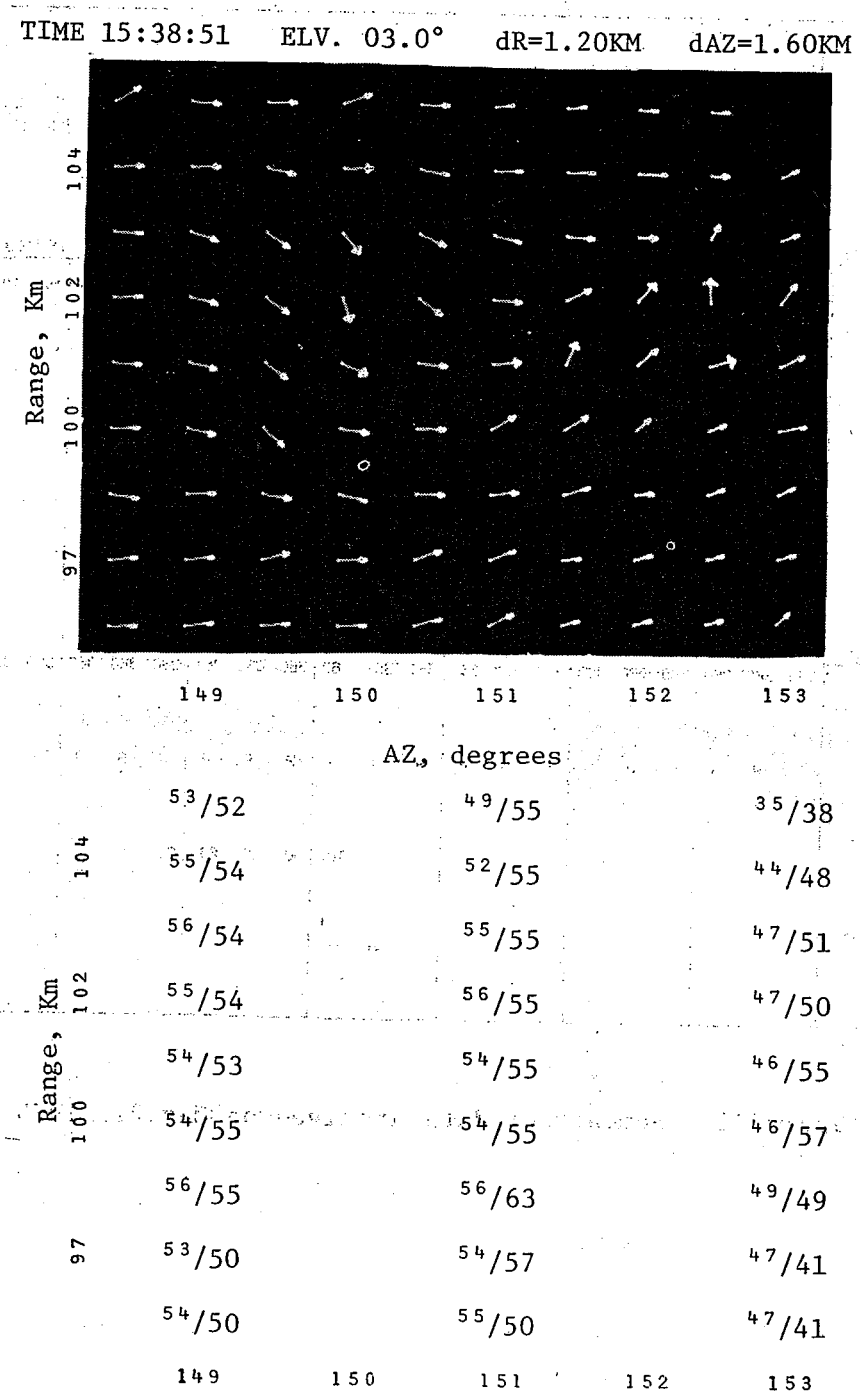

Figure 15. (top) Example of NSSL computerized, multimoment display of Doppler mean wind speeds. Rotation of arrows from right (0 velocity reference is pointing to right) indicates magnitude of wind, i.e., counterclockwise is away from the radar and clockwise is toward the radar. Full rotation to the left is 34 m s^{-1}. The spread of the arrowhead indicates spectral width. For interpretation of cyclone signature see Burgess (1976). (bottom) WSR-57 (small digits) and NRO Doppler (large digits) radar reflectivities (dBZ) for locations above, measured at 0 and 3 degree antenna tilts, respectively.

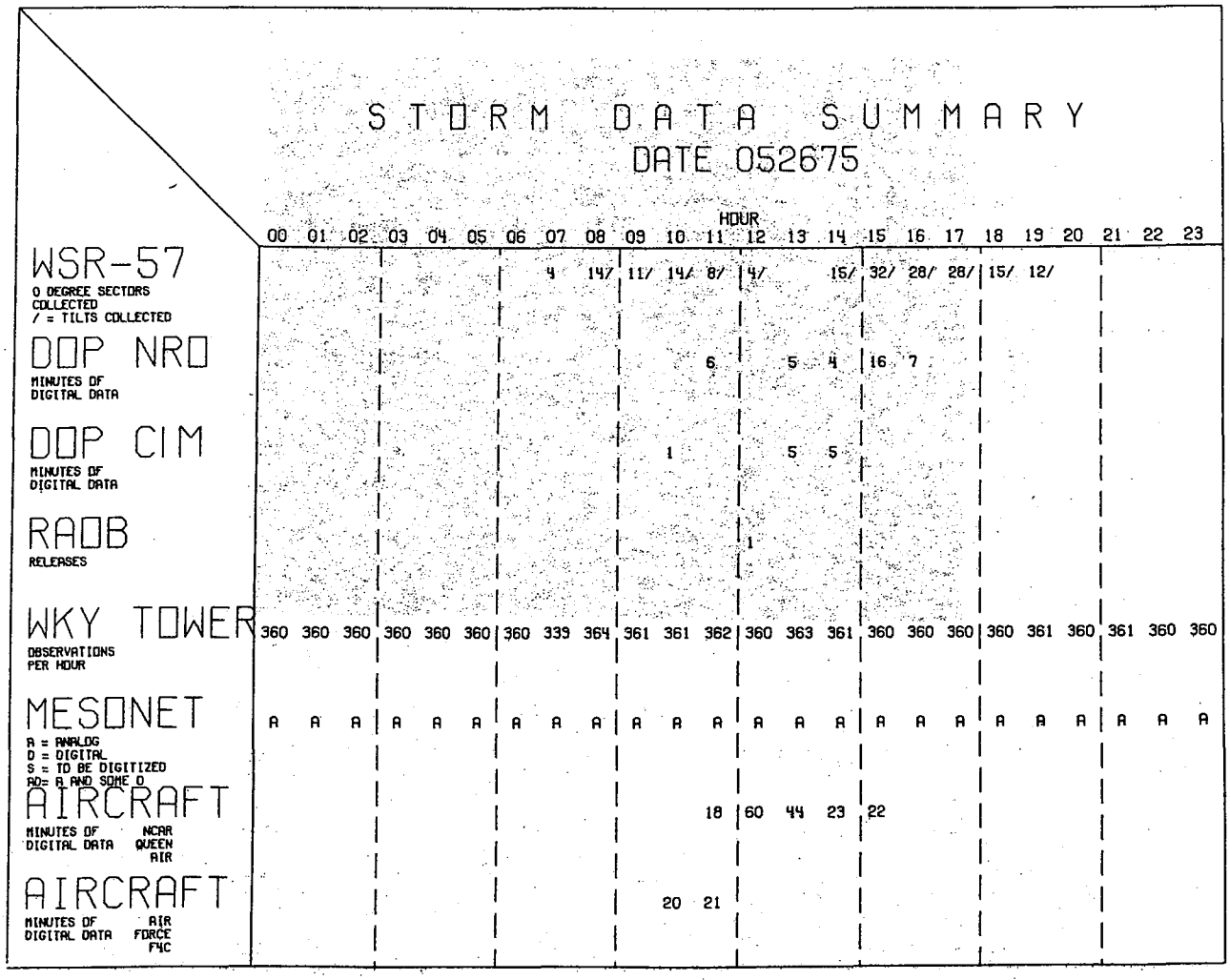

Figure 16. Summary of data archived on May 26, 1975.

CASE II

June 6, 1975

Storms in Kansas were large and severe most of the day. Individual storm movement was southeastward across northern Oklahoma until about 2100 CST, when an organized squall line moved rapidly southward into central Oklahoma and produced a major gust front, which preceded slightly ahead of the precipitation. Severe weather was first reported in northwest Oklahoma (Woods County) about 1700 CST. One of the three tornadoes sighted was rotating anticyclonically (documented on film). Heavy wind damage occurred 20 km north of Oklahoma City. Scattered hail and high winds were reported in 20 counties in northern and eastern Oklahoma (Storm Data, 1975).

The surface maps, WSR-57 radar display, and satellite photograph show the very moist air converging in the areas of thunderstorm development, and the resulting squall line. The WKY tower data contained peak gusts of 35 m s^{-1}. Multiple trip signals prevented the collection of Doppler radar data.

NOWCAST FOR 6 JUNE 1975

Based on 0900 CST data. Short wave lifting is most apparent in mid and high clouds over central and northwest Kansas, extreme northeast Colorado and southwest Nebraska and is expected to track east-southeast or southeast giving strongest activity in Kansas, north-central and northeast Oklahoma.

1200 CST data. Very strong TRW have developed in northeast Colorado, southwest Nebraska and northwest Kansas with line of CB and TCU southward to near LHX Colorado. Two other TRW have developed near CAO New Mexico. These two TRW indicate lifting is occurring further south than previously indicated by SMS and forecast progs. This indicates that northwest Oklahoma, central and southeast may eventually be involved in TRW activity during late afternoon and night.

1400 CST data. Very strong activity has developed in southwest and south-central Kansas with a field of TCU and CU southeastward. Activity has also developed in west Texas panhandle. Indications are that activity (strong to severe) will move into area around 1900 CST.

Leslie R. Lemon

Figure 17. NSSL Operational Nowcast, beginning at 0900 CST on June 6, 1975.

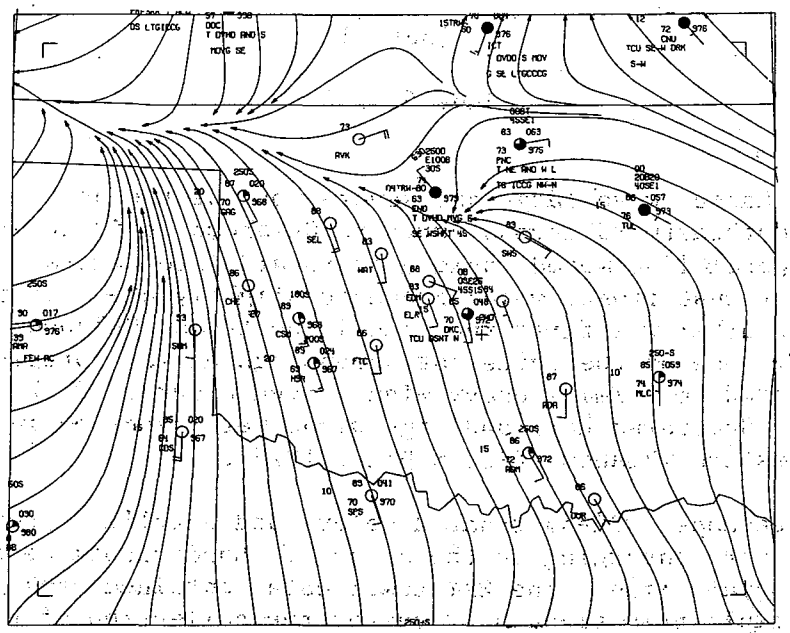

Figure 18. Surface map time 1900 CST. Boundary layer trajectories during intensification of squall line. Note the extremely high dew-point values in the air flow arriving in north-central Oklahoma from eastern Texas.

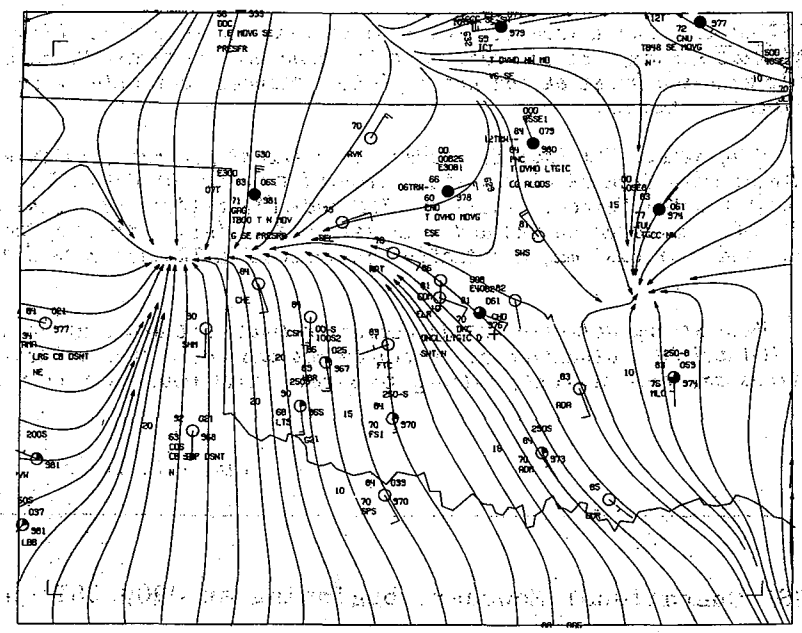

Figure 19. Surface map time 2000 CST. Boundary layer trajectories as the squall line accelerates southward and develops westward. A radar thin line appeared at 2130 CST, and moved southward at 21 m s^{-1} ahead of the precipitation (see fig. 22.)

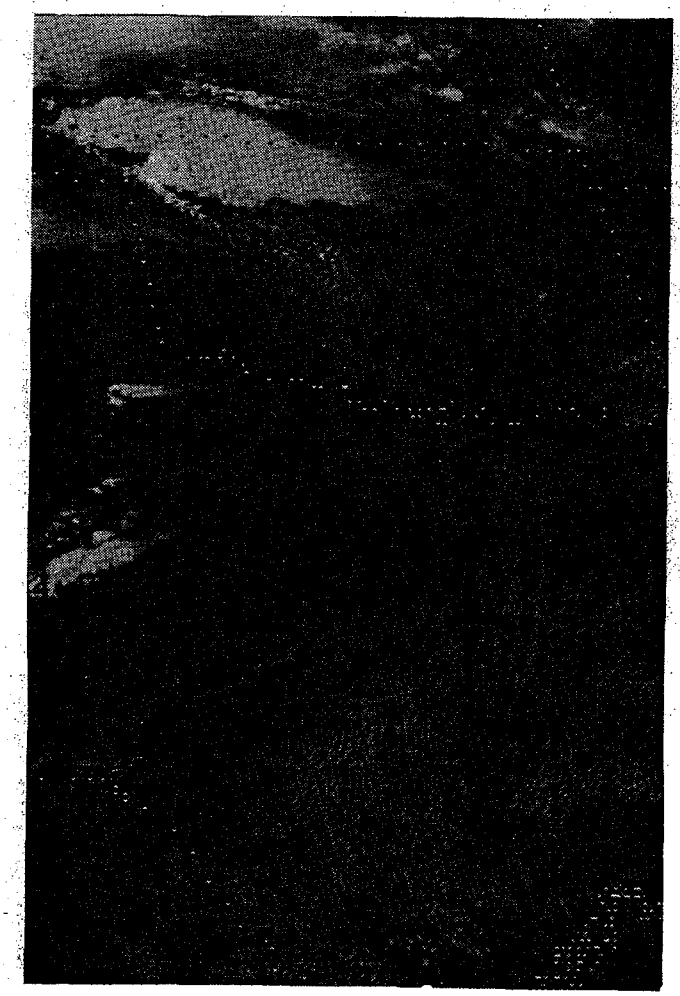

Figure 20. Satellite photograph at 1545 CST, June 6 showing advection of Gulf moisture northward to feed expanding thunderstorm activity over northwest Oklahoma.

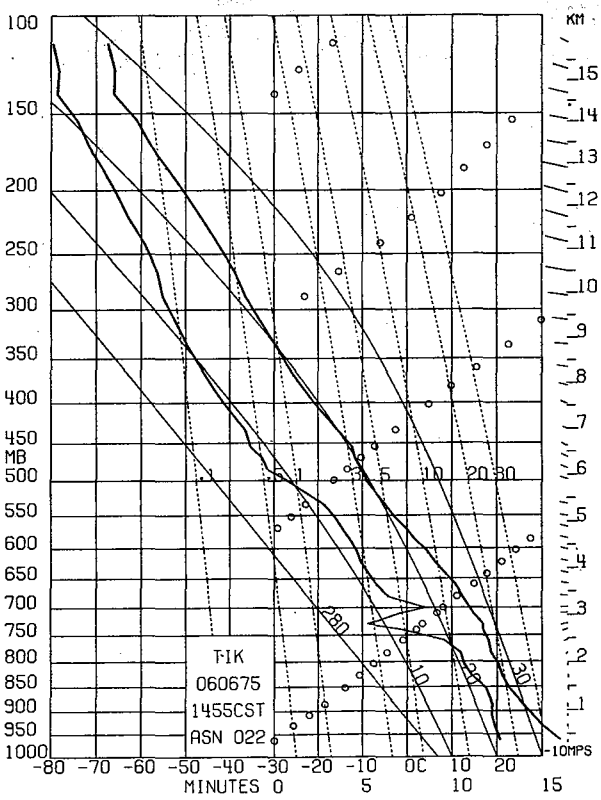

Figure 21. Temperature, moisture, and wind profiles in the conditionally unstable air mass at Oklahoma City. Sounding was made approximately six hours prior to formation of the squall line. Movement and propagation of the line was toward the southeast at 20 m s^{-1}, which is 30 degrees to the right of the mean environmental wind at a height (7.5 - 9.5 km) where the speed $\geq$ 20 m s^{-1}.

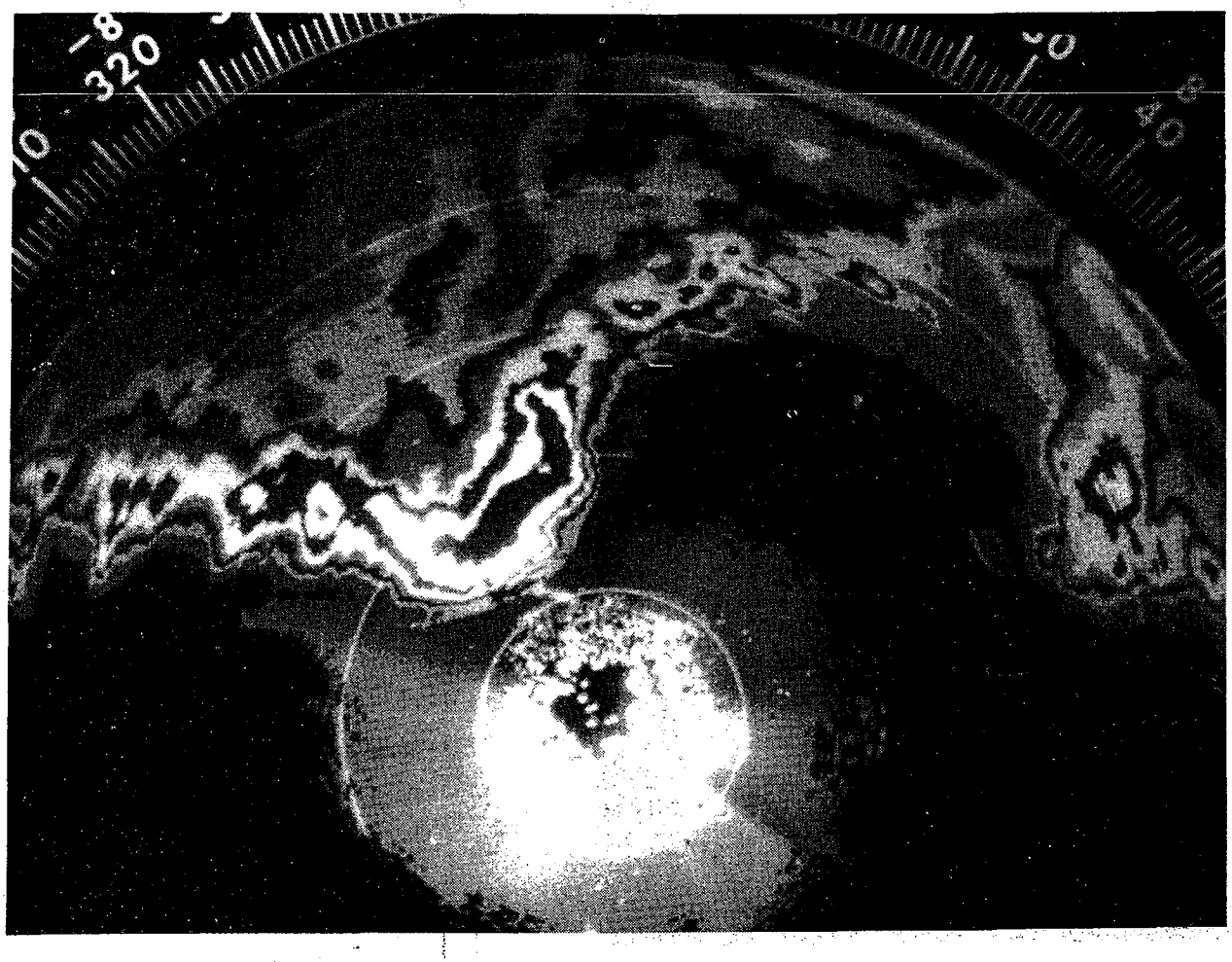

Figure 22. WSR-57 display without range normalization, showing the beginning of the gust front echo as it emerges from the line. It is now 10 minutes, or 16 km from the start of the tower section shown in Figure 23.

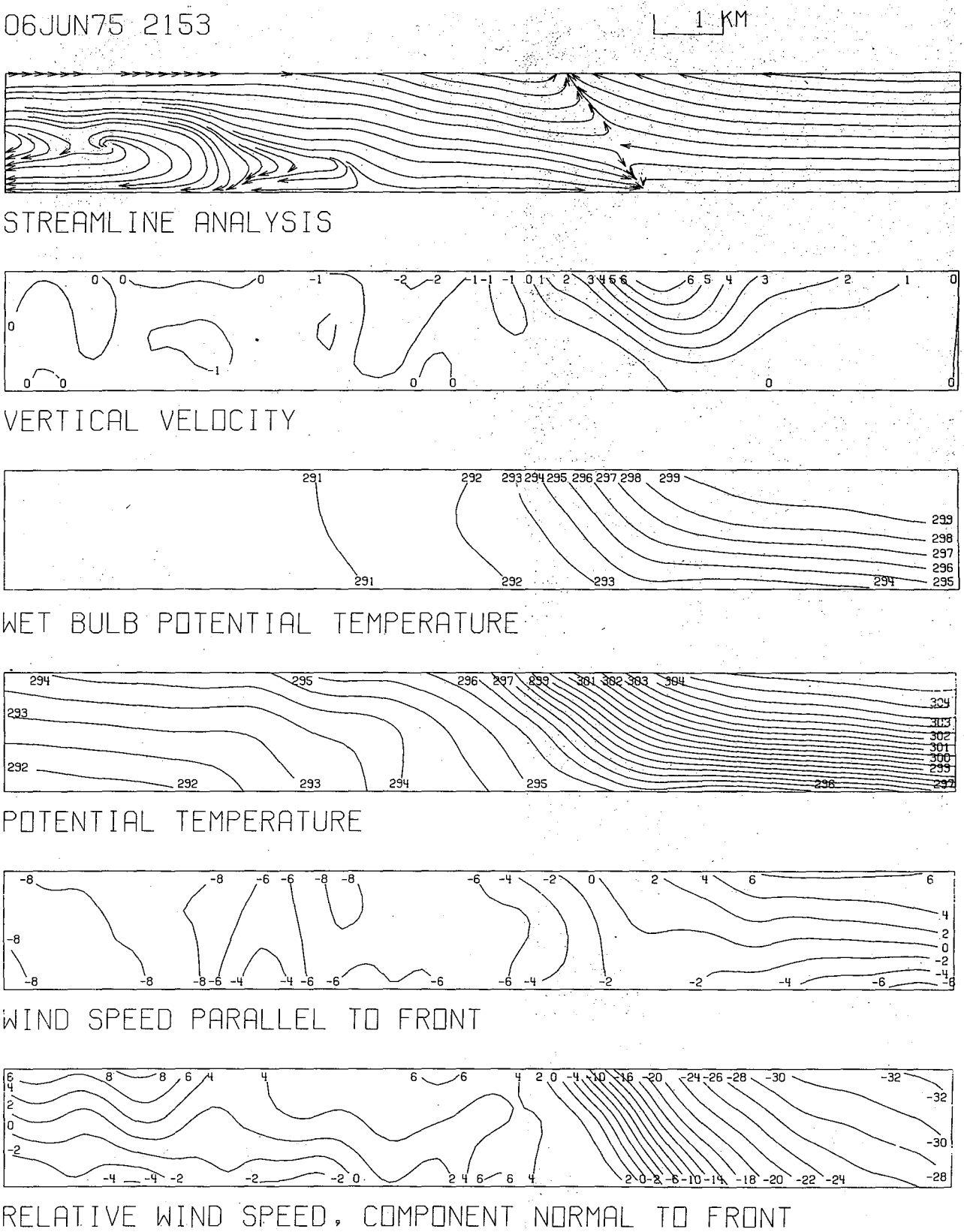

Figure 23. Time (space) section of smoothed 444 m tower data obtained during severe squall line passage, June 6, 1975. (See Goff, op. cit.)

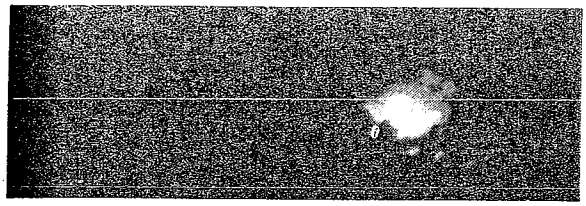

14°
(48K ft)

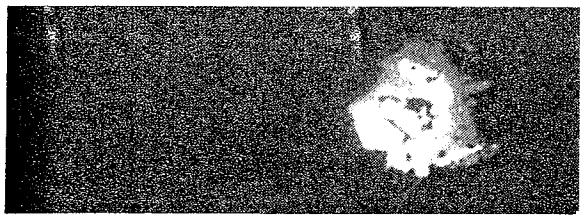

12°
(42K ft)

10°
(35K ft)

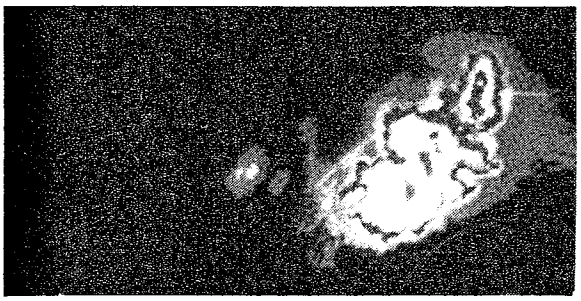

8°
(28K ft)

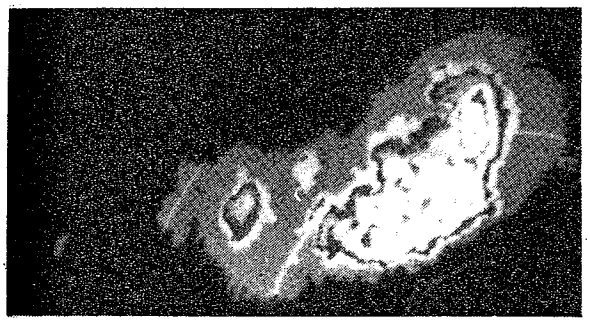

6°
(21K ft)

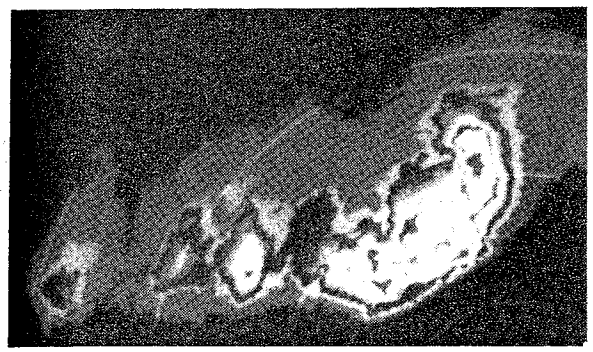

4°
(14K ft)

Figure 24. WSR-57 radar reflectivity profile at time of maximum storm development and origin of gust front.

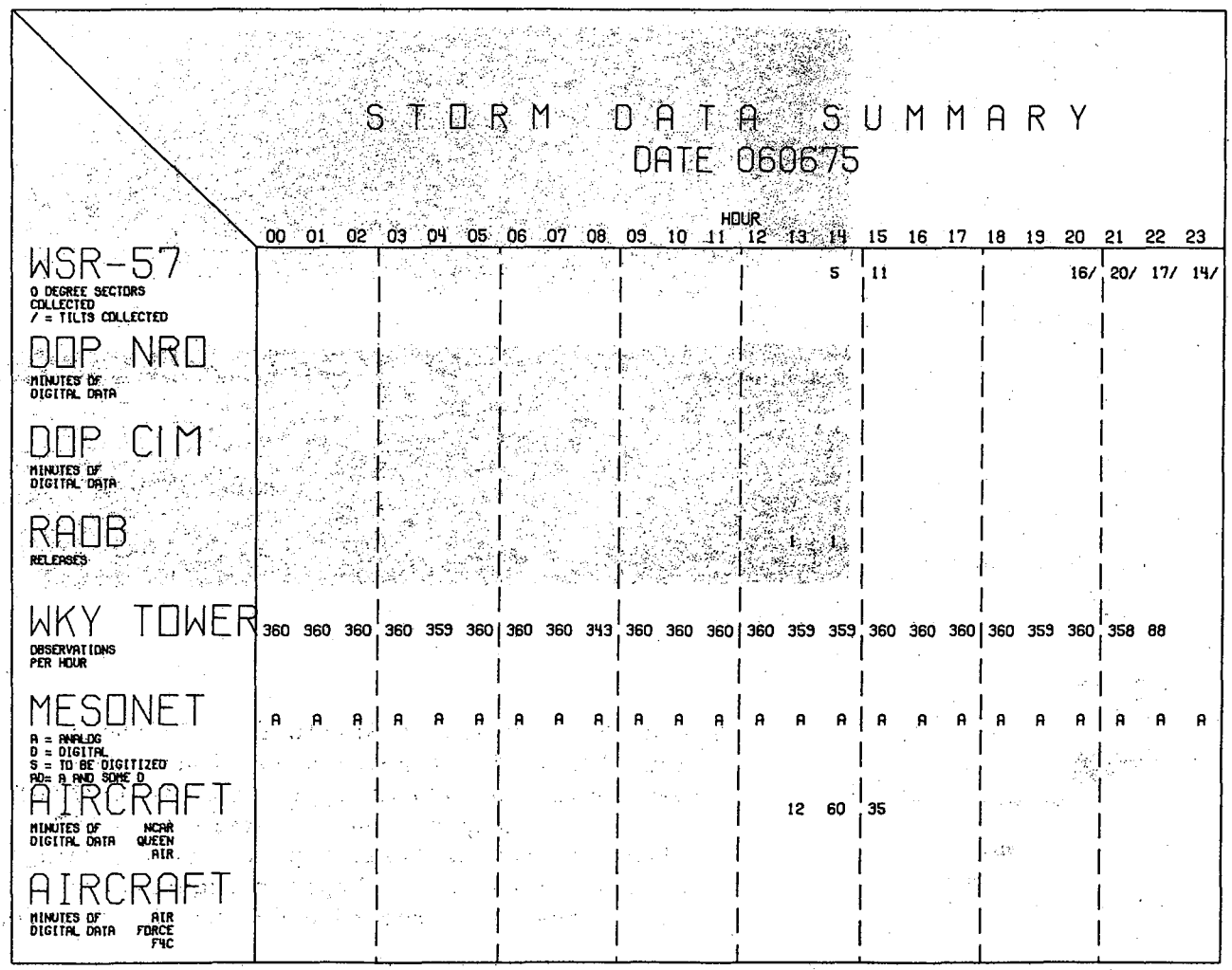

Figure 25. Summary of data archived on June 6, 1975.

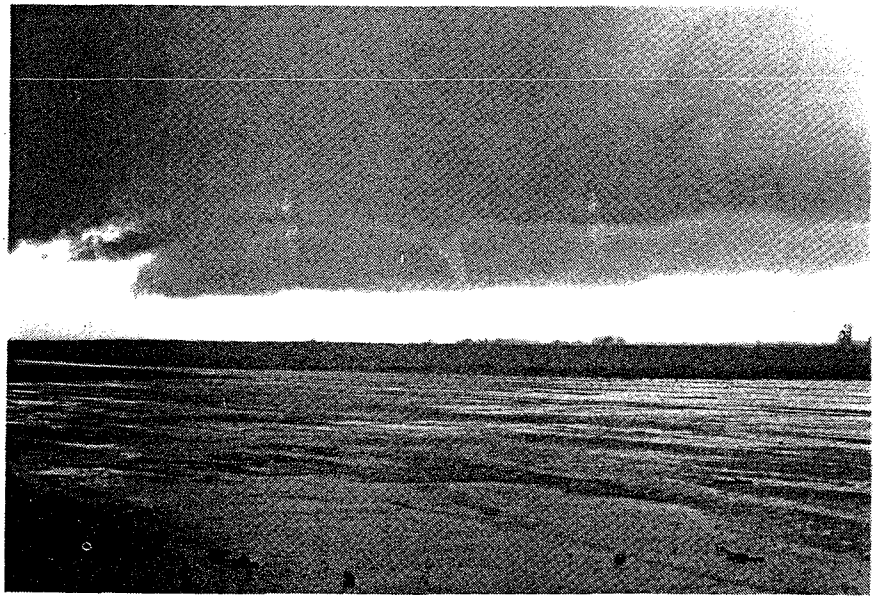

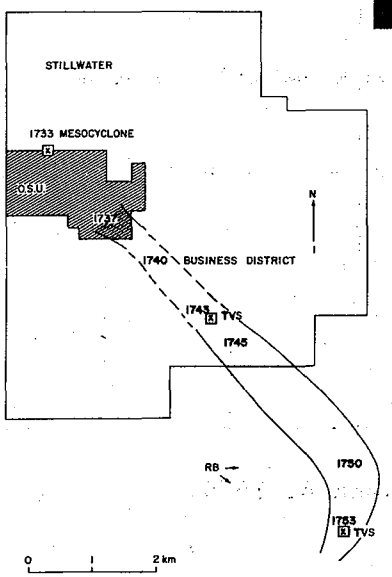

Figure 26. Tornado at Stillwater, Oklahoma, June 13, 1975. (above) Wall cloud and developing tornado at approximately 1737 CST. (below) Tornado at approximately 1753 CST, after destroying trailer park. (left) Damage path and location of Doppler radar vortex signatures (TVS) recorded during the tornado.

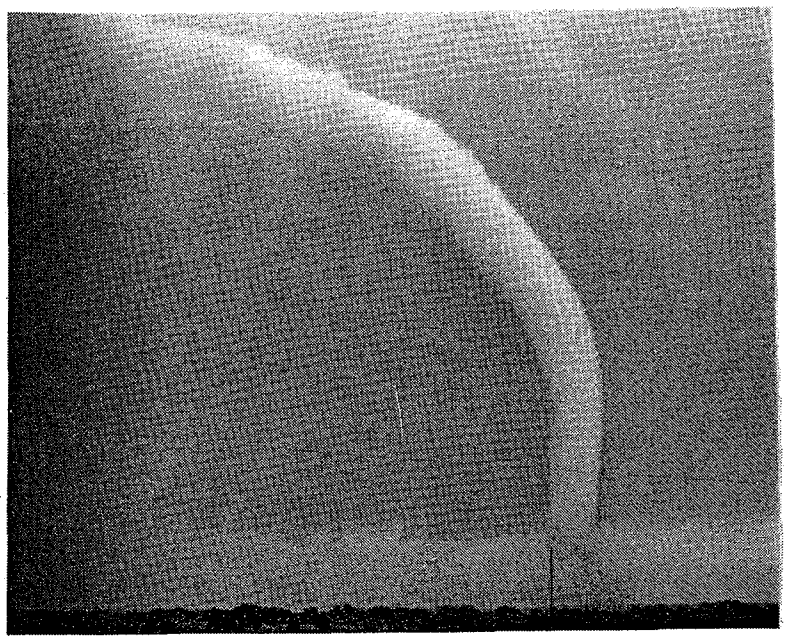

CASE III

June 13, 1975

On this day, the boundary layer flow over northern Oklahoma was southerly, weakly convergent, with mean level steering winds from the northwest. Scale of the convection, shown by satellite and WSR-57 radar was large--indicative of severe storms. A large tornado occurred at Stillwater at 1737 CST. An excellent radar data set was obtained, which is receiving special attention at NSSL and the University of Oklahoma.

NOWCAST FOR 13 JUNE 1975

Based on 1000 CST data. High, low level, moisture values (depths somewhat uncertain), fairly cold temperatures aloft and frontal system into extreme west and northwest Oklahoma. Weak moisture convergence in END area (primarily speed convergence) with TRW present. Maximum mass convergence is in Kansas along front at present time. Moisture of apparently sufficient depth to suggest TRW and potential for severe activity exists.

1100 CST data. Frontal system difficult to locate in Oklahoma but pressure trough and dry air is present. Moisture convergence continues and is increasing in the area of TRW activity in north central Oklahoma but still by way of speed convergence. Pressure trough in west is also an area for possible further development if convergence develops in response to pressure field. Activity should continue and increase in north central Oklahoma in response to increasing heating and outflow boundary generated by the persistent TRW.

1200 CST data. Drying and strong moisture gradient exist in southwest Oklahoma but convergence still lacking. Windshift or front has passed HUT and ICT Kansas area possibly indicating windshift extending down into north central Oklahoma further supporting activity there. Band of high and mid-level clouds (which may mark a "subsampling scale" wave with associated PVA and enhanced upward motion) is moving southeast from southwest Kansas and may initiate development in west Oklahoma or strengthen the already very strong activity in north central Oklahoma.

1300 CST data. Large pressure falls in southwest Oklahoma continue to make area suspect for future development but convergence has not yet developed significantly. Strong winds in central and west Oklahoma continue to funnel warm very moist unstable air into north central Oklahoma and are moderate at this time.

1400 CST data. Increasing convergence both in west and north central Oklahoma. In southwest Oklahoma winds have veered in the dryer air and backed some in more moist air with strong pressure falls continuing. An area of TCU and CB's also is present in the dryer air in west Texas indicating destabilization. Winds have backed at both PNC and END (probably induced by CB's to the southeast) and continued large temperature contrast and strong inflow to area. Continued strong to severe activity in north central Oklahoma.

1500 CST data. Basically same as above. Some TCU beginning in southwest Oklahoma. Mid and high cloud band moving southeast toward west and north central Oklahoma. One CB and some TCU developing under east end of cloud band northwest of CB complex in north central Oklahoma. Large pressure falls in southwest Oklahoma gives good possibility for development there. (Weak echo has developed.)

1600 CST data. Very strong moisture convergence in north central Oklahoma and large pressure falls at END and PNC. Pressure trough has passed END moving into and further increasing convergence in the north central Oklahoma activity. Mid and high level cloud band now overtaking END, PNC activity with new CB development beneath band. Conditions favorable for increased strength and severity of activity. Strong TRW near CDS area as that activity overtakes dry line.

Leslie R. Lemon

Figure 27. NSSL Operational Nowcast, issued hourly beginning at 1000 CST, on June 13, 1975.

As indicated in the forecast and nowcast, wind and moisture fields were not typical of severe storm days. By 1500 CST an increase in convergence was noticed in hourly data over north-central Oklahoma. The development of the large storms with an immence ice crystal cloud is well documented in the satellite data. The WSR-57 data, both photographic and digital, should be very useful in reconstructing the sequence of development of the Stillwater storm.

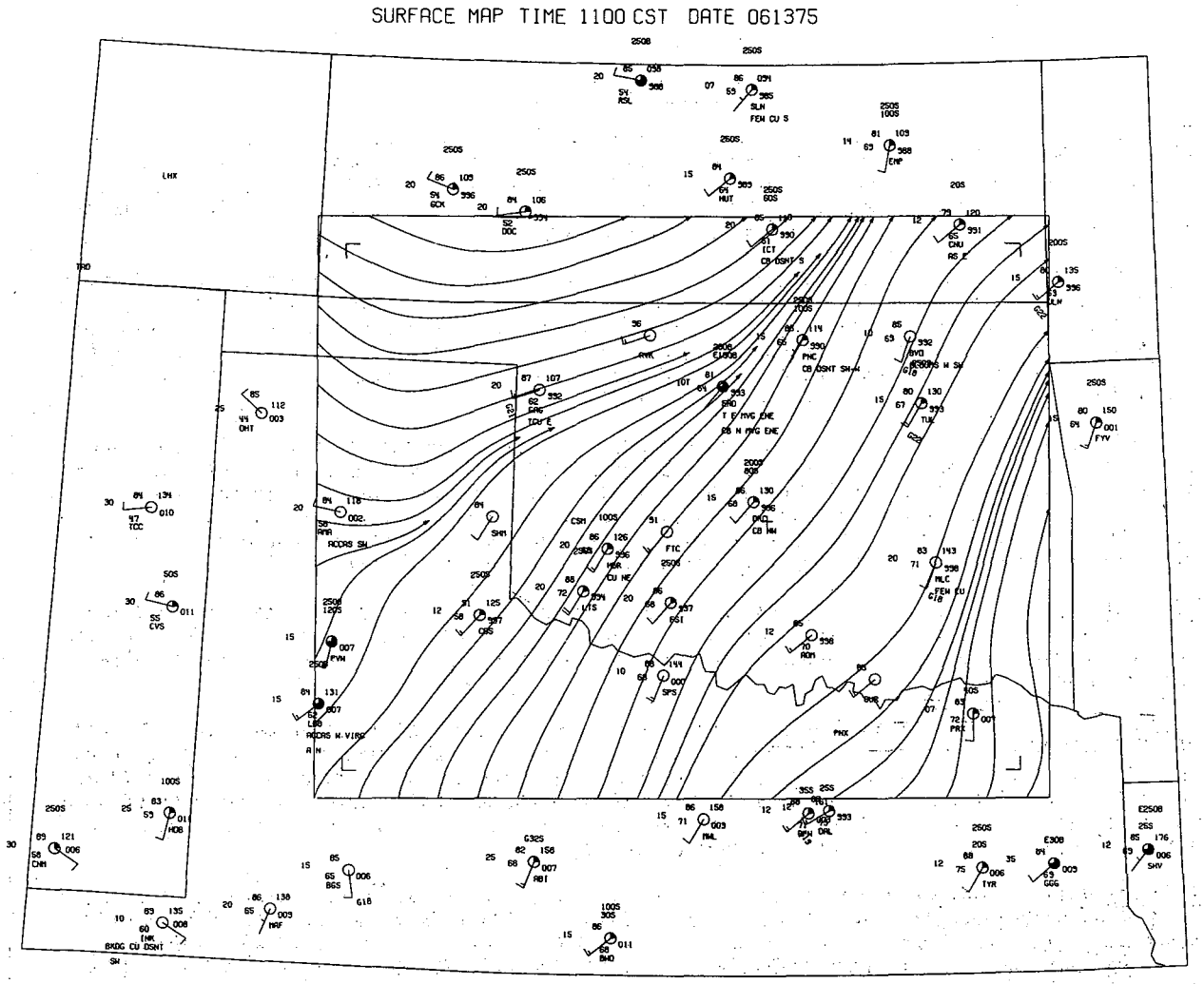

Figure 28. Surface analysis, 1000 CST, June 13, 1975.

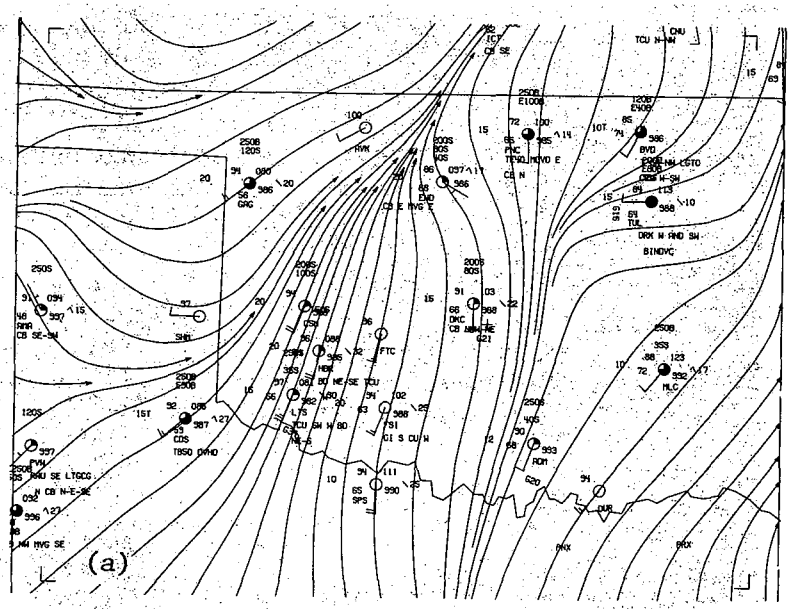

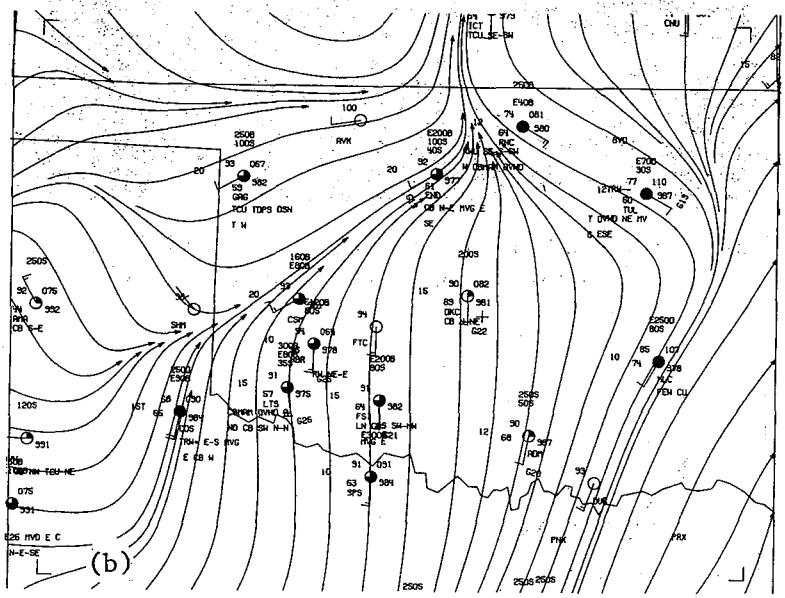

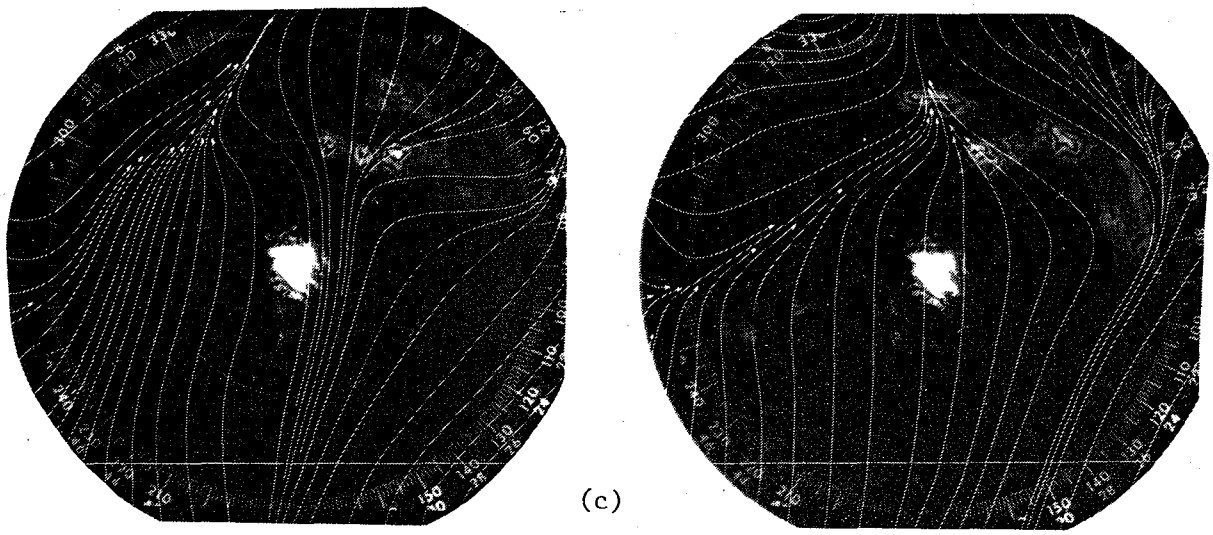

Figure 29. Surface flow fields, a) 1500 CST, b) 1700 CST, and c) WSR-57 radar displays showing origin of thunderstorms in zone of convergence over northern Oklahoma.

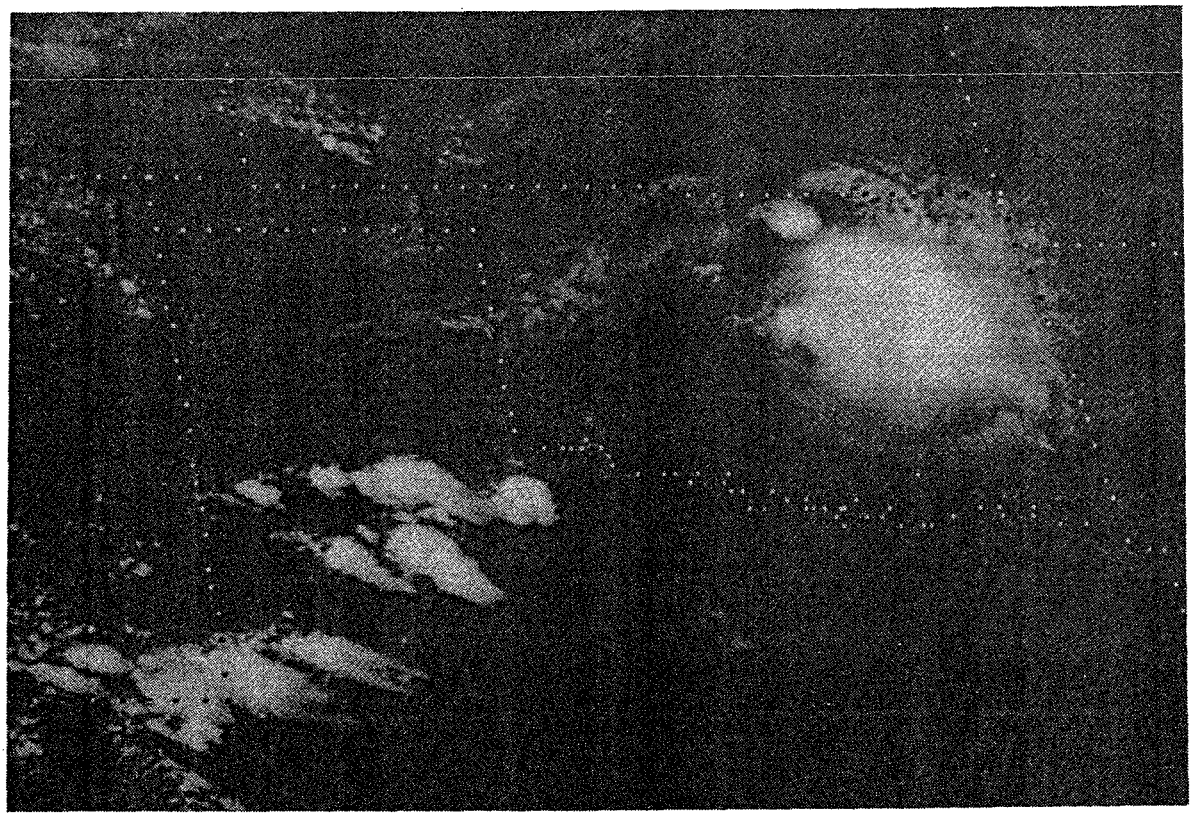

Figure 30. Satellite photograph at 1445 CST, same time as WSR-57 radar profile of precipitation rate, Figure 32.

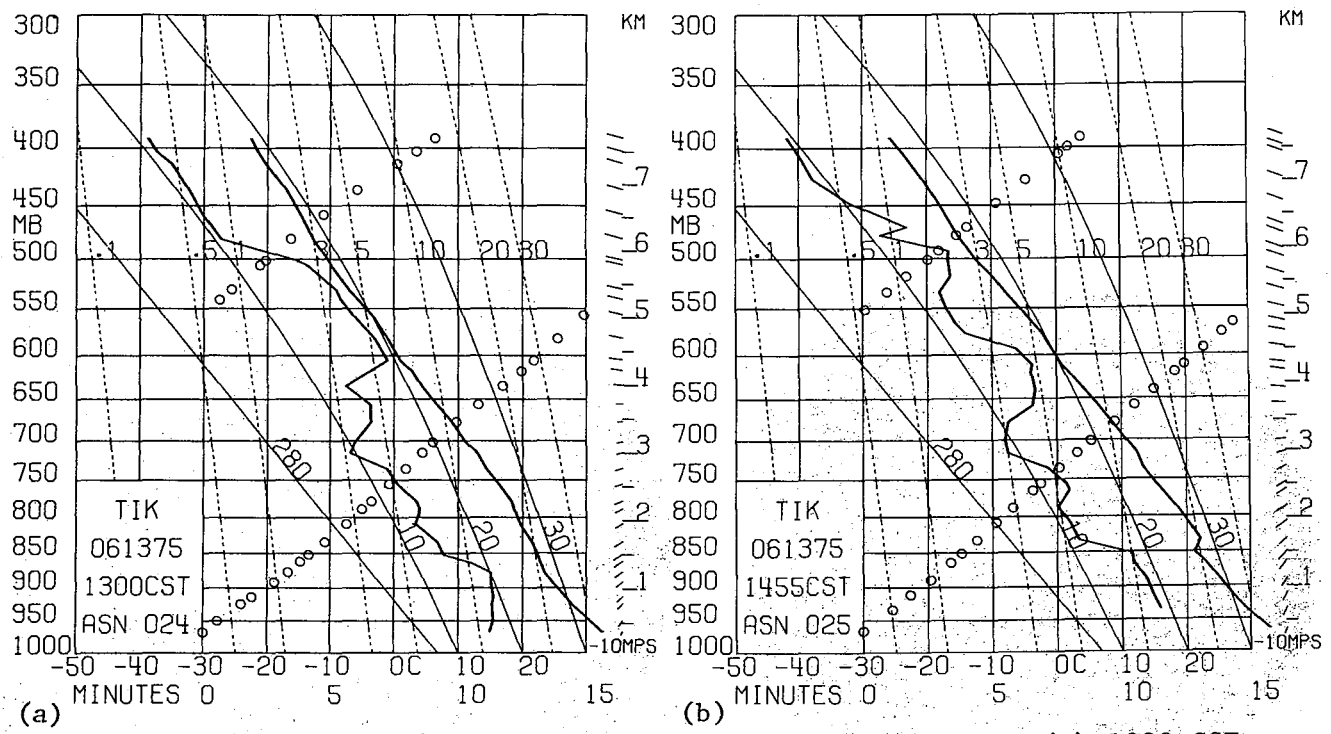

Figure 31. Soundings recorded at Tinker Air Force Base at: (a) 1300 CST, and (b) 1455 CST, 3-4 hours prior to the Stillwater tornado.

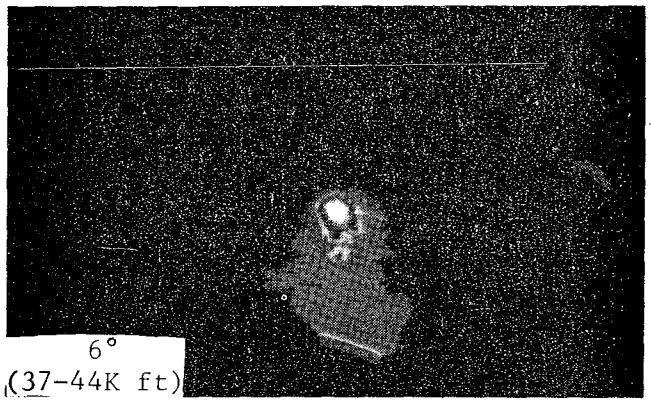

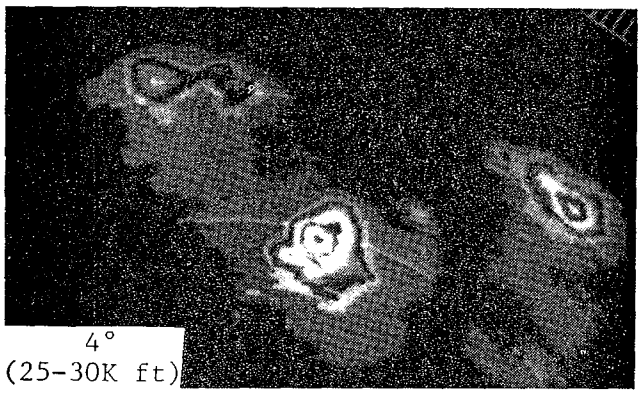

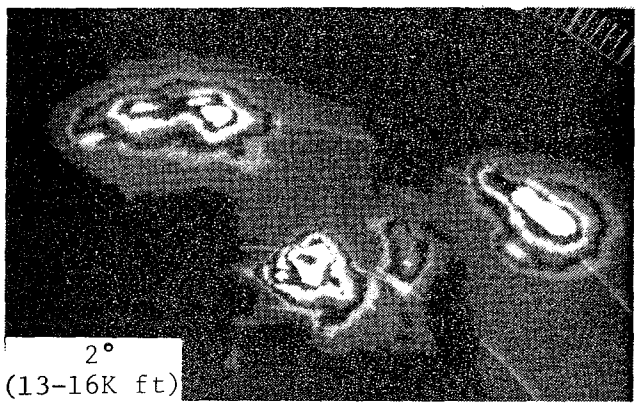

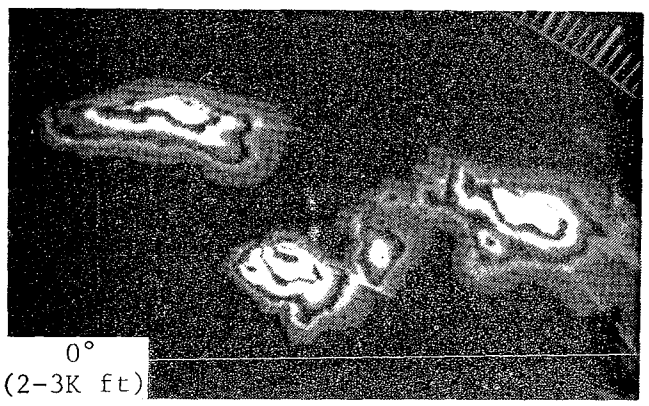

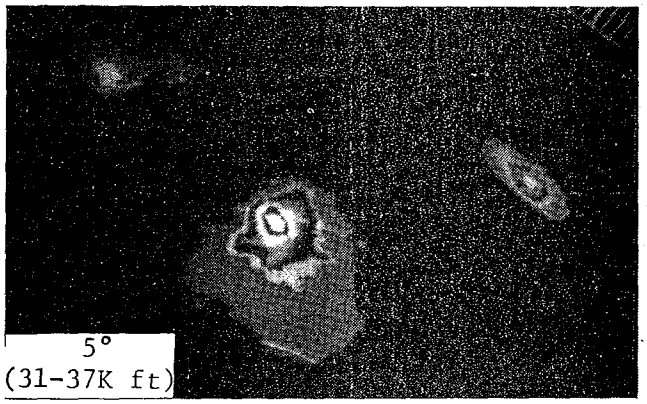

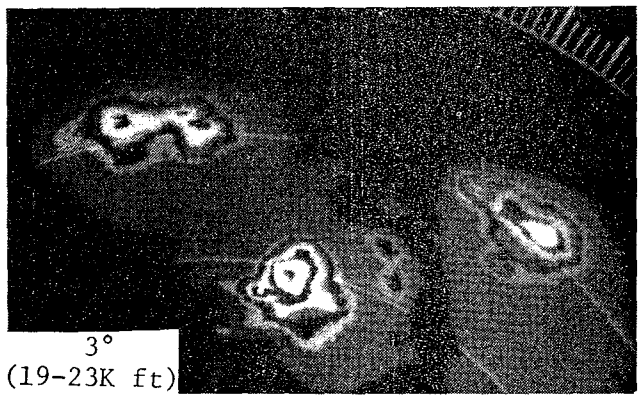

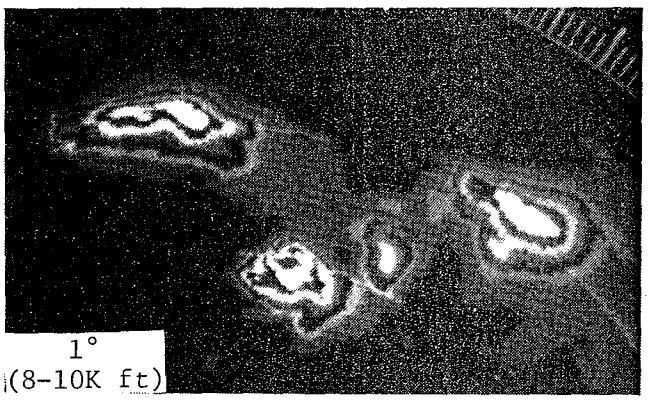

Figure 32. Vertical profile of WSR-57 reflectivity display showing multiple, large-scale thunderstorm activity, approximately three hours prior to tornado at Stillwater.

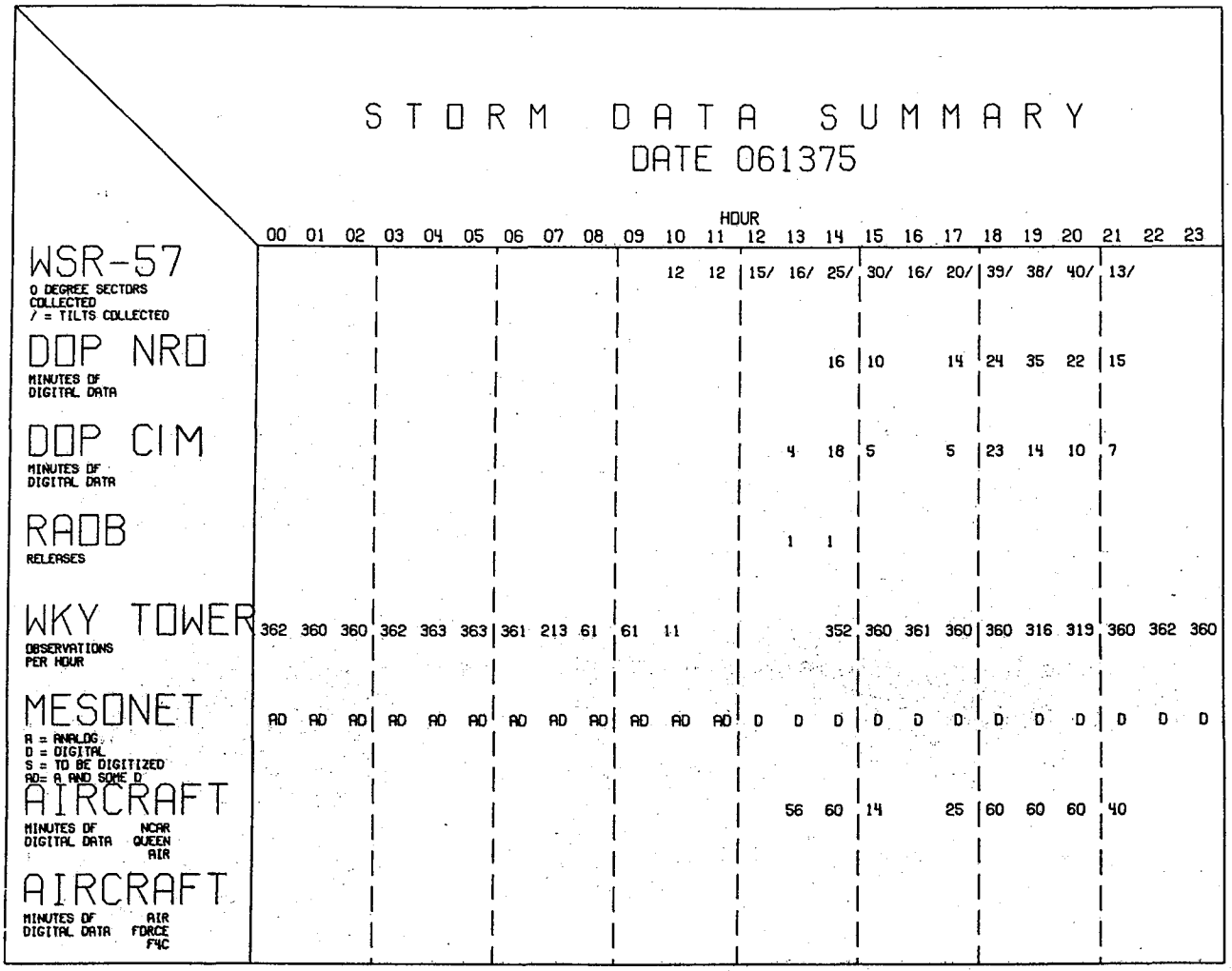

Figure 33. Summary of data archived on June 13, 1975.

SECTION 3

AUXILIARY INFORMATION

This section contains operating procedures for the rawinsonde program, a list of locations of remote observing facilities, and indices of the data archived.

Figure 34. LuCreta Butcher operates NSSL's Systems Engineering Laboratories 8600. Equipment seen in the background includes an IBM 1401, and a Calmagraphic X-Y reader/ plotter system.

U.S. DEPARTMENT OF COMMERCE
National Oceanic and Atmospheric Administration
ENVIRONMENTAL RESEARCH LABORATORIES

Date : March 21, 1975

To : Rawinsonde Network Personnel

From : Project Coordinator

Subj : NSSL Rawinsonde Operations - 1975

I. Statement of Objectives

A Rawinsonde Unit from the U.S. Air Force's Sixth Weather Squadron (Mobile) Tinker Air Force Base, Oklahoma, the U.S. Army's Rawinsonde Section at Fort Sill, Oklahoma, and the National Weather Service's Rawinsonde Unit at Oklahoma City, Oklahoma, comprise the network of upper air sites for this spring's thunderstorm observation program during the period 15 April through 15 June. The upper air network is supplemented by an automatic recording surface network, radar observations from NSSL, aircraft operations in and near thunderstorms, an instrumented television tower (WKY-TV) in Oklahoma City, and dual Doppler radars located at Norman and Cimarron Field.

The project meteorologists will use the combined data from all these sources to furnish additional information on the structure and dynamics of severe thunderstorms, and how they interact with their environment. Knowledge gained from these studies will ultimately improve forecasting these destructive storms and related phenomena.

Operationally, the upper air network has these goals:

1. Furnish high quality data in and around thunderstorms
2. Test new operational techniques
3. Furnish support data for aircraft and Doppler radar wind measurement operations and other laboratory special-purpose operations.

The operational specifications described in the following sections are the results of several years operational experience in the field and data reduction experience in the laboratory. The procedures are more unconventional than conventional, but with the purpose of simplifying the task of obtaining scientifically useful data.

II. Network Description

Site specifications are given in Table 1.

III. Daily Routine (7 days per week unless otherwise notified)

A. Period of operation will begin 15 April and end 15 June 1975.

B. Crews should be on site by 1300 CDT unless otherwise notified. When crews are not on site, one member of each crew should be available to receive telephoned instructions, and should know the whereabouts of the other crew members.

C. Perform Daily Check List and other routine maintenance and housekeeping chores.

D. RAOB CONTROL will contact each site by 1330 CDT to obtain station pressure, make time checks, and issue operational instructions. (See Section IX on Communications.)

IV. Soundings (General)

A. Pre-storm and soundings for operational forecasting purposes will be requested at certain times from one or two selected sites. Details on the reduction of these soundings will be passed on at the briefing. Use of a 300 gm balloon normal inflation will be sufficient.

B. Serial soundings using 300 gm balloons, normal inflation 300 m/min will be requested whenever thunderstorms are in or near the network or expected to develop over the network. Release times and heights of soundings will be variable for each station. RAOB CONTROL will determine this during serial sounding operations. Report release time back to RAOB CONTROL as soon as practical.

A WORD OF CAUTION: Don't be too eager! Take time to get preflight calibration checks right. If they are not right, the entire sounding is wasted and cannot be recovered.

V. Data Acquisition

A. Flight preparation and pre-release checks.

1. Balloon inflation

2. GMD

a. If strong winds or heavy precipitation have occurred since the GMD was last checked for orientation and leveling, check again before making release.

b. Keep the electronics of the tracking system in "A-OK" condition. Preventive maintenance should be a matter of daily routine.

3. Control Recorder

   a. Azimuth printer should record 360° when GMD is pointing to true north.

   b. Check condition of printer to insure that verier readings will be legible.

   c. Reset time before each flight.

   d. RESET PRINTING FREQUENCY TO 10 PRINTS PER MINUTE.

   e. Perform other checks in accordance with FMH No. 3 instructions.

4. Baseline check and outside psychrometer check.

   a. A standard baseline check is required according to FMH No. 3 instructions.

   b. Enter baseline values on both the NSSL worksheet and in lines 1 through 4, Blocks 2 and 3 of the RAOB Calibration Form (see instructions in Section VI).

   c. DO NOT CLIP TEST LEADS FROM INSTRUMENT AFTER BASELINE CHECK.

   d. Place instrument outside with the aspirated psychrometer in the instrument shelter provided by NSSL. Moisten the psychrometer wick with distilled water and turn on fan motor. DO NOT ALLOW FAN TO EXHAUST AIR DIRECTLY AT THE RAWINSONDE ELEMENTS.

   e. After one minute, short the reference lead and record a 15-second trace on the TMQ-5.

   f. Immediately after step e, obtain 15-second temperature and humidity traces, and determine the rawinsonde temperature and humidity.

   g. Determine the temperature and humidity from the psychrometer readings. (See Section VIII on psychrometer maintenance.)

   h. If the rawinsonde temperature and humidity differ from the psychrometer values by more than 1°C or 10%, recheck baseline values. If instrument is faulty, reject it and baseline a new instrument. When in doubt, contact RAOB CONTROL for instructions.

   i. Record outside check information in Block 3 of RAOB Calibration Form, and NSSL worksheet (see Section VI).

5. Setting baroswitch

   a. Double check the station barometer reading with the reading from the previous sounding. On a given day, station pressure should not vary more than one to two millibars per hour, unless a vigorous thunderstorm is overhead or a strong cold front has passed.

b. Be especially careful in determining the initial contact setting of the baroswitch. The accuracy of entire sounding depends upon this setting. However, should a discrepancy occur between set contact versus release contact, record the error according to instructions in Section VI, and do not apply the correction when evaluating the TMQ-5 record. The NSSL computer will do this for you.

c. DO NOT ADJUST YOUR BAROMETER UNLESS REQUESTED BY RAOB CONTROL. Your barometer was calibrated at NSSL prior to operations. NSSL will perform a daily computer check of station pressure across the network, and will notify you if your barometer needs further adjustment.

6. TMQ-5 pre-flight preparation

a. Wind stop watch before each sounding.

b. Keep chart drive setting at 1 INCH PER MINUTE.

c. Check ink supply daily.

d. Tension on pen should be set to eliminate overshoot or excessive drag.

e. Check zero ordinate trace for accuracy.

f. Perform other pre-flight checks according to FMH No. 3, EXCEPT it is not necessary to perform sensitivity check prior to each baseline if such a check has already been accomplished as part of the Daily Check List procedures.

g. IMPORTANT: Activate chart drive motor at least one minute before release.

h. The TMQ-5 should be calibrated with a signal generator once every two weeks in accordance with normal procedures.

B. Surface Observation at Release

1. Enter on the NSSL WORKSHEET the surface observation.

2. Estimate surface wind direction and speed and record in meters per second and nearest 10°. (Laboratory personnel will later enter the wind from the recording surface station at your site, but in case that equipment fails, we need your estimate also.)

3. Use the NSSL aspirated psychrometer to determine temperature and relative humidity.

4. Convert psychrometer temperature and humidity to ordinate values, and use these values as the surface recorder record evaluations.

C. In-Flight Check Procedures

1. GMD

   a. Man the GMD on release. It is imperative to get the GMD on target as soon as possible.

   b. The man on the GMD is responsibile for determining the azimuth to the release point on each release. The man releasing the instrument is responsible for pacing of the distance from the release point to the GMD on each release. Record these data as in c and d below.

   c. Enter release azimuth to nearest 10° on the Winds Coding Form-1 in Block 2 at time 00.0.

   d. Enter distance to release point in meters on the RAOB Calibration Form, Line 5, Block 2.

2. Control Recorder

   a. After 2 minutes of flight, switch print frequency to 2 per minute.

   b. Monitor paper feed for legible angle prints.

   c. Monitor signal strength and azimuth-elevation indicators to detect tendency for GMD to hunt or respond erratically. Correct erratic tracking tendencies as soon as feasible

   d. Note on the winds tape the time periods during which the GMD was tracking erratically or hunting.

   e. Operate reference time print switch in AUTOMATIC mode.

3. TMQ-5 Recorder Record

   a. Activate the stop watch coincident with switching the TMQ-5 from S.C. This should be done at the exact moment of instrument release.

   b. Adjust low references regularly and enter on the TMQ-5 record the corrections applied.

   c. Except for attention to reference signals and the general quality of the trace, the recorder chart should require little monitoring during the flight. The operator should closely monitor the control recorder rather than try to evaluate levels on the recorder chart during the flight.

   d. At termination, stop the stop watch at the same time the TMQ-5 is returned to S.C.

   IMPORTANT: Allow recorder to run at least one contact past the required height before turning switch to S.C.

VI. Procedures for Data Reduction

A. Recorder Record

1. FMH No. 3 rules are to be followed in picking levels for evaluation EXCEPT SUCCESSIVE LEVELS MAY NOT BE SEPARATED BY MORE THAN 25 MB (exactly 25 mb is allowable) OR BY TWO CONTACTS IN LOW LEVELS.

2. Enter on each significant level the elapsed time since release as discussed in item 4 below, and level number at left side of record starting with level 1 at surface.

3. If changes in temperature and humidity trends allow, it will be more accurate to place levels at the top of the temperature traces (whole contacts). However, do not violate FMH No. 3 rules arbitrarily for this convenience.

4. Determine elapsed time since release using the ruler provided by NSSL. Read times to the nearest 0.01 minute. Begin each measurement from the time when the S.C. signal ended at release (not the time of first trace recording), or from a line drawn across the record at each 6 minutes (the length of the ruler). Be careful to draw levels perpendicular to the ordinate lines.

5. Entries on recorder record at surface level.

   a. Contact value at release.

   b. Ordinate value corresponding to surface temperature from psychrometer reading at release.

   c. Ordinate value corresponding to surface relative humidity from psychrometer reading at release.

   d. Level number 1.

6. VERIFY ALL EVALUATIONS

B. Entries on RAOB CALIBRATION FORM

Note: Lines are labeled at left side of form. Blocks are labeled at bottom of form. Numbers inside the heavy lines are instructions to computer operator and may be ignored.

LINE	BLOCK NUMBER	SPECIFICATION
1	1	Station identification letters (see Table 1).
2		Latitude nearest hundredth degree (see Table 1).
3		Longitude nearest hundredth degree (see Table 1).
4		Height of barometer in meters.
5		Height of GMD antenna in meters.
6		Month, day, year (CST).
7		Release time nearest minute CST.
8		Surface wind direction nearest 10°
9		Surface wind speed meters per second (knots x 1.94)
10		Radiosonde serial number, last five digits only.
11		Ascension number.
12		No entries.
1	2	Baseline temperature to nearest 0.1°C.
2		Baseline temperature ordinate value to nearest tenth.
3		50.0 is constant.
4		Relative humidity ordinate value at 50% relative humidity and +40° after setting humidity evaluator on baseline information.
5		Distance from release point to GMD in meters.
6		Surface temperature at release to nearest 0.1°C from psychrometer reading.
7		1 is constant.
8		Elapsed time of sounding to nearest hundredth minute from ruler measurement of recorder record. Also enter on recorder record, measurement is from S.C. to S.C.

9		Elapsed time of sounding to nearest hundredth minute from stop watch. (See conversion Table 2.) Also enter on Recorder Record, measurement is from S.C. to S.C.
10		Correction ± to be applied to commutator bar setting. (Same as line 3, block 4).
11		Surface pressure at release* to nearest tenth millibar.
1	3	Baseline temperature ordinate.
2		Baseline temperature.
3		Baseline humidity ordinate.
4		Baseline humidity.
5		Outside check temperature ordinate.
6		Outside check temperature from Recorder Record.
7		Outside check temperature from psychrometer.
8		Outside check humidity ordinate.
9		Outside check humidity from Recorder Record.
10		Outside check humidity from psychrometer.
11		Pressure to nearest millibar at beginning of missing data layer.
12		Pressure to nearest millibar at end of missing data layer.
13-14		Beginning and ending of additional missing data layer.
15		If precipitation was occurring at release time at station, enter 1; otherwise enter 0.
16		If unusual sustained ascent rate occurred during sounding such as that due to updraft, icing, etc., enter 5; otherwise enter 0.

* Ordinarily, when pressure reading used for commutator bar setting has been made within 5 minutes of release, that pressure may be used as surface pressure. However, if more than 5 minutes has elapsed, or if a wind shift or temperature drop occurs between setting commutator and release, take another pressure, temperature and humidity reading immediately after release to use as surface values.

1	4	Contact setting value (if greater than 10 shift decimal one place to the right).
2		Contact value at release (if greater than 10 shift decimal one place to the right).
3		Correction ± to be applied to commutator bar setting (if no correction enter 00.0).
4		Radiosonde serial number (last 5 only).
5		The top of the first contact after release (example commutator bar came in at 8.2 contacts enter 9).

D. Entries on WINDS CODING FORM-1

LINE	BLOCK	TIME	SPECIFICATIONS
1	1	00.0	Elevation angle at release (always 00.00).
	2		Azimuth angle to balloon at release.
	3	00.1	Elevation angle.
	4		Azimuth angle.
	5	00.2	Elevation angle.
	6		Azimuth angle.
	7	00.3	Elevation angle.
	8		Azimuth angle.
2-25	1-8	00.4-41.5	Elevation azimuth angles entered in the same manner as on Line 1.

NOTE:
1. All angles should be read to hundredths of a degree.
2. Time increment changes at 2.0 minutes.
3. Angle data must be filled in to complete the line on which termination time falls.
4. For runs exceeding 41.5 minutes, finish entries on Winds Coding For
5. Fill out heading on form.

E. Entries on NSSL Worksheet

Heading

1. Enter station identifier letters.

2. Release data and time (CST).

3. Ascension number.

4. Radiosonde serial number (last 5 only).

Baseline Check Data

1. Make baseline check in accordance with NSSL S.O.P. Chapter V, 4a through 4e.

2. Enter all information in spaces provided.

Outside Check

1. Make in accordance with NSSL S.O.P. Chapter V, 6b, 1 through 4.

2. Enter information in spaces provided.

OTE: FURNISH ALL INFORMATION IN EACH SECTION!

F. Entries on CONTACT SETTING Form

1. Ascension number (numbered sequentially from beginning of season).

2. Surface pressure to the nearest tenth of a mb.

3. Whole Contact Value below setting.

4. Pressure at contact below setting.

5. Pressure at contact above setting.

6. Detent Click Value.

7. Radiosonde serial number (last 5 only).

Note: The above information to be called in to RAOB CONTROL. RAOB CONTRAL will call back the following information.

1. Commutator bar setting, Contact Value to the nearest tenth of a contact.

2. Number of clicks up from lower contact.

Note: Each crew will be furnished a working copy of the contact setting form in acetate and the information may be erased after it is transferred to the NSSL worksheet and RAOB calibration form.

VII. Procedures for Forwarding Original Records and Forms

A. Envelope Supply:

1. Thirty large, franked, U.S. Government mailing envelopes, return-addressed to NSSL.

2. Forty serially-numbered smaller envelopes for packaging the recorder record, control recorder tape, pressure calibration strip, and coding forms for each run individually.

B. Any run resulting in at least one minute of information will be assigned an ascension number.

C. Some Precautions:

1. Be sure the sounding information is placed in the envelope numbered for that ascension. (A few unnumbered envelopes are included in case a numbered envelope is lost.)

2. Take care not to mix records from one sounding with those from another.

D. The small envelopes should be identified by the following:

1. Station identification letters

2. Date and time of release (CST)

3. Ascension number

E. After the day's soundings have been evaluated and VERIFIED, place the unsealed envelopes in a large envelope, seal, and mail to NSSL at the earliest convenience.

VIII. Maintenance of NSSL Psychrometer

A. The aspirated psychrometer furnished by NSSL should remain a reliable instrument with nominal care. You have been supplied with the most essential items necessary to maintain an accurate instrument. If you exhaust your supplies, notify RAOB CONTROL.

1. Supplies:

a. Six 1.5v batteries (Size D).

b. One quart bottle of distilled water.

c. One small applicator bottle.

d. Wicking and string.

2. Maintenance:

a. Change wicking at least ONCE every WEEK, more often if dusty conditions prevail.

b. Change batteries every THREE weeks to insure an adequate ventilation rate.

B. DO NOT RUN THE PSYCHROMETER MOTOR CONTINUOUSLY FOR PERIOD LONGER THAN 5 MINUTES. Your batteries will maintain power much longer if this suggestion is followed.

IX. Communications

A. NSSL will serve as RAOB CONTROL. The base station call sign is KKE 793, only RAOB CONTROL CAN OPEN THE NETWORK. Telephone: 1-329-0388.

B. All stations are required to have access to commercial telephone at the rawinsonde site and at the personnel billet. When calling NSSL by telephone, CALL COLLECT if long distance.

C. Radio Communications

1. The FM transceivers which NSSL assigns to each site form a dual-channel line-of-sight communications system linking the sites to RAOB CONTROL and in certain instances to each other. RAOB CONTROL will use this means to issue general operational advisories and directives, and individual instructions to

each site. The sites may also use this means to initiate communications with RAOB CONTROL or with adjacent sites. However, you should keep in mind that you are not likely to receive all sites on your set, so take care not to interrupt communications which NSSL is having with another site. Please use discretion in the amount and type of messages transmitted by radio.

2. Except during actual transmission, these radios are to be kept in a ready-to-receive status while the site is manned.

3. NSSL's transceiver is mounted near the top of the WKY-TV tower in Oklahoma City (about 1000 ft above terrain level). These transceivers transmit on a frequency of 173.10 mHz and receive on 163.275 through the NSSL transceiver.

4. In the event of radio malfunction or other transmission difficulties, the telephone link with NSSL is to be used.

5. Transmissions on either the radio or telephone links are restricted to messages pertinent to project operations.

TABLE 1. 1975 Rawinsonde Site Specifications

Station Number	Location	Code Letters	Latitude	Longitude	Elevation Field/ Barometer	Assigned Frequency
1	TAFB	TIK	35.41	97.40	1270 ft/387M	1685
2	Fort Sill	FSI	34.66	98.41	1180 ft/362M	1680
3	Oklahoma City	OKC	35.40	97.60	1286 ft/392M	1680

TABLE II

CONVERSION TABLE SECONDS TO HUNDREDTHS

Seconds		Hundredths	Seconds		Hundredths	Seconds		Hundredths
01	=	.02	21	=	.35	41	=	.69
02	=	.03	22	=	.36	42	=	.70
03	=	.05	23	=	.38	43	=	.72
04	=	.07	24	=	.40	44	=	.74
05	=	.08	25	=	.41	45	=	.75
06	=	.10	26	=	.43	46	=	.77
07	=	.12	27	=	.45	47	=	.79
08	=	.13	28	=	.47	48	=	.80
09	=	.15	29	=	.48	49	=	.82
10	=	.16	30	=	.50	50	=	.83
11	=	.18	31	=	.52	51	=	.84
12	=	.20	32	=	.53	52	=	.86
13	=	.21	33	=	.55	53	=	.88
14	=	.23	34	=	.57	54	=	.80
15	=	.25	35	=	.58	55	=	.91
16	=	.26	36	=	.60	56	=	.93
17	=	.28	37	=	.61	57	=	.95
18	=	.29	38	=	.63	58	=	.96
19	=	.31	39	=	.65	59	=	.98
20	=	.33	40	=	.67	60	=	1.00

ENTRIES ON RAOB CALIBRATION FORM

Block	Line	
One	One	The station identifier OUN is Norman.
	Two	The latitude is 35.24 to the nearest hundredth.
	Three	The longitude is 97.47 to the nearest hundredth.
	Four	The height of the barometer is 362 meters.
	Five	The height of the antenna is 363 meters.
	Six	The date is May 20, 1974.
	Seven	The time of release is 1900 CST.
	Eight	The surface wind direction is 20 degrees.
	Nine	The surface wind speed is 2 meters per second.
	Ten	Radiosonde serial number 02643 (last 5 No. only).
	Eleven	Ascension number is 49.
	Twelve	Leave as is, no entries.
Two	One	Enter baseline temperature, 23.8 degrees C.
	Two	Enter baseline temperature ordinate from recorder record, 70.9 ordinates.
	Three	50.0, is constant.
	Four	After setting humidity evaluator on baseline information, enter ordinate value at 50% relative humidity and +40 degrees C. to the nearest tenth of an ordinate, 75.1 ordinates.
	Five	Distance from release point to GMD to the nearest meter, 55 meters.
	Six	Surface temperature at release to the nearest 0.1 degree C. from psychrometer reading, 24.8 degrees C.
	Seven	1 is constant.
	Eight	Elapsed time of sounding at termination as taken from recorder record to nearest hundredth minute, 19.62 minutes.

Block	Line	
	Nine	Elapsed time of sounding at termination to nearest hundredth minute (see conversion table) as taken from stop watch 20.12 minutes.
	Ten	Commutator bar correction, to the nearest tenth of a contact is 0.1.
	Eleven	Surface pressure, from barometer to nearest tenth of a millibar, at release, 971.4 mb.
Three	One	Baseline temperature ordinate is 70.9.
	Two	Baseline temperature was 23.8 degrees C.
	Three	Baseline relative humidity ordinate is 80.8.
	Four	Baseline relative humidity is 31%.
	Five	Outside check temperature ordinate is 71.4.
	Six	Outside check temperature converted from ordinate value is 24.8 degrees C.
	Seven	Outside temperature from psychrometer at time of check is 24.8 degrees C.
	Eight	Outside check relative humidity ordinate is 63.0.
	Nine	Outside check relative humidity converted from ordinate value is 63%.
	Ten	Outside relative humidity determined from psychrometer reading is 67%.
	Eleven	Missing data beginning at 841 millibars.
	Twelve	Missing data ending at 805 millibars.
	Thirteen Fourteen	Blocks 13 and 14 are used for beginning and ending of additional missing data if encountered.
	Fifteen	Precipitation is occurring at station at time of release (if no precipitation enter 0).
	Sixteen	Unusual ascent rate occurred at some point during sounding (if no unusual ascent rate occurred enter 0).

Block	Line	
Four	One	Contact setting was 7.4.
	Two	Commutator bar came in on 7.5 contacts.
	Three	Commutator bar correction is -0.1.
	Four	Radiosonde Serial Number is 02643 (last five only).
	Five	The top of the first contact after release is 8.0.

INDEX 1975 RAWINSONDE DATA

DATE	TIK	FSI
050275	1305	
051375	1257	
	1458	
051975	1400	
	1600	
	1832	
052075	1402	
52075	1402	
052275	1329	
	1534	
	1630	
052375	1357	
052475	1128	1219
	1329	
052675		1240
052875	1358	
052975	1328	
060275	1545	
060575	1426	
060675	1300	
	1455	
060975	1359	
061375	1300	
	1455	

INDEX OF ALL RAWINSONDE STATIONS

ANA	ANADARKO			1968								
APA	APACHE			1968								
BLA	BLANCHARD				1969	1970						
CDS	CHILDRESS	1966										
CHK	CHICKASHA	1966	1967	1968	1969	1970					1974	
CDR	CORDELL	1966	1967									
DIB	DIBBLE			1968								
EDM	EDMOND					1970	1971					
ELR	EL RENO				1969	1970					1974	
EXP	EXPRESSWAY				1969							
FSI	FORT SILL (1)	1966	1967	1968				1972	1973	1974		
FTC	FORT COBB									1974		
HIN	HINTON			1968								
LNS	LINDSAY									1974		
LTS	ALTUS	1966	1967									
MAP	MUSTANG AIRPORT						1971					
MIN	MINCO			1968	1969	1970						
MUS	MUSTANG				1969							
NEW	NEWCASTLE			1968								
NOB	NOBLE					1970						
NRO	NORMAN				1969		1971	1972	1973			
OKC	OKLAHOMA CITY	1966	1967									
OUN	NORMAN									1974		
PMT	PIEDMONT				1969	1970						
PVY	PAULS VALLEY	1966	1967									
RIN	RINGLING	1966	1967									
RSP	RUSH SPRINGS			1968								
SPS	WICHITA FALLS	1966	1967									
SIL	FORT SILL (2)			1968								1975
TAB	TINKER					1970						
TIK	TINKER	1966	1967					1972	1973			1975
TVT	WKY TOWER (2)			1968								
WAT	WATONGA	1966	1967									
WHT	WHEATLAND					1970						
WKY	WKY TOWER (1)			1968						1974		

ORIGIN NRO (WSR/57) LAT 35. 14. 17. LONG 97. 27. 43.

	LAT			LONG			R(KM)	AZ TO	AZ FRM
WHF (NRO DOP)	35.	14.	11.	97.	27.	47.	0.211	208.57	28.57
CMF (CIM DOP)	35.	28.	31.	97.	48.	47.	41.349	309.74	129.54
TWR (WKY TOWER)	35.	34.	6.	97.	29.	20.	36.808	356.20	176.19
OUN (NSSL WBRT)	35.	14.	24.	97.	27.	34.	0.314	46.40	226.40
KOCO-TV	35.	33.	44.	97.	29.	23.	36.135	356.01	176.00
KWTV	35.	32.	58.	97.	29.	50.	34.773	354.73	174.71
WKYA	35.	33.	50.	97.	30.	28.	36.470	353.47	173.45
WKYB	35.	33.	43.	97.	30.	30.	36.261	353.35	173.33
WKYC	35.	33.	41.	97.	30.	25.	36.185	353.54	173.51
WKYD	35.	33.	43.	97.	30.	24.	36.244	353.59	173.57

ORIGIN WHF (NRO DOP) LAT 35. 14. 11. LONG 97. 27. 47.

	LAT			LONG			R(KM)	AZ TO	AZ FRM
CMF (CIM DOP)	35.	28.	31.	97.	48.	47.	41.391	310.03	129.82
NRO (WSR/57)	35.	14.	17.	97.	27.	43.	0.211	28.57	208.57
TWR (WKY TOWER)	35.	34.	6.	97.	29.	20.	36.986	356.38	176.36
OUN (NSSL WBRT)	35.	14.	24.	97.	27.	34.	0.518	39.24	219.24
KOCO-TV	35.	33.	44.	97.	29.	23.	36.313	356.19	176.18
KWTV	35.	32.	58.	97.	29.	50.	34.949	354.93	174.91
WKYA	35.	33.	50.	97.	30.	28.	36.643	353.66	173.64
WKYB	35.	33.	43.	97.	30.	30.	36.433	353.55	173.52
WKYC	35.	33.	41.	97.	30.	25.	36.358	353.73	173.71
WKYD	35.	33.	43.	97.	30.	24.	36.417	353.78	173.76

ORIGIN CMF (CIM DOP) LAT 35. 28. 31. LONG 97. 48. 47.

	LAT			LONG			R(KM)	AZ TO	AZ FRM
WHF (NRO DOP)	35.	14.	11.	97.	27.	47.	41.391	129.82	310.03
NRO (WSR/57)	35.	14.	17.	97.	27.	43.	41.349	129.54	309.74
TWR (WKY TOWER)	35.	34.	6.	97.	29.	20.	31.111	70.48	250.67
OUN (NSSL WBRT)	35.	14.	24.	97.	27.	34.	41.387	129.11	309.31
KOCO-TV	35.	33.	44.	97.	29.	23.	30.822	71.62	251.81
KWTV	35.	32.	58.	97.	29.	50.	29.753	73.62	254.00
WKYA	35.	33.	50.	97.	30.	28.	29.334	70.28	250.46
WKYB	35.	33.	43.	97.	30.	30.	29.215	70.65	250.83
WKYC	35.	33.	41.	97.	30.	25.	29.314	70.85	251.02
WKYD	35.	33.	43.	97.	30.	24.	29.357	70.75	250.93

NSSL Mesonetwork - 1975

Station	Ident.	County	Latitude	Longitude	Elevation Feet MSL*	Source Map Scale x 10^2
Amber	AMB	Grady	35°09'05"N	97°52'52"W	1240	1:240
Amber E	AME	Grady	35°10'24"N	97°46'21"W	1359	1:240
Dutton Corner	DUT	Caddo	35°12'18°N	98°05'41"W	1225	1:240
Minco A	MNA	Grady	35°15'36"N	97°59'19"W	1379	1:240
Minco B	MNB	Grady	35°16'34"N	97°55'02"W	1437	1:240
Minco C	MNC	Grady	35°13'05"N	97°55'13"W	1200	1:240
Minco D	MND	Grady	35°15'00"N	97°56'03"W	1251	1:240
Minco E	MNE	Grady	35°14'33"N	97°55'04"W	1242	1:240
Minco F	MNF	Grady	35°14'24"N	97°57'13"W	1251	1:240
Minco G	MNG	Grady	35°16'11"N	97°57'10"W	1402	1:240
Minco NE	ONE	Grady	35°19'07"N	97°53'43"W	1317	1:240
Minco SW	MSW	Grady	35°15'23"N	98°02'30"W	1412	1:240
Minco W	MNW	Grady	35°20'02"N	97°59'47"W	1402	1:240
NSSL CHK	CHK	Grady	35°06'07"N	97°57'43"W	1148	1:240
Pocasset SW	PSW	Grady	35°10'27"N	98°00'44"W	1219	1:240
Tuttle	TUT	Grady	35°17'32"N	97°49'45"W	1298	1:240
Tuttle S	TTS	Grady	35°13'38"N	97°51'12"W	1273	1:240

*Add four (4) feet to get the elevations of the instrument shelter.

NSSL SUBSYNOPTIC NETWORK - 1975

Station	Ident.	County	Latitude	Longitude	Elevation Feet MSL*	Source Map Scale x 10^2
Ada	ADA	Pontotoc	34°48'14"N	96°40'28"W	1008	1:240
Alva	AVK	Woods	36°46'37"N	98°40'02"W	1470	1:240
Cheyenne	CHE	Roger Mills	35°36'33"N	99°42'01"W	2035	1:625
Choctaw	CHO	Oklahoma	35°29'54"N	97°16'04"W	1160	1:240
Clinton Sherman	CSM	Washita	35°21'23"N	99°11'53"W	1919	1:625
Durant	DUR	Bryan	33°56'39"N	96°23'51"W	690	1:625
Edmond	EDM	Oklahoma	35°39'16"N	97°28'38"W	1200	1:240
El Reno	ELR	Canadian	35°31'09"N	97°58'27"W	1392	1:240
Ft. Cobb	FTC	Caddo	35°08'53"N	98°28'01"W	1379	1:625
Lindsay	LNS	Garvin	34°47'08"N	97°36'33"W	1135	1:240
NSSL (50' TWR)	MWF	Cleveland	35°14'13"N	97°27'43"W	1175	1:240
Perkins	SWS	Payne	35°59'57"N	97°02'39"W	965	1:625
Seiling	SEL	Dewey	36°06'04"N	98°55'27"W	1925	1:250
Shamrock	SHM	Wheeler	35°14'24"N	100°11'30"W	2369	1:100
Watonga	WAT	Blaine	35°51'35"N	98°25'09"W	1534	1:240
NSSL's Radar, Rawinsonde, and Tower Facilities						
NSSL (Radar)	NRO	Cleveland	35°14'17"N	97°27'43"W	1175	1:240
NSSL (Doppler)	WHF	Cleveland	35°14'11"N	97°27'47"W	1172	1:240
WKY Tower	TWR	Oklahoma	35°34'06"N	97°29'20"W	1148	1:240
Cimarron Field	CMF	Canadian	35°28'33"N	97°48'47"W	1310	1:240
NSSL (WBRT)	OUN	Cleveland	35°14'24"N	97°27'34"W	1183	1:240

*Add four (4) feet to get the elevations of the instrument shelter.

APRIL 1975 ARCHIVED RADAR

NUMBER OF ZERO DEGREE TILT SECTORS COLLECTED

DATE \ HOUR	00	01	02	03	04	05	06	07	08	09	10	11	12	13	14	15	16	17	18	19	20	21	22	23
1																								
2																								
3																								
4																								
5																								
6																								
7																	94	186	169	144	9			
8																								
9																								
10																								
11																								
12																								
13																								
14																								
15																								
16																								
17																		5	12	25	12	12	1	
18																								
19																								
20																								
21																								
22															8	12	12	12	12	12	12	12	12	12
23	12	12	12	12	12	12										6	11		8	12	12	12	12	12
24	12	12	12	12	12	12	3											19/	24/	10/	12	12	12	12
25	12	12	12	12	12	8																		
26																								
27													5	12	12	28	86	98	71/	44	12	12	12	12
28	12	12	12	12	12	12	5																	
29																			143	115				
30																								

/ -TILT DATA COLLECTED

MAY 1975 ARCHIVED RADAR

NUMBER OF ZERO DEGREE TILT SECTORS COLLECTED

DATE \ HOUR	00	01	02	03	04	05	06	07	08	09	10	11	12	13	14	15	16	17	18	19	20	21	22	23
1																								
2																								
3																								
4																								
5																								
6												49	178	31										
7																								
8																								
9											9	12	9		11	12	12	12	12	14/	6			
10								11	10/	8 /	12	12	12						5	10				
11									0 /	11/	12	7			4 /	10/								
12						7	12	14/	6	9 /	20/	12/	1											
13						9 /	13/	48/	18/	15/	6		11/	29/	17/	13/	4 /	8 /	13/	14/	10/			
14																								
15																								
16																								
17																								
18																								
19											12	12	14/	27/	13/	53/	18/	14/	15/	12/	3			
20						9	12	3								12								
21																	4	12	60/	3 /				
22											2	15/	18/	17/	17/	17/	48/	51/	115					
23						7	12	11	12	17/	11/	12	10	4	12	12								
24								4	12	12	11	12/	24/	12	12	22/	10/							
25																								
26								4	14/	11/	14/	8 /	4 /	0 /	15/	32/	28/	28/	15/	12/				
27						7	11/	12	12	12	1													
28						1	12	12	73	47	12	12	5	12	12	12								
29							11	165	180	167	54	12	8	7	19/	29/	28/	12	12	120	152	138	7	
30																								
31																								

/ -TILT DATA COLLECTED

JUNE 1975 ARCHIVED RADAR

NUMBER OF ZERO DEGREE TILT SECTORS COLLECTED

DATE \ HOUR	00	01	02	03	04	05	06	07	08	09	10	11	12	13	14	15	16	17	18	19	20	21	22	23
1																								
2																								
3																								
4																	3	12	12	19/	27/	21/		
5						5	12	8						9 /	14/	16/	18/	18/	24/	25/	3 /			
6															5	11					16/	20/	17/	14/
7																								
8													12/	17/	12	12	12	23/	25/	21/	24/	4 /		
9						4	9	3	15/	12	8			5	29/	29/	26/							
10						10	12	12	12	12	12	12	12	53	12	12	3							
11						7	12	12	11	12	12	12	11							1		0 /	0 /	
12																								
13											12	12	15/	16/	25/	30/	16/	20/	39/	38/	40/	13/		
14									71	104	1	12	6	6	6	6	1		11/	5 /				
15																								
16															4	12	12	12	12	13	12	6		
17																								
18																								
19																								
20																								
21																								
22																								
23																								
24																								
25																								
26																								
27																								
28																								
29																								
30																								

/ -TILT DATA COLLECTED

MAY 1975 DOPPLER (RAW DATA)

TOTAL MINUTES OF DIGITAL DATA

N-NORMAN C-CIMARRON H-HIGH PRF

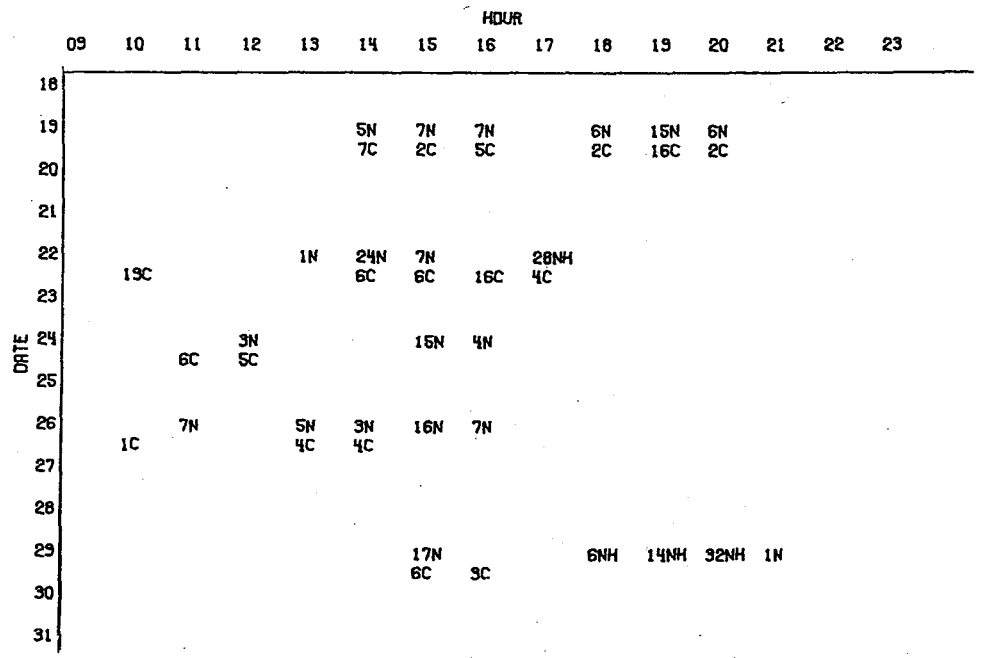

JUNE 1975 DOPPLER (RAW DATA)

TOTAL MINUTES OF DIGITAL DATA

N-NORMAN C-CIMARRON H-HIGH PRF

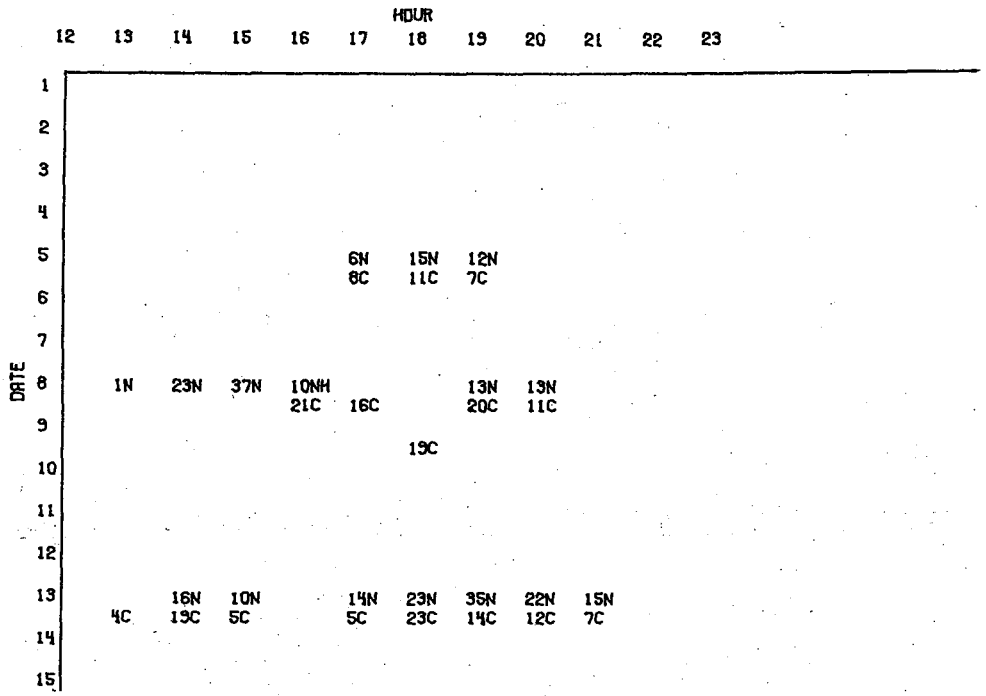

APRIL 1975 WKY TOWER

NUMBER OF OBSERVATIONS PER HOUR

DATE \ HOUR	00	01	02	03	04	05	06	07	08	09	10	11	12	13	14	15	16	17	18	19	20	21	22	23
1																								
2																								
3																								
4																								
5																								
6																								
7																273	362	360	360	360	360	360	361	361
8	361	360	361	360	360	361	361	343	360	360	360	360	360	360	360	362	360	360	360	361	361	363	359	360
9	361	360	360	360	360	360	360	328	360	360	360	360	360	361	360	360	360	360	360	360	361	360	360	360
10	359	361	360	361	362	360	360	345	359	361	362	361	360	361	359	361	361	361	361	363	361	361	360	361
11	360	361	361	359	360	361	361	361	345	360	361	361	359	361	360	360	361	360	360	361	359	360	360	361
12	359	359	361	360	360	360	360	334	360	362	359	362	360	360	360	361	361	360	360	359	361	361	361	360
13	360	360	361	361	360	360	361	345	360	360	360	360	360	360	361	360	361	360	361	361	361	360	360	361
14	360	360	360	360	360	360	361	337	361	360	360	360	361	361	360	360	360	361	360	360	360	361	360	360
15	361	361	360	360	360	359	361	359	345	361	360	361	360	360	360	360	360	361	361	360	360	360	360	360
16	360	360	360	360	360	361	360	346	361	360	361	360	360	360	361	361	361	361	360	360	360	360	360	361
17	360	360	360	360	360	360	361	337	362	360	360	360	361	360	361	360	360	360	360	360	360	360	360	360
18	360	360	360	361	360	361	360	344	360	361	362	361	360	242	124	361	360	363	360	360	360	360	361	360
19	360	361	361	360	360	360	361	337	360	360	361	360	360	360	360	362	362	360	360	361	360	361	360	360
20	360	360	360	360	361	360	233	185	360	360	361	360	361	360	360	362	360	360	360	361	360	360	361	361
21	360	361	360	362	361	360	361	344	360	361	360	360	360	360	360	360	360	360	360	360	360	361	360	360
22	361	360	363	360	360	360	183	298	360	360	360	361	360	361	361	360	360	360	360	361	360	360	361	360
23	360	360	360	360	361	360	360	341	362	360	360	360	360	360	360	361	359	360	360	360	361	361	360	360
24	361	360	359	361	360	360	361	342	360	360	360	360	360	360	360	360	360	361	360	362	360	361	360	360
25	360	361	360	360	360	361	360	362	343	362	361	360	361	360	360	361	360	361	361	359	359	360	360	360
26	360	360	360	361	360	360	360	337	360	360	360	360	360	361	359	361	360	360	360	359	360	360	360	360
27	360	359	361	361	360	361	359	345	360	360	360	360	360	360	360	359	360	360	360	360	362	360	361	361
28	361	360	360	360	361	360	360	360	335	360	360	361	360	360	361	359	361	360	360	360	360	360	361	361
29	360	361	360	360	360	361	361	344	361	360	361	360	360	361	360	360	360	360	360	360	360	360	361	361
30	360	360	361	360	360	360	361	361	360	360	343	360	360	361	360	360	360	361	360	360	360	360	360	360

MAY 1975 WKY TOWER

NUMBER OF OBSERVATIONS PER HOUR

DATE \ HOUR	00	01	02	03	04	05	06	07	08	09	10	11	12	13	14	15	16	17	18	19	20	21	22	23
1	360	360	360	360	361	360	360	360	360	349	360	360	360	361	361	360	360	360	236	94	110	79	6	96
2	188	202	280	78				287	360	259	360	360	110											
3																								
4																								
5																186	360	361	361	360	360	361	360	360
6	360	360	360	360	360	360	360	334	360	360	361	360	360	361	361	360	360	360	361	360	360	360	361	360
7	360	360	361	360	359	361	360	340	360	360	361	360	361	360	360	360	360	361	359	360	361	361	359	361
8	360	360	359	360	361	361	360	342	360	363	360	360	360	360	360	360	360	360	360	360	360	362	360	360
9	361	359	361	360	360	360	360	360	360	360	360	360	321	294	360	360	360	361	360	359	360	359	361	360
10	360	360	360	361	360	360	359	343	360	359	360	360	360	361	360	360	361	360	360	360	361	360	360	360
11	360	360	360	345						309	359	362	359	361	359	361	360	360	359	360	360	361	360	360
12	360	360	360	361	360	361	359	359	325	360	360	360	360	360	360	360	361	360	359	360	360	360	360	360
13	359	360	360	358	361	360	360	337	355	360	360	360	271	360	360	331	267	360	360	359	359	361	360	360
14	359	360	360	361	361	360	360	337	360	108														
15								153	360	360	360	360	360	360	360	360	360	360	360	360	360	360	360	360
16	360	360	360	360	360	360	360	360	345	360	359	360	359	361	360	360	360	360	360	360	360	360	360	360
17	360	360	360	360	360	361	360	342	360	360	360	360	360	360	361	360	360	360	360	360	360	360	360	360
18	360	360	360	360	360	360	361	360	360	360	340	360	360	360	360	360	360	360	360	360	360	360	360	360
19	360	360	360	360	360	361	360	344	361	360	360	359	358	360	360	360	361	360	360	360	360	360	360	360
20	360	360	360	361	360	361	360	338	360	360	360	360	360	360	360	360	360	361	362	358	361	360	360	360
21	360	360	360	360	360	359	360	340	360	360	360	360	360	360	360	360	360	361	360	360	360	360	360	360
22	360	360	360	360	360	360	360	336	360	360	359	360	356	360	360	360	360	359	122					
23										157	359	361	360	360	360	359	359	360	361	359	359	360	360	360
24	360	360	360	360	360	360	360	329	360	360	359	359	360	359	359	360	361	360	360	360	360	360	360	360
25	360	360	360	360	360	360	360	360	360	360	344	360	360	360	360	360	360	360	360	360	360	360	360	360
26	360	360	360	360	360	360	360	339	364	361	361	362	360	363	361	360	360	360	360	361	360	361	360	360
27	360	360	361	360	360	361	360	361	345	361	360	360	361	361	361	360	360	360	360	360	360	362	360	360
28	360	363	360	360	364	360	360	341	1184	1121	360	362	360	360	362	360	360	360	361	361	360	360	360	360
29	360	360	361	360	361	361	361	360	239	360	360	361	360	360	361	360	360	360	360	360	360	360	361	360
30	360	360	360	360	360	360	360	341	360	360	361	360	360	360	360	360	360	363	361	360	360	360	360	360
31	360	360	360	360	361	360	359	339	361	360	360	360	360	360	360	360	360	360	360	360	360	360	360	360

JUNE 1975 WKY TOWER

NUMBER OF OBSERVATIONS PER HOUR

DATE \ HOUR	00	01	02	03	04	05	06	07	08	09	10	11	12	13	14	15	16	17	18	19	20	21	22	23
1	360	360	360	363	360	363	360	367	361	363	341	362	360	364	362	361	363	360	363	361	365	361	364	365
2	362	361	362	361	361	361	362	342	361	360	360	360	360	360	360	360	360	360	360	360	360	361	363	360
3	361	361	362	360	361	360	362	344	360	360	360	360	360	360	360	360	360	360	360	360	360	360	360	359
4	360	359	360	360	345	360	360	341	360	360	360	360	360	360	360	359	360	360	360	360	360	360	359	359
5	360	359	360	359	360	360	360	360	345	360	360	360	360	359	360	360	360	360	360	360	360	360	360	360
6	360	360	360	360	359	360	360	360	343	360	360	360	360	359	359	360	360	360	360	359	360	358	88	
7									199	361	360	359	360	359	360	360	360	360	360	360	360	360	359	360
8	361	360	360	360	360	360	360	360	359	359	360	359	360	359	360	360	360	360	360	360	360	361	360	360
9	360	360	360	360	360	360	360	332	360	360	359	360	360	361	360	360	360	360	360	360	360	360	360	360
10	360	360	360	360	360	360	360	342	360	360	360	360	360	360	360	360	360	361	360	360	360	360	360	360
11	360	360	360	360	360	360	360	360	360	360	335	359	361	368	364	367	360	362	363	361	363	362	361	362
12	361	365	361	361	361	360	360	361	362	360	361	362	361	361	361	361	361	363	360	360	364	361	361	360
13	362	360	360	362	363	353	361	213	61	61	11				352	360	361	360	360	316	319	360	362	360
14	364	361	363	361	360	361	360	331	360	361	363	361	360	361	361	361	360	360	360	360	360	360	363	360
15	360	362	361	360	360	360	360	363	361	361	360	361	360	362	360	360	360	360	361	162				
16								47	63	64	61	63	62	65	61	61	61	65	62	61	62	45		
17																								
18																								
19																								
20																								
21																								
22																								
23																								
24																								
25																								
26																								
27															54	61	60	60	62	62	60	60	60	61
28	60	62	63	61	61	61	62	62	64	62	62	60	60	60	61	60	61	61	62	61	61	61	62	61
29	61	63	65	61	61	61	64	61	62	64	62	62	61	62	61	62	63	62	60	61	63	62	64	61
30	64	61	62	61	62	61	62	38								40	62	65	63	61	62	66	61	61

REFERENCES

Barnes, Stanley L., et al., 1974a: Papers on Oklahoma thunderstorms, April 29-30, 1970. NOAA Tech. Memo. ERL NSSL-69, 233 pp.

Barnes, Stanley L., 1974b: Summary of the 1974 severe thunderstorm observation season and operations. NSSL In-house Report, 144 pp.

Brown, Rodger A., Donald W. Burgess, and Kenneth C. Crawford, 1973: Twin tornado cyclones within a severe thunderstorm: single Doppler radar observations. Weatherwise, 26, No. 2, 63-69,71.

Burgess, D. W., L. D. Hennington, R. J. Doviak, and P. S. Ray, 1976: Multimoment Doppler display for severe storm identification. In press, J. Appl. Meteor.

Goff, R. Craig, 1975: Thunderstorm-outflow kinematics and dynamics. NOAA Tech. Memo. ERL NSSL-75, 63 pp.

Lemon, Leslie R., 1976: The flanking line, a severe thunderstorm intensification source. J. Amos. Sci., 33, 4, 686-694.

Martner, Brooks E., 1975: The University of Wyoming's participation in NSSL project storm intercept, 1975 (data analysis). Final Report, NOAA Contract #03-5-022-6, 14 pp.

NOAA, Environmental Data Service, 1975: Storm Data, 17, 6, Asheville, N.C., p. 21.

Vlcek, Charles L., 1973: Observations of severe storms on 26 and 28 April 1971. NOAA Tech. Memo. ERL NSSL-63, 19 pp.

OBJECTIVES AND ACCOMPLISHMENTS OF THE NSSL 1975 SPRING PROGRAM

PART II

RADAR QUALITY CONTROL PROGRAM

D. Sirmans, J. Dooley, J. Carter, and W. Bumgarner

National Severe Storms Laboratory
Norman, Oklahoma
July 1976

TABLE OF CONTENTS

		Page
INTRODUCTION		1
SECTION 1	Digital Integrator Calibration - General Considerations in Quality Control Testing	15
SECTION 2	ADC Quantization - General Considerations In Quality Control Testing	19
SECTION 3	Note on Norman Doppler Image Gates	25
SECTION 4	Note on Spectrum Background Noise Level	26
SECTION 5a	Range Calibration of Cimarron-Norman Digital Integrator Data Records	31
SECTION 5b	Range Timing Check for Norman Doppler	35
SECTION 6	Sun Flux Measurement Comparison	40
SECTION 7	Standard Deviation of Estimates	43
REFERENCES		46

INTRODUCTION

The accuracy of NSSL's weather radar data can be estimated generally by comparison with raingages (Wilson, 1970; Brandes, 1974), or by comparison among radars. However, it is obviously important to routinely examine the various receiver and signal processing components using calibrated test signals and document the performance of each radar system.

The following sections of this report describe results of calibration procedures developed and tested in 1975 for the NSSL Doppler radars. These techniques are part of the daily routine in preparing for severe storm surveillance. The material is provided as an aid to users in selection of data sets and in evaluation of meteorological inferences. It is intended as a tabulation of descriptive parameters, subjective evaluations and listing of known problems associated with the data listed in the Data Summary Log. It is not intended as a comprehensive discussion of parameters or techniques. For details, the reader is referred to one or more of the supplemental attachments or references.

Table 1 lists radar system characteristics utilized during the Spring Program and supercedes the preliminary table dated March 14, 1975. Note that some radar system characteristics are subject to variation and must be determined from the daily logs.

Tables 2 and 3 are tabulations of parameters pertaining to radar intensity calibration. Quantities listed in Table 3a are derived from the receiver calibrations made before and after data acquisition.

Table 4 tabulates noise introduced by the complex video digital quantization process based on measured ADC performance. The scheme used in this measurement is given in Section 2 (ADC Quantization - General Considerations in Quality Control Testing).

Spectrum image suppression level is tabulated by data set in Table 5. Values given for the Norman radar do not include the systematic high image at certain gates prior to May 27, 1975. This is discussed in Section 3 (Note on Norman Doppler Image Gates).

The noise level in the frequency domain, spectrum background level, is tabulated in Table 6. This quantity was estimated from scattergram values taken from spectra plots. Interpretation of this quantity is discussed in Section 4 (Note on Spectrum Background Noise Level).

Results of sun-scan orientation checks are given in Table 7.

A list of known data problems is in Table 8. This is not all inclusive, of course, since problems of a more subtle nature will probably be found during data analysis.

An example of a ranging check is given in Section 5 for both the Norman (NRO) and Cimarron (CIM) radars. An estimate of ranging uncertainty is also given in this discussion.

Section 6 contains the results of received power calibration check by sun flux density for both the Norman and Cimarron systems.

The measured standard deviation of intensity and velocity estimates are compared with theoretical values in Section 7.

TABLE 1a.

NSSL Doppler Radar Characteristics
June 25, 1975

Parameter	Cimarron (CIM)	Norman (NRO)	Hi PRF (NRO)
Antenna			
Shape	Parabolic	Parabolic	Parabolic
Diameter	9.15 m	9.15 m	9.15 m
Half-power Beam Width	0.80 deg	0.81 deg	0.81 deg
Gain	46 dB	46.8 dB	46.8 dB
First Side Lobe Level	21 dB	21 dB	21 dB
Polarization	Horizontal	Vertical	Vertical
RMS Surface Deviation	2.5 mm	2.8 mm	2.8 mm
Transmitter			
Wavelength	10.97 cm	10.52 cm	10.52 cm
Frequency	2735 MHz	2850 MHz	2850 MHz
Pulse Repetition Time	768 μsec	768 μsec	288 μs
Pulse Width	1 μsec (150 m)	1 μsec (150 m)	0.35 μs (52 m)
Peak Power*	500 kw	700 kw	200 kw
Receiver			
System Noise Figure	4.1 dB	3.3 dB	5 dB**
Transfer Function	Doppler-linear Intensity-logarithmic	Doppler-linear Intensity-logarithmic	Doppler-linear Intensity-logarithmic
Dynamic Range	70 dB	70 dB	70 dB
Bandwidth (6 dB)	4.52 MHz	2.88 MHz	0.81 MHz***
Intermediate Frequency	30 MHz	30 MHz	30 MHz
Min. Detectable Signal (SNR=0 dB)*	-103 dBm	-106 dBm	-105 dBm
Doppler Time Series Data Acquisition			
No. of Simultaneous Range Gates	16	16	6
No. of 16-Gate Blocks Along Radial	Unlimited	8	8
Range Gate Spacing	300, 350...1200, 1350m	150, 300, 600, 1200m	150, 300, 600, 1200m
Azimuthal Sample Spacing	0.1 to 9.9 deg	0.1 to 9.9 deg	0.1 to 9.9 deg
Automatic Elevation Increment	0.5 to 9.9 deg	0.1 to 9.9 deg	0.1 to 9.9 deg
Number of Samples in Time Series†	2^n n=1, 2...13	2^n n=1, 2...13	2^n n=1, 2...13
Complex Video Digital Word Length	10 bits (binary)	12 bits (binary)	12 bits (binary)
Intensity Data Acquisition			
No. of Range Gates	762	762	192
Range Gate Spacing	150 m	150 m	225 m
Number of Samples in Estimate††	2^n-1 n=4...11	2^n-1 n=4...11	2^n-1 n=4...11
Time Window Function††	Linear or exponential	Linear or exponential	Linear or exponential
Intensity Estimate Word Length (Recorded)	6 bits (binary)	6 bits (binary)	6 bits (binary)
General Features			
Azimuthal Antenna Rotation Rate	0.1 to 24.0 deg sec^{-1}	0.1 to 10 deg sec^{-1}	0.1 to 10 deg sec^{-1}
Maximum Unambiguous Range	115 km	115 km	43 km
Maximum Unambiguous Velocity	$\pm$ 35.6 m sec^{-1}	$\pm$ 34.2 m sec^{-1}	$\pm$ 91 m sec^{-1}
PPI Capability	Yes	Yes	Yes
RHI Capability	Yes	Yes	Yes
Coplane Capability	No	No	No

* Representative value: see Table 2 or daily log for particular data set.

** 8 dB before May 22, 1975

*** 2.03 MHz before May 22, 1975

† Most data taken with N=64 for normal PRF and N=128 for Hi PRF.

†† Practically all data taken with Ns=127 and exponential time window.

TABLE 1b.

Calibration and Timing Parameters
June 25, 1975

Parameter	Cimarron (CIM)	Norman (NRO)	Hi PRF (NRO)
Radome Loss (two way)	2.0 dB	2.0 dB	2.0 dB
Coupler Loss	36.5 dB	36.2 dB	36.2 dB
Cable Loss	6.7 dB	9.5 dB	9.5 dB
Waveguide Loss (two way)	3.6 dB	2.0 dB	2.0 dB
Receiver Detection Loss	0.43 dB	.69 dB	6.81 dB*
Delay to Tx Pulse	4.4 μs	4.0 μs	4.4 μs
Doppler Sample-Hold Aperture	0.07 μs	0.4 μs	0.4 μs
Integrator Start Delay	4.2 μs	3.7 μs	4.0 μs
Integrator Spacing	1.0 μs	1.0 μs	1.5 μs
Receiver Rise Time	.22 μs	.35 μs	1.67 μs†
Receiver Initial Delay	0.1 μs	0.1 μs	0.1 μs
Plumbing Delay	0.33 μs	0.1 μs	0.1 μs

* Loss was 3.31 dB prior to May 22, 1975.

† .37 μs before May 22, 1975.

TABLE 2

RADAR PEAK POWER MEASUREMENTS

Date	Cimarron (CIM)	Norman (NRO) "A"	Norman (NRO) "B" (Hi PRF)
5-13-75	*	683 kw	217 kw
5-19-75		470 kw	216 kw
5-22-75		450 kw	220 kw
5-24-75		730 kw	
5-26-75		730 kw	
5-28-75		730 kw	
5-29-75		730 kw	
6-02-75		718 kw	195 kw
6-04-75		718 kw	
6-05-75		706 kw	
6-06-75		706 kw	
6-08-75		730 kw	220 kw
6-11-75		740 kw	
6-13-75		706 kw	

* Maintained 500 kw during periods of data collection.

TABLE 3a

Logarithmic Receiver Noise Level and Logging Constant

Date	Norman (NRO)		Cimarron (CIM)	
5-19-75	-107.3 dBm	0.62 AGC/dB		
5-22-75	-103.0 dBm	0.64 AGC/dB	-100.7 dBm	0.76 AGC/dB
5-24-75	-107.4 dBm	0.62 AGC/dB	- 97.3 dBm	0.86 AGC/dB
5-26-75	-105.2 dBm	0.62 AGC/dB	-103.3 dBm	0.78 AGC/dB
5-29-75	-102.3 dBm	0.62 AGC/dB	-101.0 dBm	0.76 AGC/dB
6-05-75	-105.0 dBm	0.64 AGC/dB	- 98.0 dBm	0.83 AGC/dB
6-08-75	-102.1 dBm	0.65 AGC/dB	-102.6 dBm	0.88 AGC/dB
6-09-75			- 98.2 dBm	0.80 AGC/dB
6-13-75	-106.7 dBm	0.71 AGC/dB	-100.9 dBm	0.82 AGC/dB

TABLE 3b

Magnitude of Intensity Calibration Drift

Date	Norman (NRO)	Cimarron (CIM)
5-19-75	<0.3 dB	Malfunction
5-22-75	<1.0 dB	1 to 5 dB
5-24-75	<0.1 dB	Unknown
5-26-75	<0.5 dB	0 to 3 dB
5-29-75	<0.8 dB	1 to 5 dB
6-05-75	2 to 4 dB	Unknown
6-08-75	3 to 4 dB	3 to 5 dB
6-09-75	—— · ——	Unknown
6-13-75	<0.5 dB	0.5 dB

TABLE 4

Signal to ADC Quantization Noise Ratio

Date	Norman (NRO)	Cimarron (CIM)
5-19-75	>45 dB	>35 dB
5-22-75	>45 dB	>35 dB
5-24-75	>45 dB	>35 dB
5-26-75	>45 dB	>35 dB
5-29-75	>45 dB	>40 dB
6-05-75	>45 dB	>35 dB
6-08-75	>45 dB	>40 dB
6-09-75	——·——	>40 dB
6-13-75	>45 dB	>35 dB

TABLE 5

Spectrum Image Suppression*

Date	Norman (NRO)	Cimarron (CIM)
5-19-75	>20 dB	
5-22-75	>20 dB	~10 dB
5-24-75	>15 dB	~15 dB
5-26-75	>20 dB	~15 dB
5-29-75	>15 dB	~15 dB
6-05-75	>15 dB	>15 dB
6-08-75	>15 dB	~15 dB
6-09-75	——·——	
6-13-75	>15 dB	>15 dB

*This does not include the systematic image at certain gates of the Norman radar (see Note on Image Gates).

TABLE 6

Spectrum Background Level (dB below Signal Mode)*

Date	Norman (NRO)	Cimarron (CIM)
5-19-75	35 dB	
5-22-75	30 dB	25 dB
5-24-75	30 dB	20 dB
5-26-75	35 dB	22.5 dB
5-29-75	27.5 dB	27.5 dB
6-05-75	30 dB	25 dB
6-08-75	35 dB	20 dB
6-09-75	——·——	20 dB
6-13-75	32.5 dB	30 dB

* The value given is an estimate at a SNR = 20 dB and serves only as a qualitative index. For a more comprehensive discussion see Note on Spectrum Background Noise Level.

TABLE 7

Antenna Orientation Checks (Sun Scans)

Site	Date	Deviation	
		Azimuth	Elevation
Norman (NRO)	8 May 1975	.07° ccw	.01° low
	3 June 1975	——·——	.16° low
	25 June 1975	0	.64° low
	16 July 1975	.30° cw	.71° low
Cimarron (CIM)	8 May 1975	.01° cw	.09° high
	25 June 1975	.16° cw	.15° high
	16 July 1975	.06° ccw	.16° high

TABLE 8

Malfunctions, Glitches, and other Pesty Things

Date	Norman (NRO)	Cimarron (CIM)
5-19-75		1. Intensity record malfunction - data recovery not feasible. Velocity data recovery possible by special processing.
5-22-75	1. Gate 8 of header intensity has intermittent 1 bit.	1. Gate 16 of header intensity has intermittent 8 bit.*
5-24-75	1. Gate 8 of header intensity has intermittent 1 bit.	1. Gate 16 of header intensity has intermittent 8 bit.* 2. Complex video clipping at SNR ≈ 30 dB.*
5-26-75	1. Gate 8 of header intensity has intermittent 1 bit. 2. Complex video clipping at SNR≈50 dB.	1. Gate 16 of header intensity has intermittent 8 bit.*
5-29-76	1. Gate 8 of header intensity has intermittent 1 bit.	1. Gate 16 of header intensity has intermittent 8 bit.*
6-05-75	1. Gate 8 of header intensity has intermittent 1 bit.	1. Intensity record malfunction. Data not recoverable. Doppler header intensity valid.* 2. Gate 16 header intensity has intermittent 8 bit.
6-08-75	1. Gate 8 of header intensity has intermittent 1 bit.	1. Complex video clipping.*
6-09-75	1. No data taken.	1. Header intensity values are shifted by one gate.*
6-13-75	1. No velocity data from 1803 CST to 1900 CST, Tapes DP7571 through DP7574, Intensity data valid.	1. Header intensity values are shifted by one gate. 2. Gate 6 of header intensity has intermittent 2 bit.

* All data sets have header intensity values shifted by one gate; location 1 is gate 2, location 2 is gate 3, etc..., location 16 is gate 1.

General Hardware Problems:

1. NRO actual antenna speed varies significantly from specified value.
2. No antenna speed parameter in CIM housekeeping.
3. CIM complex video contains intermittent noise. (See Section 4.)

1975 CIMMARON DOPPLER COLLECTION LOG

TAPE	DATE	START TIME	STOP TIME	START AZM	STOP AZM	TILT
CP7503	051975	144459	145154	179	210	04•1
CP7504	051975	154659	154928	174	179	04•1
CP7505	051975	160808	161009	179	215	05•1
CP7505	051975	161252	161538	179	220	07•1
CP7506	051975	185820	190110	209	240	10•1
CP7506	051975	190441	190745	199	240	08•1
CP7507	051975	191525	192132	189	240	09•1
CP7508	051975	192839	193409	184	240	08•1
CP7509	051975	200439	200659	158	241	06•1
CP7510	052275	145255	145901	249	300	20•1
CP7511	052275	153549	153640	221	265	11•1
CP7511	052275	154709	155114	221	265	11•1
CP7512	052275	155906	160519	221	265	12•1
CP7513	052275	160942	161414	224	270	11•1
CP7514	052275	162255	163008	239	290	16•1
CP7515	052275	173337	173824			•
CP7516	052275	101159	103108	068	074	01•0
CP7519	052475	114951	115606	049	060	02•3
CP7519	052475	120052	120123	049	060	02•5
CP7519	052475	121703	121814	114	135	02•6
CP7519	052475	122233	122630	114	135	02•5
CP7521	052675	105520	105600	119	135	02•1
CP7523	052675	135134	135513	040	070	03•5
CP7523	052675	135557	135718	037	070	01•5
CP7524	052675	140149	140629	040	070	03•5
CP7528	052975	154915	155102	244	275	03•6
CP7528	052975	155224	155403	244	275	03•1
CP7529	052975	155759	160050	249	270	03•1
CP7529	052975	160116	160226	249	270	03•1
CP7529	052975	160248	160330	249	270	02•1
CP7532	060575	173650	174059	329	345	11•3
CP7533	060575	174604	175007	329	350	12•0
CP7534	060575	180144	180521	334	355	10•0
CP7535	060575	182039	182446	334	355	12•0
CP7536	060575	184504	184914	334	000	09•0
CP7537	060575	190302	190716	334	010	07•0
CP7538	060575	192044	192411	339	015	05•0
CP7540	060875	160829	161048	294	320	04•0
CP7540	060875	161238	161441	294	320	02•0
CP7541	060875	162605	162841	295	320	03•0
CP7541	060875	162935	163250	295	320	03•4
CP7542	060875	164022	164337	295	320	03•4
CP7542	060875	164827	165124	295	320	03•5
CP7543	060875	165727	170314	310	330	09•0
CP7544	060875	171146	171743	310	330	09•0
CP7545	060875	173322	173636	314	335	09•1
CP7545	060875	173713	173953	314	335	07•0

TAPE	DATE	START TIME	STOP TIME	START AZM	STOP AZM	TILT
CP7546	060875	190555	191149	214	245	19.0
CP7547	060875	191737	192407	204	245	17.1
CP7548	060875	193329	194054	179	235	15.1
CP7549	060875	201319	201901	139	190	19.4
CP7550	060875	203008	203325	029	050	13.0
CP7550	060875	204233	204459	029	050	13.0
CP7552	061375	134723	134920	359	030	8.6
CP7552	061375	135054	135252	359	030	9.5
CP7553	061375	135952	140348	009	040	12.0
CP7553	061375	140625	140808	014	040	09.1
CP7554	061375	142553	142856	024	055	11.0
CP7554	061375	143209	143426	024	055	08.0
CP7555	061375	144105	144342	024	055	10.1
CP7555	061375	145016	145337	029	060	06.1
CP7556	061375	145844	150439	030	060	07.5
CP7557	061375	175207	175702	035	060	05.5
CP7558	061375	180319	180815	035	060	05.5
CP7559	061375	181604	181940	024	075	03.1
CP7560	061375	182641	183133	024	075	10.1
CP7561	061375	183833	184307	029	060	13.1
CP7562	061375	185022	185451	029	060	13.1
CP7563	061375	190052	190404	034	070	12.2
CP7563	061375	190617	190718	034	080	03.1
CP7564	061375	192319	192719	034	085	09.1
CP7565	061375	193604	194006	034	085	09.1
CP7566	061375	195745	200237	059	100	13.1
CP7567	061375	203949	204504	358	096	16.2
CP7567	061375	205033	205507	059	100	05.1
CP7568	061375	210447	210917	064	110	14.0
CP7569	061375	211906	212211	079	115	12.0
CP7570	060975	182719	183047	267	330	01.0
CP7570	060975	183306	184740	267	330	01.0

1975 NORMAN DOPPLER COLLECTION LOG

TAPE	DATE	START TIME	STOP TIME	START AZM	STOP AZM	TILT
DP7503	051975	144458	145018	249	280	06•1
DP7504	051975	154703	155147	229	260	05•0
DP7504	051975	155257	155447	229	260	05•1
DP7505	051975	160810	161106	239	270	08•0
DP7505	051975	161259	161640	239	280	07•0
DP7506	051975	182500	182627	239	270	06•4
DP7506	051975	184411	184641	239	270	06•4
DP7506	051975	185822	190138	239	270	08•0
DP7506	051975	190451	190729	239	270	06•0
DP7507	051975	191522	191631	229	270	02•0
DP7507	051975	191727	192131	229	270	09•0
DP7508	051975	192841	193246	229	270	09•0
DP7509	051975	200359	201020	219	270	07•0
DP7510	052275	134029	134043	254	283	01•0
DP7510	052275	140421	141226	259	280	02•5
DP7511	052275	141603	142030	259	280	02•5
DP7511	052275	142248	142625	259	280	02•5
DP7512	052275	143204	144011	259	280	02•5
DP7513	052275	154717	155359	239	280	05•0
DP7514	052275	171545	172555	189	210	08•1
DP7515	052275	173029	173813	189	210	10•0
DP7516	052275	174540	175409	189	220	12•1
DP7516	052275	175500	175636	189	220	01•1
DP7520	052475	123951	124246	049	070	02•0
DP7521	052475	151212	151435	289	310	02•0
DP7521	052475	151810	152035	289	310	02•0
DP7521	052475	152342	152621	289	310	02•0
DP7522	052475	153501	153858	299	320	02•0
DP7522	052475	154231	154628	299	320	02•0
DP7523	052475	160529	160702	169	200	08•1
DP7523	052475	160809	160942	169	200	08•1
DP7526	052675	111526	112149	109	140	01•5
DP7527	052675	135140	135636	009	050	02•8
DP7528	052675	140140	140500	009	050	04•0
DP7529	052675	153455	154413	129	160	05•1
DP7530	052675	154756	155431	129	160	06•1
DP7531	052675	160055	160733	139	170	06•6
DP7537	052975	151631	152326	259	290	01•5
DP7537	052975	152622	153039	259	290	01•5
DP7538	052975	153331	153540	259	290	01•5
DP7538	052975	153618	153948	269	300	01•5
DP7540	052975	184532	185202	280	338	09•9
DP7541	052975	190506	190846	330	019	27•8
DP7541	052975	191049	191224	330	048	13•9
DP7542	052975	195116	201745	219	300	04•9
DP7543	052975	203104	203614	049	096	05•1

TAPE	DATE	START TIME	STOP TIME	START AZM	STOP AZM	TILT
DP7544	052975	205110	210118	049	096	05.1
DP7548	060575	172707	173246	029	070	03.1
DP7549	060575	182033	182958	309	340	06.1
DP7550	060575	184502	185124	319	340	08.1
DP7551	060575	190302	190934	319	350	06.1
DP7552	060575	192047	192531	329	359	06.5
DP7555	060875	135919	140819	209	230	01.6
DP7556	060875	144512	150956	289	320	03.0
DP7557	060875	151404	153642	289	320	03.0
DP7558	060875	154221	154358	289	320	01.6
DP7558	060875	155258	155438	289	320	01.5
DP7558	060875	160711	161005	289	320	05.0
DP7559	060875	161344	162120	309	320	04.1
DP7560	060875	190702	191018	259	290	09.0
DP7560	060875	191847	192156	269	290	10.1
DP7561	060875	193441	194157	259	300	15.0
DP7562	060875	201428	202257	239	300	19.6
DP7563	060875	203115	203351	339	359	05.0
DP7563	060875	204341	204515	339	359	05.0
DP7565	061375	142420	143207	009	030	05.0
DP7566	061375	144106	144749	003	030	05.5
DP7567	061375	145856	150447	009	030	08.1
DP7568	061375	151706	152150	029	050	06.1
DP7569	061375	174155	174905	009	040	05.1
DP7570	061375	175215	175838	009	040	06.0
DP7571	061375	180321	181020	019	040	09.0
DP7572	061375	181610	182320	019	050	10.0
DP7573	061375	182653	183320	009	050	07.0
DP7574	061375	183835	184145	009	030	05.1
DP7575	061375	190105	191233	009	050	11.0
DP7576	061375	192321	193345	019	060	12.1
DP7577	061375	193556	194542	029	070	12.1
DP7578	061375	195746	200442	339	359	16.1
DP7579	061375	201232	201940	039	080	07.0
DP7580	061375	203954	204505	009	120	09.1
DP7581	061375	205330	205850	019	070	14.1
DP7582	061375	210448	210954	029	090	12.1
DP7583	061375	211900	212404	039	100	12.1
DP7584	061375	213913	214357	049	110	11.1

MAY 1975 DOPPLER (RAW DATA)

TOTAL MINUTES OF DIGITAL DATA

N-NORMAN C-CIMARRON H-HIGH PRF

DATE \ HOUR	09	10	11	12	13	14	15	16	17	18	19	20	21	22	23
18															
19						5N 7C	7N 2C	7N 5C		6N 2C	15N 16C	6N 2C			
20															
21															
22		19C			1N	24N 6C	7N 6C	16C	28NH 4C						
23															
24				3N			15N	4N							
25			6C	5C											
26		1C	7N		5N 4C	3N 4C	16N	7N							
27															
28															
29							17N 6C	9C		6NH	14NH	32NH	1N		
30															
31															

JUNE 1975 DOPPLER (RAW DATA)

TOTAL MINUTES OF DIGITAL DATA

N-NORMAN C-CIMARRON H-HIGH PRF

DATE \ HOUR	12	13	14	15	16	17	18	19	20	21	22	23
1												
2												
3												
4												
5						6N 6C	15N 11C	12N 7C				
6												
7												
8	1N	23N	37N		10NH 21C	16C		13N 20C	13N 11C			
9												
10							19C					
11												
12												
13	4C	16N 19C	10N 5C			14N 5C	23N 23C	35N 14C	22N 12C	15N 7C		
14												
15												

SECTION 1

Digital Integrator Calibration - General Considerations in Quality Control Testing

The logarithmic receiver-digital integrator calibration is given in detail in Sirmans and Barclay (1973), Sirmans and Doviak (1973), and Sirmans (1974a). What follows is a summary of the technique as well as an abbreviated discussion of statistical considerations and noise measurements (Sirmans, 1974b).

Procedure

Digital integrator calibration is a three-step procedure:

1. The boundaries of input quantization categories (i.e., the ADC classes) are measured by injecting a known signal level into the receiver.

2. An incremental integration is performed (increments are input digital categories) on the theoretical probability density of a meteorological signal having a specified mean power. The relative frequency of occurrence of digital classes thus obtained are assigned digital class weights (at the ADC ouput), and the mean of these weights is the digital output corresponding to the specified input mean power.

3. The entire receiver input power-digital integrator output transfer characteristic is then determined by "lagging" the theoretical mean input power through the dynamic range of the receiver. Thus, the calibration gives a mean input power versus the corresponding digital output. Difference between calibration (signal generator) power corresponding to given digital output and theoretical input power of a meteorological signal corresponding to this digital output is termed bias which is corrected by the calibration procedure.

This bias is a composite of the probability density effect, the receiver transformation, and the quantization by truncation. Note that in the logarithmic region of receiver response the bias is 2.5 dB plus 1/2 of the input quantization increment (Sirmans and Barclay, 1973). Bias increases near the upper extreme due to saturation and decreases near the lower extreme due to the additive noise effect.

Statistics of the Calibration

The technique contains two major sources of error (other than the human element): (1) the quantization boundary uncertainty, and (2) the signal source accuracy. We will examine the boundary uncertainty first. Normally, the "logging constant" of digital output-input power transfer is about 1.25 dB/digit, thus the quantization width (one least significant digit) is larger

than input signal increment (1 dB = .8 digit) and the S.D. of the digital boundaries is just the quantization S.D.

Since the quantization standard error

$$\sigma_B = \frac{1}{2\sqrt{3}} = .29 \text{ digits} \quad (1)$$

is small compared to the standard rms error of the input weather signal, 4.46 digits, we may assume the error of derived relative frequency of occurrence, i.e., the increment integral of theoretical probability density (over the class) is linearly related to the width of the class. Since width of the class has a variance twice that of either boundary (statistically independent boundaries)(Lee, 1964), we find the variance of the calibration estimate to be:

$$\sigma^2 = 2\sigma_B^2 = \frac{1}{6} \text{ digits}^2 = (.41)^2 \text{ digit}^2 \quad (2)$$

or a standard deviation of about 0.5 dB for the usual transfer characteristic.

Signal source will also constitute an uncertainty since no real source is purely deterministic. This uncertainty, however, is more in the form of a bias rather than a variance since the mechanism is an inability to control exact power injected into the system and is largely repeatable and consistent from run to run. Absolute accuracy of most sources is about $\pm$ 2 dB and it can be improved to 1 percent by comparing the source against a power meter at the higher input power levels (>-20 dBm). Unfortunately, the source cannot be calibrated over the entire dynamic range of the receiver due to power meter limitation. "Tracking accuracy" of the signal source used (i.e., the dB difference between true output power and power indicated by the dial) is about $\pm$ 1 dB and should be entered in the daily calibration log.

Besides providing measurement standards, the calibration listing can serve to monitor performance of the hardware. For example, the 1 dB increment should be a continuum on the digital scale, i.e., the digital output should vary in steps of about one. Calibration points should fit a smooth regression line, not necessarily straight but without abrupt changes or discontinuities. Histograms of the output variable should reflect these properties.

Logarithmic Receiver Noise Power Determination

Determination of receiver noise power is necessary for certain studies requiring a signal-to-noise ratio, total variance of the signal plus noise power estimate or specification of detectable signal level. Noise power can be measured directly although it is not done routinely for any of the NSSL radars since this quantity has no meteorological significance. Instead, the following graphic technique of estimating noise power from the response characteristic of the logarithmic receiver-digital integrator is offered.

Integrator output values, D, of a logarithmic receiver are related to the total meteorological signal plus noise power $P_T = P_s + P_N$ by

$$D = \alpha\ 10\ \log_{10}\ [\frac{P_T}{P_{ref}}] + K \tag{3}$$

where α is the "logging constant", K is the offset of digital intercept value, P_{ref} is the reference power, ($P_{ref} = 10^{-3}$ watts for power in dBm). The logging constant, α , may be determined by selecting a region of logarithmic response where $P_S >> P_N$, and calculating the slope

$$\alpha \simeq \Delta[D]/\Delta[10\ \log \frac{P_S}{P_{ref}}] \tag{4}$$

Transfer characteristic of this logarithmic segment of the response may be expressed as

$$D_\ell = \alpha\ (10\ \log_{10}\ \frac{P_S}{P_1}) \tag{5}$$

where P_1 is the input power intercept value at D = 0 (see fig. 1). To determine the noise power from the receiver calibration with a known signal power, it is necessary to establish a relationship between the digital output of known signal plus unknown noise power. There are two convenient graphic methods. One method is based on a calibration curve using weather type signals by simply noting that the digital output and thus, the calibration signal input power corresponding to a signal-to-noise power ratio of unity is given by

$$D = \alpha\ [10\ \log_{10}\ \frac{2P_N}{P_{ref}}] + K = 3\alpha + \alpha[10\ \log_{10}\ \frac{P_N}{P_{ref}}] + K \tag{6}$$

at $P_S = P_N$

or at the (D,P_S) value which is 3 logging constants (if α is in digits/dB) above the D (intercept) corresponding to $P_S << P_N$ (intercept with the ordinate on fig. 1).

A second method can be devised by making the following assumptions:

1. The calibration signal source has an output power standard deviation small compared to the digital integrator quantization increment.

2. The noise amplitude probability density (in our case we assume Gaussian statistics) is the same as that of a meteorological signal.

The first assumption stipulates the only bias in the calibration signal power estimate to be due to quantization by truncation. The second stipulates that the bias of the noise power estimate is 2.5 dB plus the truncation bias. We may then determine input signal power corresponding to unity signal-to-noise ratio at the intercept of the logarithmic transfer and a D which is 2.5 logging constants above the D corresponding to $P_S \ll P_N$. (This 2.5 dB is bias of the noise power estimate due to its probability density.)

These two methods are illustrated in Figure 1 for the NRO radar. The two calibrations of Figure 1 also show the techniques are not sensitive to the offset or digital intercept value so long as the noise is not "thresholded" below digital two.

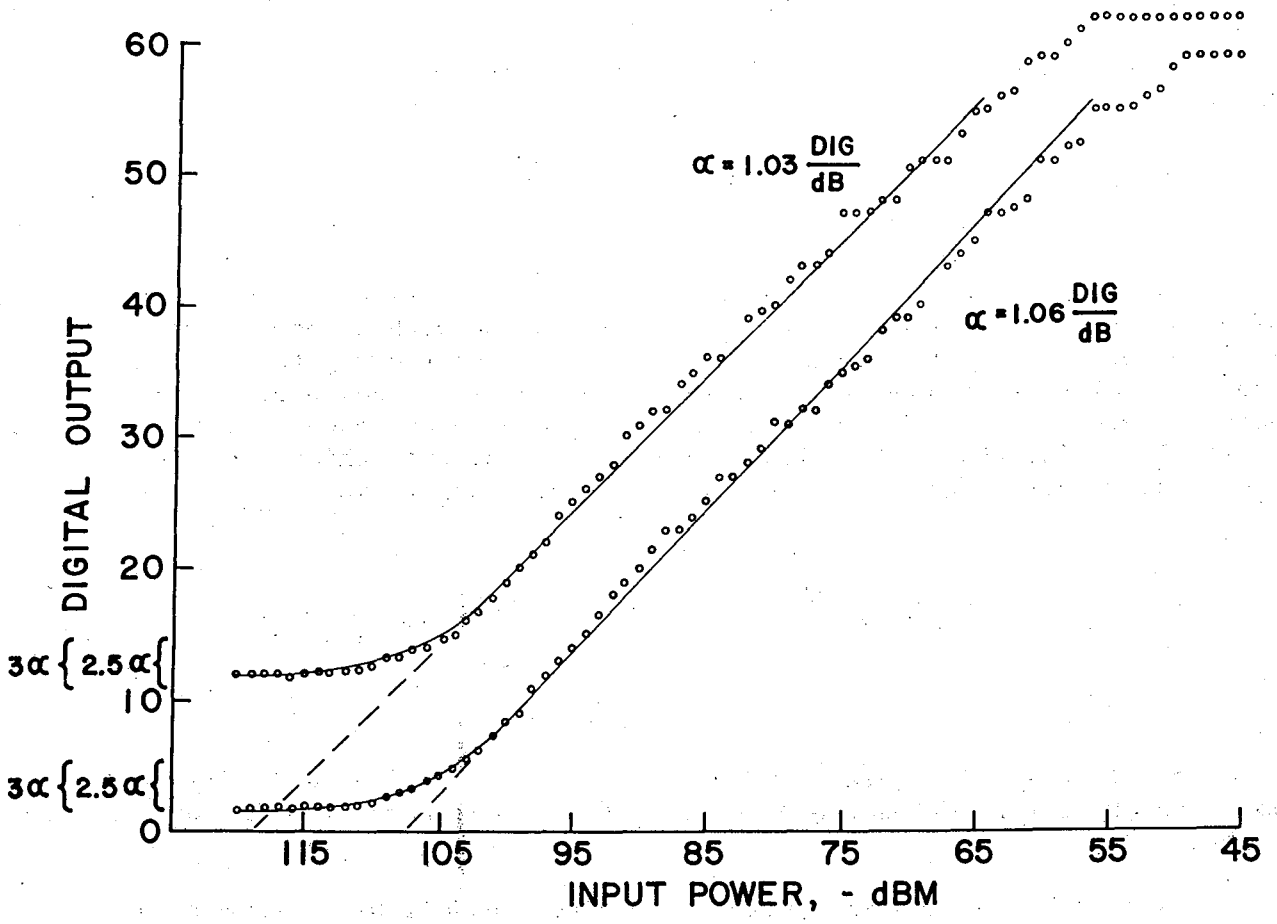

Figure 1. Transfer function from the receiver input to the output of a digital integrator.

SECTION 2

ADC Quantization - General Considerations In Quality Control Testing

Two parameters of analog to digital conversion (ADC) are of primary importance in data quality control checks. These are: (1) "differential linearity," which is the variation of actual class widths from the ideal width (1 LSB), usually given as ± 1/2 LSB, and (2) "conversion linearity," which is the deviation of class midpoints from a linear input-output conversion, usually given as about ± 1 LSB. A differential linearity of ± 1/2 LSB merely implies a ratio of maximum class width to minimum class width of three. A conversion linearity of ± 1 LSB requires that maximum deviation of any category from a linear conversion is not more than one ideal category width.

To measure the differential linearity, a test signal having a uniform distribution across the conversion range is injected and a "large number" of conversions are made to insure a statistically significant sample. The ratio of number of occurrences in a given class to the total in all classes is then a measure of the fractional width (fraction of conversion range) of that class. The listing of the number of occurrences in each class is the ADC histogram. Statistical parameters of ADC, as reflected in the histogram, can be developed as follows:

Let i be the index of the digital output number of a b bit converter, i.e., $i = 0, 1, 2, \ldots, 2^b - 2, 2^b - 1$ (for a 10 bit converter i = 0, 1, 2, ..., 1022, 1023). Let N_i be the number of occurrences of the ith digit.

For the uniform input variable, the expected number of entries for classes having the ideal width (1 LSB) is

$$\overline{N} = \frac{1}{2^b} \sum_{i=0}^{2^b-1} N_i = \frac{1}{2^b} N_T \tag{7}$$

where N_T = total number of samples; the ratio

$$\Delta q_i = \frac{N_i}{N_T} \tag{8}$$

is an estimate of the i^{th} fractional width.

Finally, the average width is

$$\widehat{\Delta q} = \frac{1}{M} \sum_{i=0}^{2^b-1} \frac{N_i}{N_T} = \frac{1}{M} \tag{9}$$

where M is the number of non-zero width entries.

Statistics associated with the estimated class width, $\widehat{\Delta q}$, can be found by noting that the number of occurrences in a given class is described by the binomial distribution (Burlington and May, 1958).

Let P_i be the probability that the sample falls in the i^{th} class

$$p_i \approx \frac{N_i}{N_T} \tag{10}$$

and q_i the probability that the sample does not fall in the i^{th} class

$$q_i \approx 1 - \frac{N_i}{N_T} \tag{11}$$

then the observed number of entries has a standard deviation of

$$\text{S.D. } [N_i] = [N_T\, p_i q_i]^{1/2} \tag{12}$$

Normalizing the S.D. by expected number of entries and substituting the estimates,

$$\frac{\text{S.D.}[N_i]}{N_i} = \frac{[N_T\, p_i q_i]^{1/2}}{N_T p_i} = \frac{[1 - \frac{N_i}{N_T}]^{1/2}}{N_i^{1/2}} \tag{13}$$

provides a convenient measure of the uncertainty associated with class width measurement. For example, for a 10 bit ADC a number of entries, N_i greater than $5(10^2)$ and $N_T = 5(10^5)$, creates a fractional S.D. less than 5 percent of the measured value.

The class width, Δq, determines the uncertainty associated with analog to digital conversion and thus the "noise" generated by ADC process (Sirmans, 1971; Sirmans, 1974c; Bendat and Piersol, 1971). For the ideal case of equi-width classes, the "noise" power introduced by quantization P_{Nq} (for the assumption of uniform probability across the class): and conversion of 0 to 1 is given by

$$P_{Nq} = \frac{(1/2^b)^2}{12} \tag{14}$$

With varying widths the uncertainty is different for each digital number but the total noise power is the summation of the noise power "per sample" in the same fashion as signal power is the summation of signal power per sample.

The statistics of the signal and noise may be developed as follows:

Let $\overline{X_i^2}$ = the expected mean square of the input for conversion in the i^{th} class; ϵ_i = the uncertainty associated with the conversion.

$$\text{prob } [\varepsilon_i] = \frac{1}{\Delta q_i} \qquad -\frac{\Delta q_i}{2} < \varepsilon < \frac{\Delta q_i}{2}$$
$$= 0 \qquad \text{otherwise} \tag{15}$$

The noise sample power generated by a conversion in the i^{th} class is

$$P_{N_{q_i}} = \frac{(\Delta q_i)^2}{12} \tag{16}$$

and signal sample power for the i^{th} class by

$$P_{S_i} = X_i^2 \tag{17}$$

for K samples we find the signal and noise power

$$P_{S+N_q} = \frac{1}{K} \sum_{j=1}^{K} (X_j + \varepsilon_j)^2 = \overline{X^2} + \overline{\Delta q^2}/12 \tag{18}$$

since the signal and noise are uncorrelated, the parameter usually given is the signal to quantization noise ratio in dB, i.e.,

$$SNR_q = 20 \log_{10} \frac{X_{rms}}{\Delta q_{rms}/2\sqrt{3}}$$
$$= 10 \log_{10} \left[\frac{12\ \overline{X^2}}{\overline{\Delta^2 q}} \right] \tag{19}$$

Note that the noise power depends on: (1) the particular classes involved in the conversion, and (2) the mean square width, (Δq^2). We therefore define the "effective" quantization width as the rms of Δq^2:

$$[\overline{\Delta q^2}]^{1/2} = \left[\frac{1}{M} \sum_{i=1}^{M} \left(\frac{N_i}{N_T} \right)^2 \right]^{1/2} \tag{20}$$

This width will specify quantization noise so long as the input signal is distributed over the entire conversion range.

An equivalent number of equi-width classes N_e which would produce the same quantization noise as the measured widths can be found from the rms width:

$$N_e = \frac{1}{[\overline{\Delta q^2}]^{1/2}} \quad . \tag{21}$$

Thus, the increase in measured noise power over theoretical noise (Eq. 14) also serves as a measure of ADC performance and is the quantization noise factor adjustment

$$QNF = 20 \log_{10}\left(\frac{2^b}{N_e}\right) \tag{22}$$

needed to specify, for example, the signal spectrum mode to average quantization noise level in the frequency domain.

In practice, it may be necessary to calculate the quantization noise as a function of input signal rms for a specified amplitude (class) distribution. For quality control testing, a Gaussian density (truncated) is used with signal rms to conversion range ratios of about 10^{-2}, 10^{-1}, and $3(10^{-1})$. The quantities pertaining to quantization given in the routine ADC quality control listings are:

1. Number of entries in each digital class (listing), N_i.
2. Total number of entries - all classes, N_T.
3. Number of non-zero width classes, M.
4. The average number of class entries, $\overline{N_i}$.
5. The fractional width estimates - listing (percent of ideal width), $\Delta q_i/\Delta q$.
6. Standard deviation of N_i.
7. RMS width, Eq. 20.
8. The quantization noise power for each class $(\Delta q_i)^2/12$.
9. The number of equi-width classes specified by the quantization noise, Eq. 21.
10. The increase of quantization noise power due to the measured widths over the theoretical noise of the ideal converter for the uniform amplitude density, Eq. 22.
11. A/D quantization noise level for a Gaussian amplitude density of simulated input signal with an ADC transfer generated by a computer using the result of step 5 above. (As a special option.)

Conversion linearity can be best checked experimentally. However, it may be calculated from the estimated differential linearity by "piecewise approximation". The difference between the line connecting the midpoints of the interval, Δq_i, to the origin and the corresponding line of the ideal ADC

$$X_L = X \tag{23}$$

is the conversion linearity of the i^{th} category.

Statistics of conversion linearity will, of course, reflect the statistics of width estimates as well as the particular width configuration. The observed length of the i^{th} conversion category is given by

$$D(\Delta q_i) = \sum_{\ell=0}^{i} (\Delta q_\ell) \quad , \quad 0 \le i \le 2^b - 1 \ , \tag{24}$$

whereas the corresponding length for an ideal ADC is $DL_i = (i + 1/2)\ \Delta q$ so that the conversion linearity, CL_i becomes:

$$\begin{aligned} CL_i &= (D_{L_i} - \frac{\Delta q}{2}) - [D(\Delta q_i) - \frac{\Delta q_i}{2}] \\ &= (i\Delta q) - [D(\Delta q_i) - \frac{\Delta q_i}{2}] \quad . \end{aligned} \tag{25}$$

As mentioned earlier, this parameter, (CL) is usually specified as $\pm$ 1 LSB and if there were no uncertainty in the estimates of class width, the CL distribution would be truncated at $\pm$ 1 LSB or $\pm\ 1/2^b$. However, in practice the S.D. (approximately 4 percent) associated with the measured class widths will result in a continuum of the distribution and it is necessary to establish a statistical confidence on the conversion linearity measured. We use the 1 percent level for a Gaussian density as the level above which the CL is assumed to be due to hardware. For example, if

$$\left| CL_i \right| > \frac{1}{2^b} + (2.575)(.04)(\Delta q_i) \quad , \tag{26}$$

the class linearity is not within $\pm$ 1 LSB.

Some parameters of the ADC in service at NRO are in Table 9 and for CIM in Table 10. A complete analysis is available from the quality control testing.

TABLE 10

	Norman ADC Characteristics	Datel #11044
1.	Non-zero classes	3065
2.	Number of equivalent bits based on non-zero classes	11.582
3.	Equivalent quantization noise width	2014
4.	Number of equivalent bits based on noise	10.976
5.	Quantization noise increase over ideal 12 bit converter	6.143 dB

TABLE 11

	Cimarron ADC Characteristics	I Com Lab #304074 Q Com Lab #504152	
1.	Non-zero classes	I 1022	Q 1022
2.	Number of equivalent bits based on non-zero classes	I 9.997	Q 9.997
3.	Equivalent quantization noise width	I 1015	Q 1015
4.	Number of equivalent bits based on noise	I 9.987	Q 9.987
5.	Quantization noise increase over ideal 10 bit converter	I .06 dB	Q .06 dB

SECTION 3

Note on Norman Doppler Image Gates

Prior to May 27, 1975, there existed a logic error in the Norman Doppler signal recording scheme which resulted in unusually large "image" spectrum at certain gates under certain conditions. The problem was due to multiplexing logic which resulted in a shift of one component of the complex video signal by one pulse repetition time (PRT) causing a deviation from phase quadrature. This anomoly (i.e., the data shift) occurred consistently at prescribed gates for a given gate spacing and block step as shown in Table 12.

However, the appearance of an image depends not only on the shift being present, but also on the true velocity at the gate (fig. 2) since the time shift of one PRT causes a phase shift which is proportional to input signal frequency, and if the phase shift was not sufficient, an image did not appear. The hardware problem was corrected May 27, and data taken after this time does not contain this type "image".

TABLE 12

High Image Gates

Gate Spacing	Gate			
	150 m	300 m	600 m	1200 m
Step				
0	-	-	-	-
1	1	-	2	4
2	-	2	-	7
3	-	3	5	10
4	2	-	-	-
5	-	4	8	-
6	-	5	-	-
7	3	-	11	-

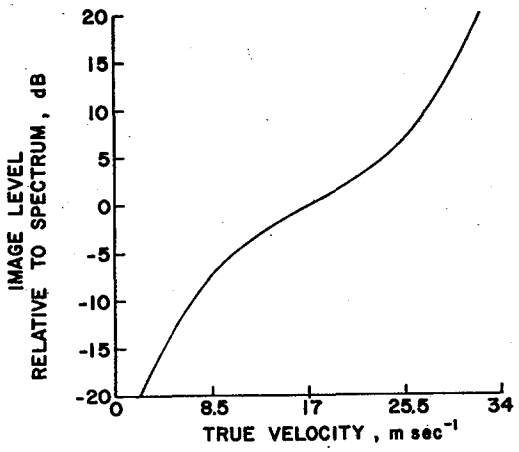

Figure 2. Image level of anomalous gates versus input velocity.

SECTION 4

Note on Spectrum Background Noise Level

Spectral density background "noise" can be divided into two broad classes: (1) uncorrelated white noise which has constant spectral density, and (2) extraneous signals which appear as discrete spectral lines or as a well defined spectrum. These are usually due to either signal processing distortions or stray pickup.

The first noise class is, in general, a colored noise but, when aliased into the Nyquist co-interval, appears for all practical purposes as white (constant spectral density). Usually it is a composite of: (1) receiver noise, (2) analog to digital quantization noise, and (3) Doppler phase noise. Contributions from the various mechanisms depend on received signal power, ADC operating range and radar signal spectral purity as outlined in Sirmans (1974c). However, background noise level observed in the frequency domain depends not only on composite signal-to-noise ratio but also on the weighting function used. With the rectangular weighting, leakage dominates the background level at SNR > 20 dB.

Quantization noise power for the ideal ADC (fig. 3) is small (over 35 dB below signal) if the rms of the digital signal σ_A is kept above 30. The usual operating range for σ_A is 100 to 600 at Norman and 50 to 200 at Cimarron.

The ratio of spectrum mode to average noise density (excluding the window effects) is shown in Figure 4 for an assumed Gaussian spectrum. Considering

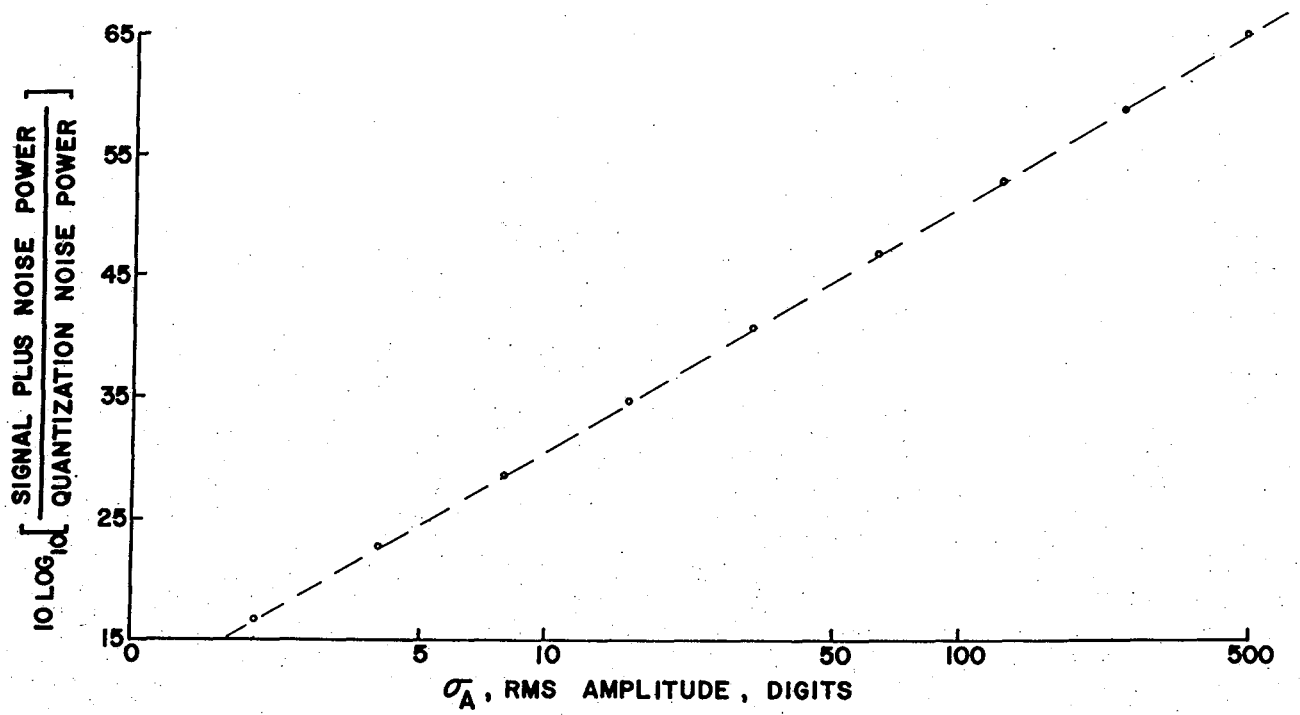

Figure 3. Signal plus noise to quantization noise ratio versus digital RMS amplitude, σ_A.

the relative magnitude of noise components, it is noted that the spectrum background noise level is dominated by receiver noise up to SNR $\simeq$40 db and by quantization and phase noise above this level. This implies a spectrum mode to average noise density ration-SNR dependency: A ratio of about 10 dB (depending on spectrum width) at a SNR of 0 dB, ratio increasing almost linearly with increasing SNR to a value of about 45 dB and inflecting with asymotope of about 55 dB.

However, this expected behavior is modified considerably at the larger SNR by the window function, especially that associated with the rectangular weight used routinely. As shown in figure 5, the window (sinx/x) has a first sidelobe level of 13.2 dB and skirt sidelobe level of about 39 dB with 64 time samples. Behavior of the observed background level is shown in figures 6, 7, and 8.

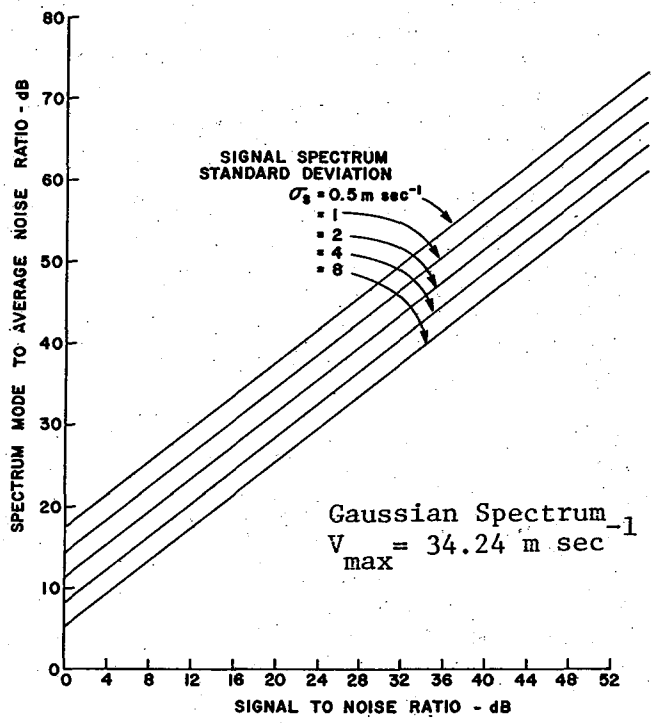

Figure 4. Spectrum mode to average noise ratio as related to signal-to-noise power ratio and spectrum standard deviation.

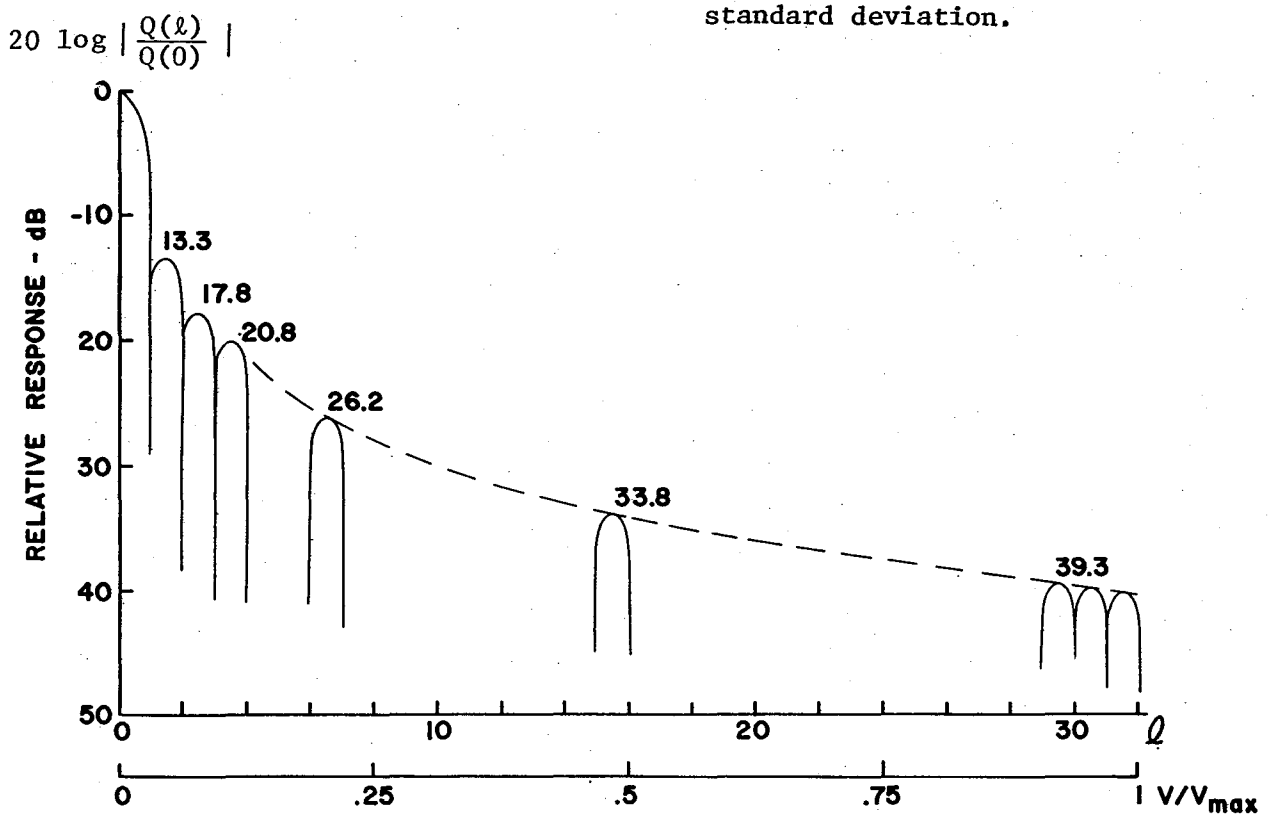

Figure 5. Rectangular weighting function and its discrete Fourier transform: $q(n) = 1$ $\quad n = 1, 2, \ldots N$; $Q(\ell) \approx \sin \pi\ell/\pi\ell$ $\quad \ell = 0, \pm 1, \pm 2, \ldots N/2 - 1$

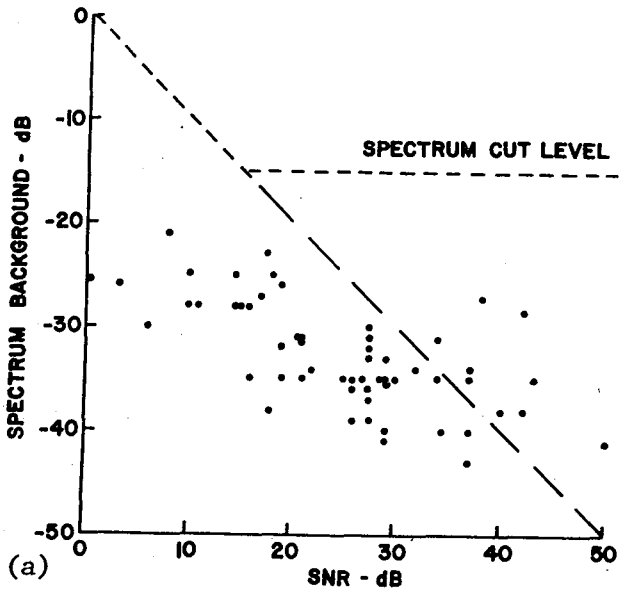

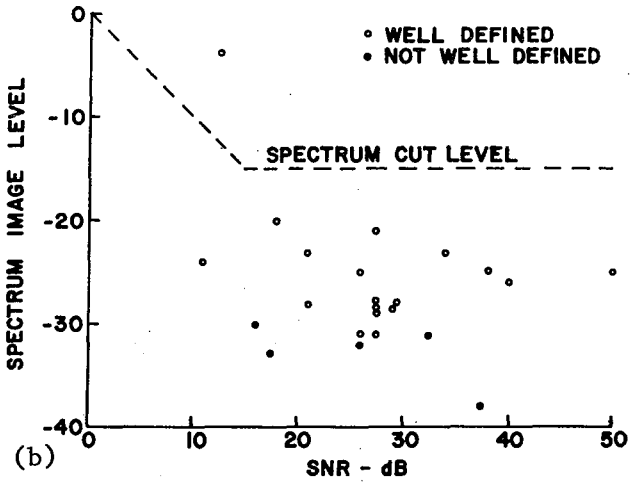

Figure 6. (Above) (a) Spectrum background level. Tape DP 7521, May 19, 1975. (Above, right) (b) Spectrum image level. Tape DP 7521, May 29, 1975. Spectrum cut level of 15 dB below peak is used routinely in the Fourier analysis.

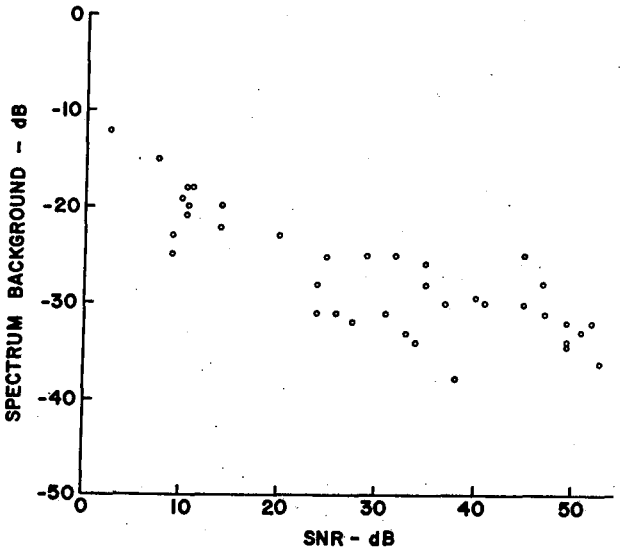

Figure 7. (Right) Spectrum background level. Tape CP 7553, June 13, 1975.

Figure 8. (Below) (a) Spectrum background level. Tape DP 7567, June 13, 1975. (Below, right) (b) Spectrum image level. Tape DP 7565, June 13, 1975.

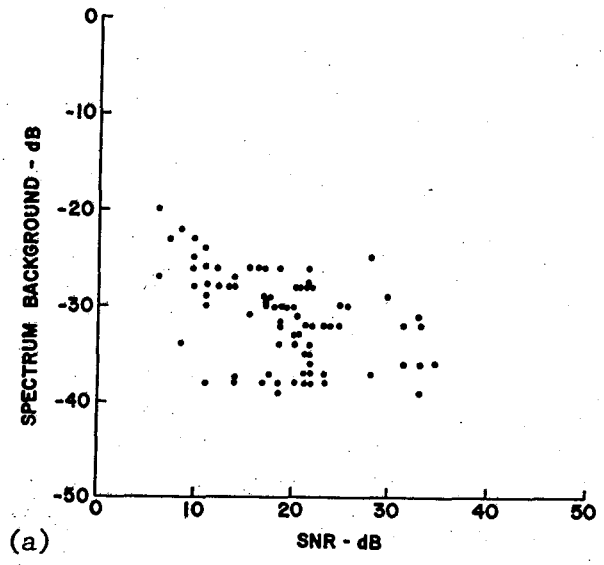

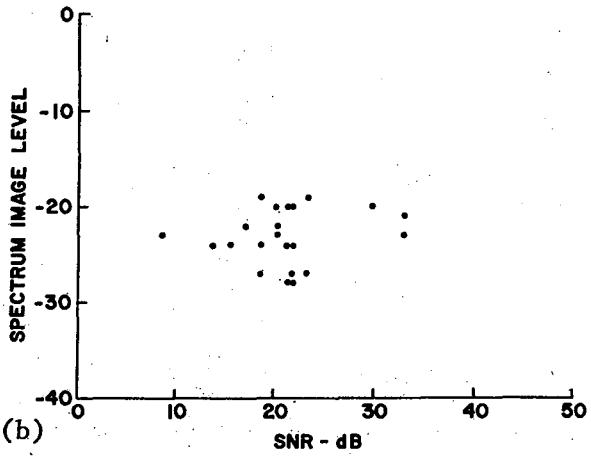

These scattergrams were plotted from spectrum plots (spot checks of the 1975 data) with average noise level estimated by eye. Note in particular that the background level is limited even at large SNR (>30 dB) to a level commensurate with the skirts of the window function.

It is interesting to compare the background level measured with rectangular weighting to that measured using a weighting function whose transform has lower sidelobes such as the Hanning function (Brigham, 1974) given in Figure 9. This window has a first sidelobe level of 31.4 dB, skirt level well below the expected noise background level with 64 samples but a main lobe width about 1.6 times that of the rectangular window (Nathanson, 1969). The background noise level scattergram (fig. 10) and spectrum width estimate scattergram (fig. 11) illustrate the influence of the two windows.

The CIM complex video contains another type of noise due to spurious convert command to the ADC's. This noise appears as an abrupt discontinuity of the complex video and thus has a uniform spectral density. Certain conditions (depending on the SNR, number and magnitude of the glitches)

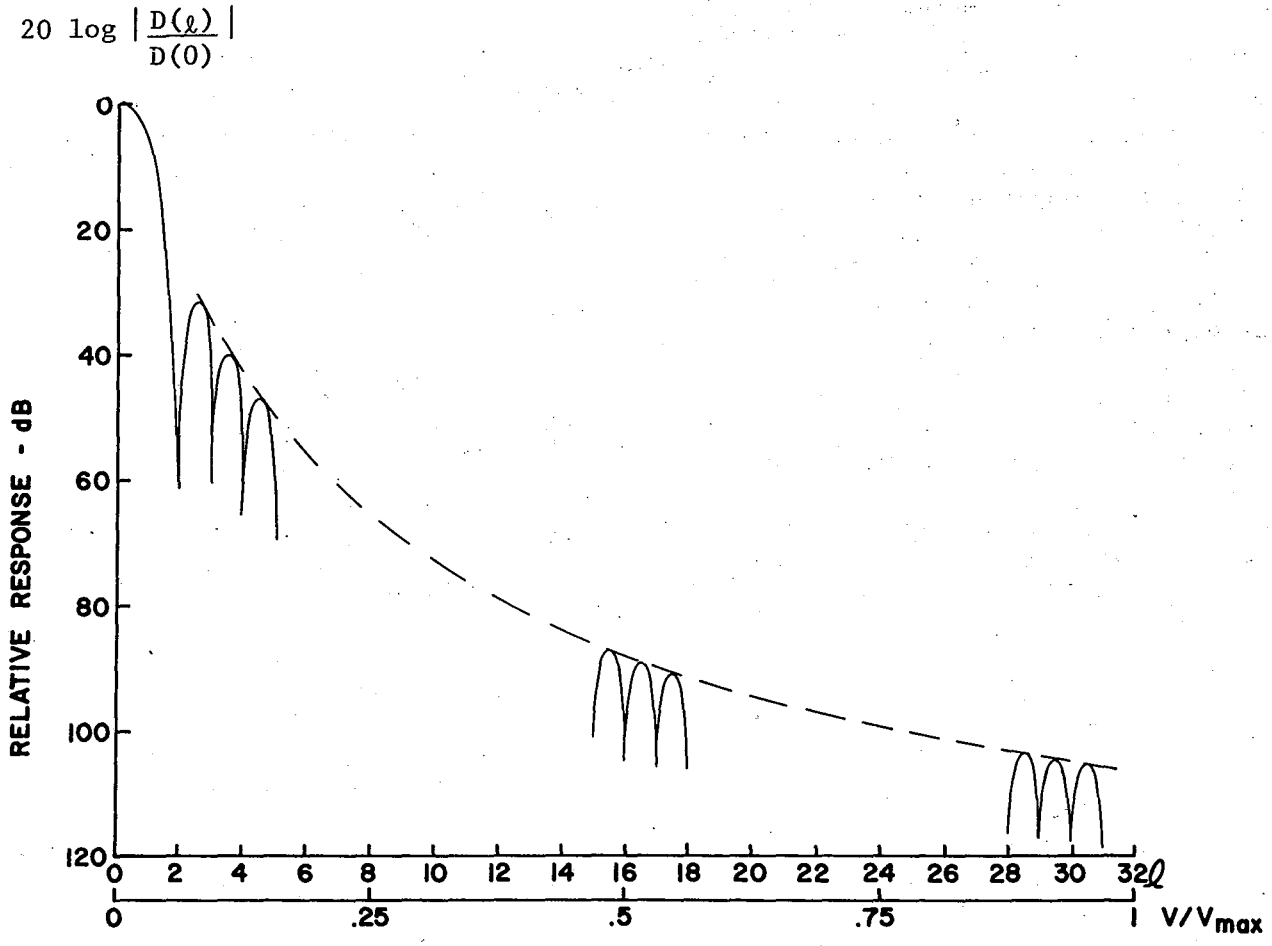

Figure 9. Hanning weighting function: $w(n) = .5(1-\cos\frac{2\pi n}{N})$ $n = 1, 2, 3 \ldots N$

$D(\ell) = 1/4\ Q(\ell - 1) + 1/2\ Q(\ell) + 1/4\ Q(\ell + 1)$ $\quad \ell = 0, +1, \pm 2, \ldots \frac{N}{2} - 1$

$Q(\ell) \approx \frac{\sin \pi\ell}{\pi\ell}$.

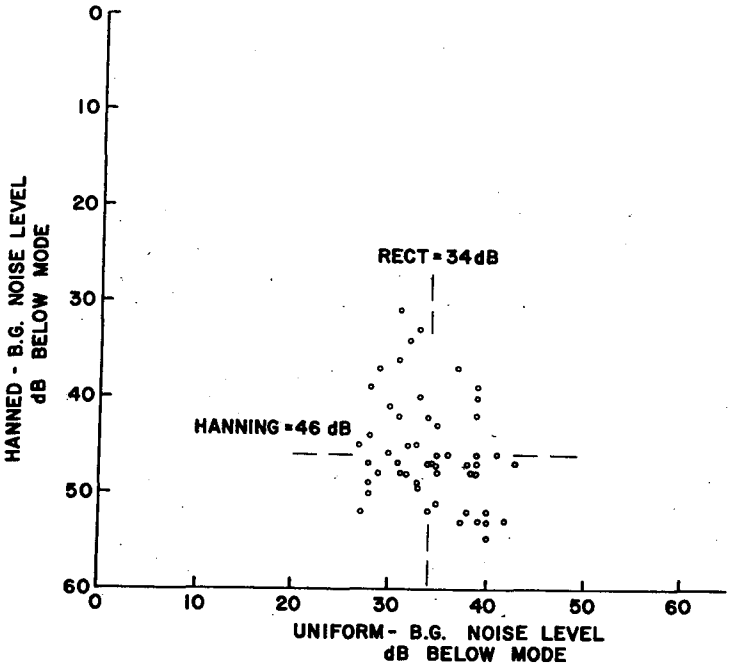

Figure 10. (Left) Background noise level with Hanning wind versus the level with a rectangular window, May 2, 1975. 16 dB < SNR < 57 dB.

Figure 11. (Below) FFT spectrum width estimate, Hanning versus rectangular window, May 2, 1975. 16 dB < SNR < 57 dB.

increase the spectrum background noise level above the spectrum cut threshold and result in a bias of the FFT mean and width estimate, particularly the width estimate. The covariance mean velocity estimate is not biased, although the standard deviation is increased in about 15 percent of the data and appears as an abnormally large width estimate (> 10 m s^{-1}). No effort is made to correct these in post analysis, therefore, quantitative estimates of spectrum width from the CIM radar should be made after subjective correction.

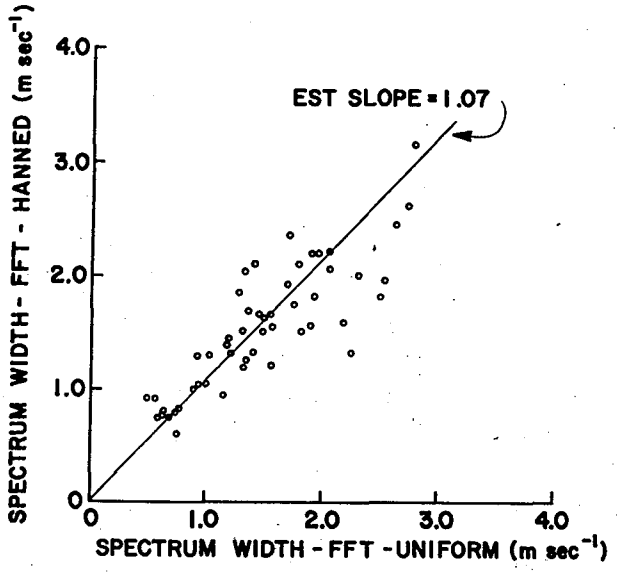

Spurious signals due to stray pickup are usually easy to recognize since stray signal frequencies are often multiples of the power service frequency (60 Hz, 120 Hz) and are not in phase quadrature (i.e., appear at both positive and negative frequencies). Although these can be suppressed after the fact, they should be eliminated in signal handling. Little evidence of such signals was noted in the 1975 data. Spurious waveforms due to signal processing appear as harmonics of the input--for instance, the negative first harmonic (image) due to the imbalance of the two video components and odd harmonics with alternating sign generated by clipping of the complex video (Sirmans, 1974c). The third harmonic in particular becomes appreciable (within 30 dB of signal mode) when the ADC maximum span to signal rms ratio is less than about 3. Anomalies of this type were noted in the 1975 data where complex video clipping occurred but present a problem only in studies involving spectrum functional form.

SECTION 5a

Range Calibration of Cimarron-Norman Digital Integrator Data Records

Apparent ranges of DI gate locations are derived from observations of known range to fixed point targets (television towers), relative to the radar transmitter pulse, as they appear in the DI data record. True measured target range is obtained by correction of apparent range for transmitter pulse displacement from DI range sampling time, receiver bandwidth, waveguide propagation time and atmospheric refractive index effects. Corrected measured range is then compared with calculated topographic range to verify that all sources of ranging error have been considered.

Cimarron Radar

(1) Apparent range: Figure 12 shows that the transmitted pulse appears in DI gate location number four. The apparent range of gate N, defined as R_o, is therefore:

$$R_o = (N - 4)\ (\tau)\ \frac{c}{2}\ m \qquad (27)$$

where

N = DI gate of interest

τ = DI range sampling interval = 1 μs

c = energy propagation speed corrected for atmospheric refractive index. (See Section 2.)

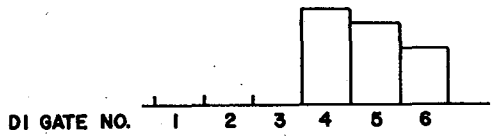

Figure 12. Digital integrator data record.

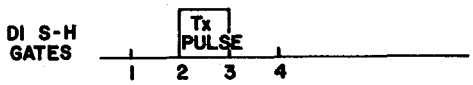

Sample and hold gates S-H with transmitted pulse T_x.

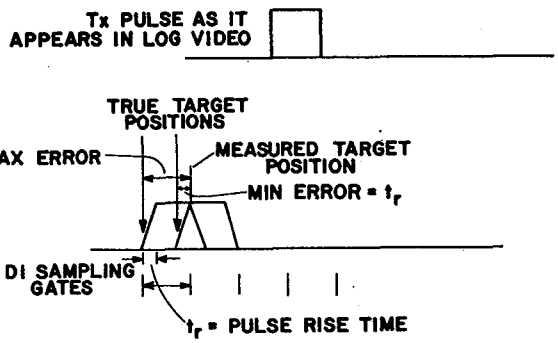

Effects of sampling gates and receiver band width (rise time) on the range correction R_2.

(2) Correction terms:

a. Transmitter pulse displacement. The transmitter pulse leading edge precedes the DI gate in which it appears by 300 nanoseconds (fig. 12). A correction term R_1 must be added to the apparent range R_0.

$$R_1 = 0.3\ (10^{-6})\ \left(\frac{c}{2}\right)\ m \tag{28}$$

b. Receiver bandwidth. The arrival of the return pulse at the DI is delayed by approximately .31 μs, the reciprocal of the receiver 3 dB bandwidth (3.2 MHz). Note also the effect of the DI range sampling interval on apparent target position (fig. 12). As a general correction factor, R_2, these two effects are combined:

$$\left(\frac{1}{BW_{3dB}}\right)\left(\frac{c}{2}\right) \leq R_2 \leq \left(\frac{\tau c}{2}\right) \tag{29}$$

with a mean value of $R_2 = -.65\ .10^{-6}\ c/2$

c. Waveguide propagation delay. Topographic ranges are calculated from known locations of target and radar antenna. Two way propagation times of energy from antenna to radar must be accounted for in range measurements in order to compare them with computed topographic ranges. Energy propagation speed in the waveguide is reduced by a factor of 1.6 from that in free space. Measured propagation delay correction factor is defined as R_3.

$$R_3 = 1.6\ D_{WG} \tag{30}$$

where

D_{WG} = physical length of waveguide run.

d. Refractive index effects. The constant c used in all the above range calculations is the energy propagation speed in vacuum divided by a factor of 1.0003.

$$c = \frac{2.998\ (10^8)}{1.0003}\ m\ s^{-1} \tag{31}$$

(3) Range calibration equation for point target measurements:

$$R = R_o + R_1 + R_2 + R_3 \tag{32}$$

$$R = [N - 4.347]\ 1.4985\ (10^2)\ m \pm 52.89\ m - 49.6\ m$$

(4) Measured range of fixed targets. Figure 13 shows the true and measured positions of three television towers from the CIM radar.

a. KWTV Tower

N = 204

$R = 29.8686\ (10^3)$ m $\pm$ 52.89 m

b. KOCO Tower

N = 211

$R = 30.9176\ (10^3)$ m $\pm$ 52.89 m

c. WKY-TV Tower

N = 213

$R = 31.2166\ (10^3)$ m $\pm$ 52.89 m

Norman Radar

(1) Apparent range: The transmitter pulse appears in gate number two. R_o is now defined

$$R_o = (N - 2)\ \tau\left(\frac{c}{2}\right) \tag{33}$$

(2) Correction terms:

a. Transmitter pulse displacement. For the NRO radar the transmitter pulse precedes the DI sampling gate by 700 nanoseconds. Therefore,

$$R_1 = 0.7\ (10^{-6})\ \frac{c}{2} \tag{34}$$

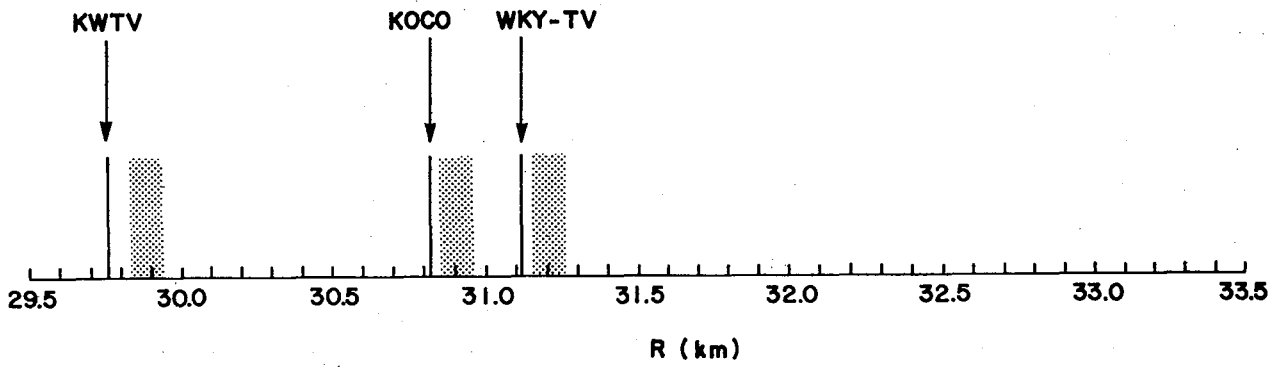

Figure 13. CIM radar derived ranges (shaded areas) within the uncertainty error given by Eq. (29) and true tower ranges (lines).

b. Receiver bandwidth. Measured receiver 3 dB bandwidth is 2.0 MHz. Range sampling interval is 1.0 μs. Correction factor R_2 is defined in the same way as for the CIM radars using the above parameters.

c. Waveguide propagation delay. Measured waveguide length is 15.24 meters, however, the transmitter timing measurement is made at the end of a 16.46 m cable which is a one-way waveguide delay (section 5b). Thus, the correction is given by

$$R_3 = 12.2 \text{ m} \tag{35}$$

(3) Range equation.

$$R = R_o + R_2 + R_3 \tag{36}$$

$$R = [N - 1.3]\ 1.49\ (10^2)\ \text{m} - 136.4\ \text{m} \pm 37.46\ \text{m}$$

(4) Measured range of fixed targets. Figure 14 shows the true and measured positions of three television towers from the NRO radar.

a. KWTV Tower

N = 235

$R = 34.895\ (10^3)\ \text{m} \pm 37.46\ \text{m}$

b. KOCO Tower

N = 244

$R = 36.244\ (10^3)\ \text{m} \pm 37.46\ \text{m}$

c. WKY-TV Tower

N = 249

$R = 36.993\ (10^3)\ \text{m} \pm 37.46\ \text{m}$

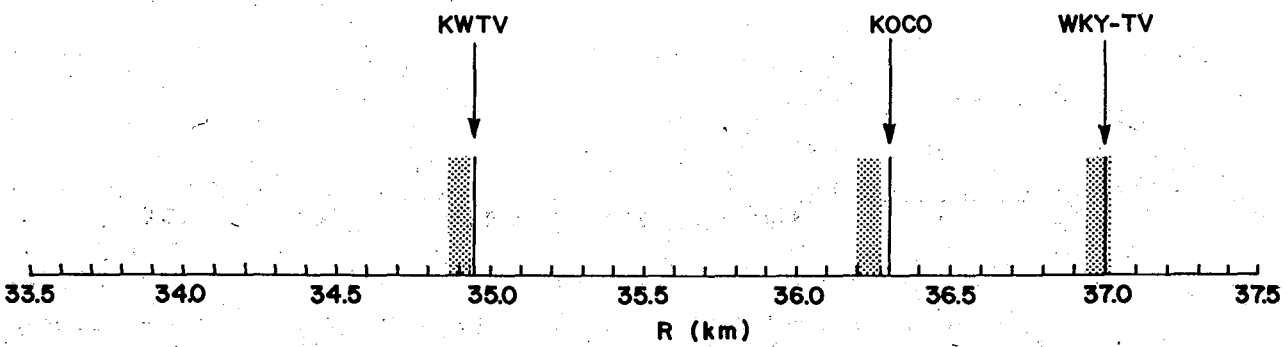

Figure 14. Norman radar derived (shaded) and true (lines) tower ranges.

Section 5b

Range Timing Check for Norman Doppler

The following description of a ranging check (using "known" range of WKY tower) illustrates the technique used in determining slant range with NSSL radars, and offers an error analysis of measured radar parameters.

A sketch of the radar integrator timing is shown in Figure 15. Important parameters are the time (T_D) between the leading edge of the transmitter pulse (time zero) and first integrator sample hold location (L_1), and the spacing between samples (S). In making this measurement the T_x pulse is viewed at the end of a 16.46 m coax (RG-8) and 15 dB coax attenuator connected to forward power jack of the directional coupler. Delay due to this cable is approximately 0.09 μs or about the same as delay from directional coupler to antenna aperture (one-way waveguide run). In the ranging calculation a correction (T_A) of 0.1 μs is made for the delay from aperture to directional coupler.

The intensity sample-hold command is approximately 40 ηs wide with leading edge occurring 50 ηs prior to data sample (uncertainty of ± 300 pico s). The data sample is the input data value exponentially weighted from the trailing edge of the sample window with time constant of about 10 ηs. These uncertainties are small compared to that associated with definition and measurement of the T_x pulse leading edge and are not accounted for in the ranging delay.

Time between sample-hold commands for A channel is the radar system Coho signal period divided by 30, i.e., for a 30 MHz reference the spacing is 1 μs, for B channel the division is 30 x 2/3 and the spacing is 1.5 μs. For the NRO Doppler this signal was 30.0079 MHz (for the WKY test, May 15, 1975) with associated spacing of 0.9997367 μs. Time delay, DLY, corresponding to a given integration location (1 designates the first location) is given by:

$$DLY = [(Location - 1)(spacing) - 0.3]\mu s \ . \qquad (37)$$

The observed delay to a target at a given range is the sum of delay due to range (from the antenna) and any fixed delays in the receiver chain. In the case of NRO Doppler the receiver chain delay is composed of two parts: the delay from the aperture to directional coupler, T_A, and the delay from directional coupler to sample hold input or receiver initial delay, T_I. This

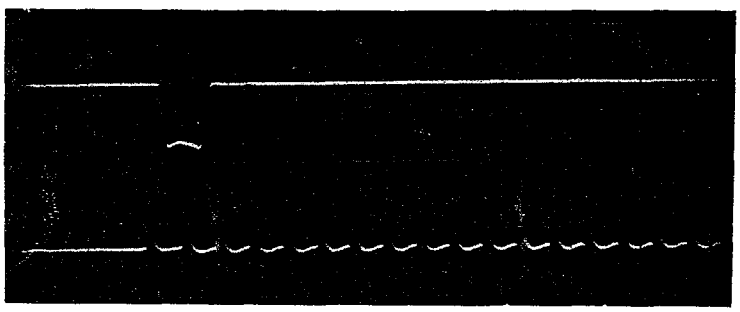

Transmitter pulse

Integrator sample hold commands

Figure 15. Time base = 2 μs/cm

second parameter is loosely related to number of stages and values of the lumped constants in the receiver chain and has a measured value of 0.1 μs for both the linear and log receivers.

The return signal is subject to a further delay due to finite receiver response. This "rise time" (T_R) is an inverse function of receiver 6 dB bandwidth (BW_{6dB}) and is given to a good approximation (Skolnik, 1969) by

$$T_R = \frac{1}{BW_{6dB}} = \frac{1}{2.88\ MHz} = .35\ \mu s\ . \tag{38}$$

Thus, the target delay (from time zero) is

$$DLY = \frac{Range}{c/2} + T_R + T_A + T_I \tag{39}$$

where c is the propagation constant.Eq. (31).

The range from the NRO Doppler to WKY tower based on longitude-latitude is calculated to be 36.986 km with estimated uncertainty of 30 m. Delay to WKY tower is given by

$$DKY_{WKY} = [\frac{36986}{299.686/2} + .55]\mu s = (246.83 + .55)\mu s - 247.38\ \mu s\ . \tag{40}$$

Substituting this DLY_{WKY} into Eq. (37) and solving for location, we have

$$LOCATION = \frac{(247.38 + 3)}{.9997367} = 248.74 \tag{41}$$

Since the above delay is measured from the leading edge of the 1 μs T_x pulse (time zero) this is the position of the target full response which should appear on the digital listing (fig. 16a) at location 249 (which it does).

The basic range resolution of 150 m that sampling imposes can be reduced for point target measurement by noting target relative response on the integrator output (i.e., the digital listing, fig. 16a) or examination of the log video relative to sample hold commands (fig. 16b). The latter must be done carefully, however, since the log receiver response to leading and trailing edges of a point target is not symmetrical and there is a stretching of the full response width.

Tabulation of uncertainties associated with the timing parameters is given in Table 13.

In practice the problem is not to verify location of a known target but to assign a representative range to the sample taken at a precribed time, i.e., what is the range associated with a given intergrator location? This is found by first combining receiver initial delay and rise time to form the receiver nominal delay, T_N (Ruston and Bordogna, 1966), i.e., delay from excitation (transmitter pulse leading edge) to 50 percent response ($T_I + T_R/2$),

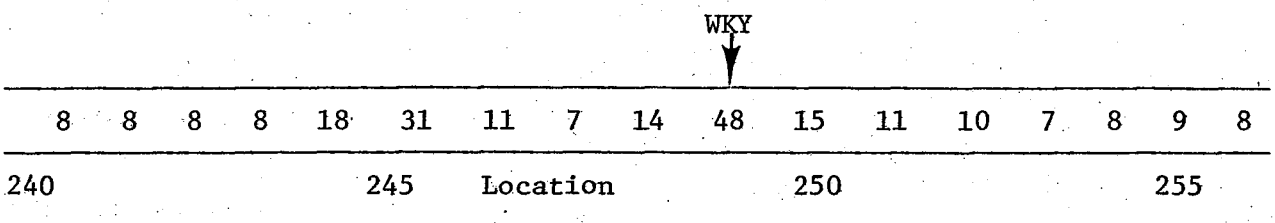

(a)

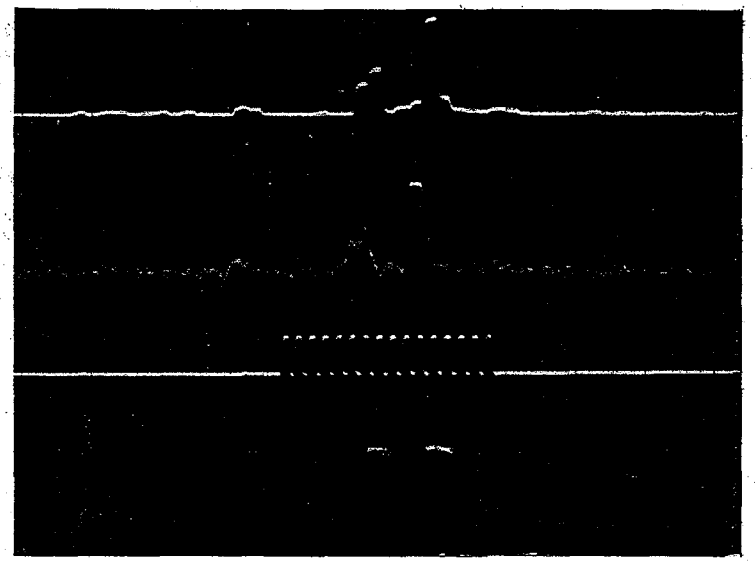

Integrator Analog Output

Log Video (strongest signal is from WKY tower)

Doppler Gates
Delay to the first gate = 242 μs
Doppler gate spacing = 1 μs

Time Base = 5 μs/cm

(b)

Figure 16. (a) Integrator listing of range-intensity for point targets (WKY tower complex). AZ = 256.2°, E_L = 1.0°, May 15, 1975. (b) "A" scope display of WKY tower complex.

which gives an integrator location range equation:

$$R_L = [(L - 1)S - T_D - T_A - T_N]\frac{c}{2} \tag{42}$$

where

R_L = range of location L (m)

L = integrator location

S = integrator spacing (s)

T_D = delay from leading edge of T_x pulse (s) to first sample hold location

T_A = delay from aperture to directional coupler (s)

TABLE 13

Timing Parameters

Parameter	Value	Estimated Uncertainty
Initial delay, T_D	-0.3 μs	0.1 μs
Spacing, S	0.99974 μs	0.0001 μs*
Rx initial delay, T_I	0.1 μs	.05 μs
Rx rise time, T_R	0.35 μs	.05 μs
Delay from T_x measurement port to antenna aperture, T_A (waveguide delay)	0.1 μs	-

In addition, the measurement is subject to variations in propagation time of the order of 10^{-4} (0.01 percent).

*This is based on a measured standard deviation of 410 Hz for seven measurements of the reference signal from May 15 to June 20, 1975. The mean value was 30.007743 MHz.

T_N = receiver nominal delay correction = $T_I + T_R/2$

T_I = receiver initial delay (s)

T_R = receiver rise time (s)

The reference (T=0, R=0) in this measurement (Eq. 43) is the transmitter leading edge. Thus, the measurement represents a volume in space having maximum range of R_L and minimum range of $R_L - c\tau/2$ where τ is the transmitter pulse width (fig. 17).

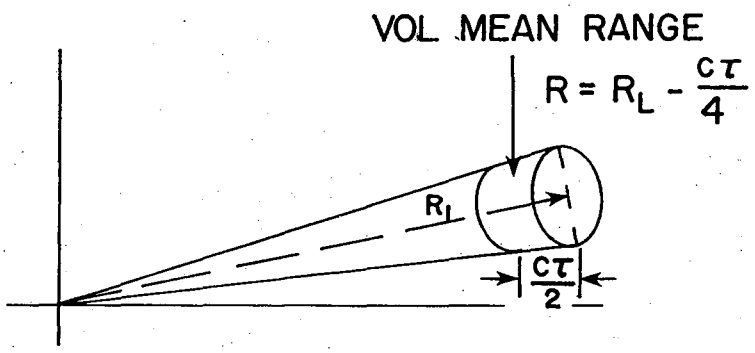

Figure 17. Radar sample volume.

The range to the center of the volume

$$R = R_L - \frac{c\tau}{4} \tag{43}$$

is probably the most convenient range parameter for routine use. In terms of this range and for mean spacing of .99974 μs, the range equation for the NRO Doppler digital integrator is given by

$$R = [(L - 1)S - T_D - T_A - T_N - \frac{\tau}{2}] \frac{c}{2} \tag{44}$$

$$R = [(L - 1)(.99974) - 1.175] \frac{c}{2} (10^{-6}) \text{ m} \quad . \tag{45}$$

The uncertainty of this range is, of course, the combined uncertainty of the various parameters as given in Table 13. The most significant of these is the measurement of T_D (~0.1 μs) and the specification of receiver nominal delay time (~.05 μs). Treating all uncertainties as uncorrelated random variabiles, the estimated standard deviation of the range measurement is 20 m.

SECTION 6

Sun Flux Measurement Comparison

CIM-NRO Dual Sunshot, June 2, 1975

Solar radiation in the S-band portion of the electromagnetic spectrum offers a convenient source for comparing measurements by NSSL's radar with an independent measurement made by the Alconquin Radio Observatory in Ottawa, Canada. Solar flux measurements with accuracy of 0.1 dB are made at the Observatory and reported on NBS radio station WWV hourly. The comparison will help establish the accuracy to which received power is measured at each radar site.

Received Power Calculation

Predicted values of power received at the radar are computed from sun flux and radar system parameters.

$$P_r(\text{dBm}) = 10 \log [F\, A_{eff} BW_N] - I_{WG} - L_R + 30 \qquad (46)$$

where

$P_r(\text{dBm})$ = predicted power incident at receiver input port in dBm units

F = Observatory measured solar flux watts (m^{-2} Hz^{-1})

A_{eff} = effective antenna aperture (m^2) calculated from measured antenna gain G

$A_{eff} = G\lambda^2/4\pi$

λ = radar wavelength (m)

BW_N = receiver noise equivalent bandwidth (Hz)

$= 1.06\ BW_{3dB}$ (where BW_{3dB} is the half power bandwidth)

L_{WG} = one way waveguide loss (dB)

L_R = one way radome loss (dB)

Cimarron Radar (CIM)

$F = 67.02\ (10^{-22})\ W m^{-2} Hz^{-1}$ [Datum from Observatory. Measurement made June 2, 1975, 1200 CST.]

$A_{eff} = 38.1\ m^2$

$L_{WG} = 1.8$ dB

$L_R = 1.0$ dB

$BW_N = 3.39\ (10^6)$ Hz

$P_r = 10 \log[6.702(10^{-21})\ 2.91(10^{-1})\ 3.39(10^6)] - 2.8 + 30 = -93.4$ dBm

Measured received power, P_{rm}, is derived from the data tape digital integrator record and the radar calibration curve.

$$P_{rm} = P_S - L_c + A_{LOG} + B_t \tag{47}$$

where

P_{rm} = observed power at receiver input port with antenna pointing at sun

P_S = observed sun power derived from receiver calibration

L_c = cable loss of the signal generator used in calibration

A_{LOG} = correction required due to log receiver signal averaging, i.e., signal generator and sun signals having different amplitude statistics

B_t = digital integrator truncation bias of .6 dB

$P_{rm} = [-90.0 - 6.7 + 2.5 + .6]$ dBm $= -93.6$ dBm

Differences in measured and calculated received powers ($P_r - P_{rm} = -.2$ dB) reflect uncertainties in measured radar parameters. This value indicates an error of -0.2 dB with CIM inferring a solar flux .2 dB less than reported by the Observatory.

Norman Radar (NRO)

Following the same procedure as for the CIM radar, yields calculated power of -94.2 dBm obtained using the NRO parameters:

$A_{eff} = 42.1\ m^2$

$L_{WG} = 1.0$ dB

$BW_N = 2.12\ (10^6)$ Hz

$L_R = 1.0$ dB

$P_r = -94.2$ dBm

$P_{rm} = [-88.7 - 9.5 + 2.5 + .6]$ dBm $= -95.1$ dBm

Difference between calculated and measured powers is -.9 dB and the difference between the two radars is about 0.7 dB with NRO inferring a solar flux less than CIM.

CIM-NRO Dual Sunshot, June 16, 1975

Another set of measurements were taken on June 16 with the following results:

CIM

P_r = -92.6 dBM

P_{rm} = -93.9 dBm

Difference = -1.3 dB

NRO

P_r = -93.6 dBm

P_{rm} = -94.6 dBm

Difference = -.8 dB.

Conclusion

Powers from the common source measured by the two radar differ by less than 1 dB. This difference is attributed to radar parameter (i.e., antenna gain, losses, etc.) measurement errors and is well within practically achievable tolerances.

SECTION 7

Standard Deviation of Estimates

Standard deviations of the estimates of mean velocity, spectrum width and intensity have been previously analyzed and the 1975 data is little different from previous data sets. However, the hardware changes (ADC and AGC at both sites) and tighter quality control provide valid estimates over a wider range of sign levels.

Data suitable for deriving standard deviation of estimates were taken at various times during the season but only that of May 29 has been extensively analyzed. These results, as well as results from some of the 1974 data (Sirmans, 1975) are given in the following scattergrams.

A scattergram of standard deviation of intensity estimate versus estimated spectrum width parameter is shown in Figures 18a and b. The time constant of 64 system periods (T_s) shown in Figure 18b (k=3) was used in routine data acquisition during the 1975 season. Note that the standard deviation of the intensity estimate approaches 3 dB for smaller values of spectrum widths encountered (~1 m s^{-1}).

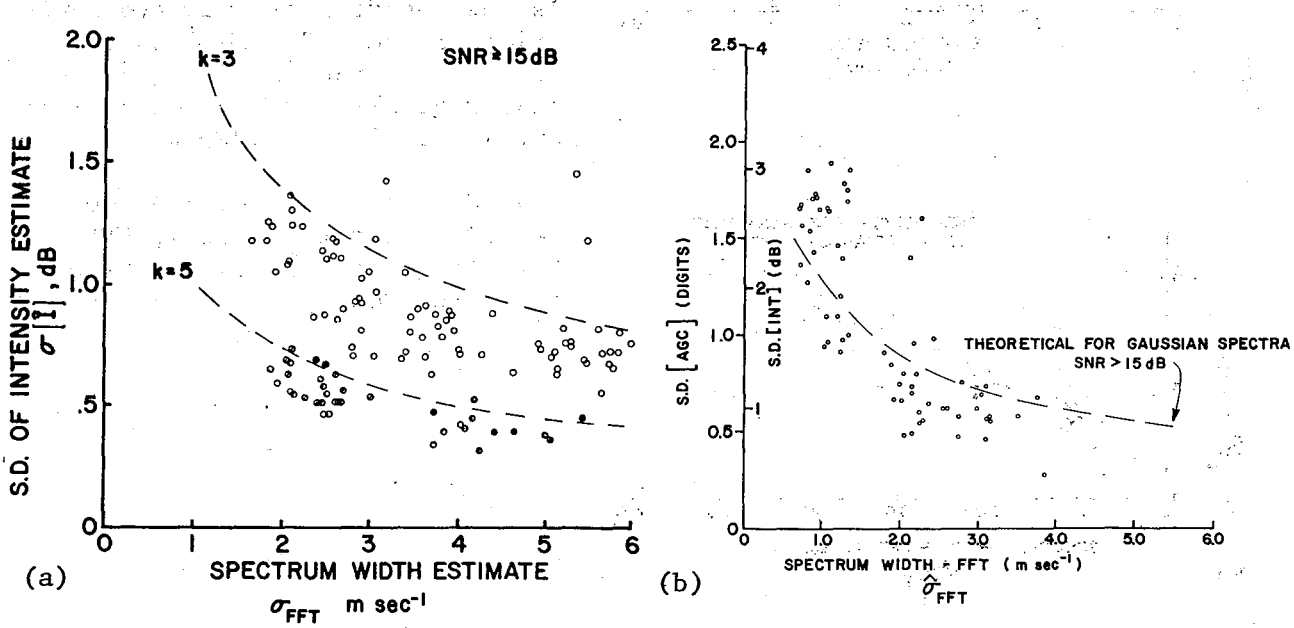

Figure 18. (a) Scattergram of intensity estimate standard deviation versus estimated spectrum width. SNR > 15 dB. Dashed curves are theoretical for Gaussian spectra. k is the time constant parameter in recorded data header, ($T_e = 2^{k+3} T_s$), k = 3 is a time constant of 64 radar periods, k = 5 is a time constant of 256 radar periods. Mean trend has been removed by linear regression. Data taken April 27, 1974 with Norman Doppler. (b) Standard deviation of intensity estimate, k = 3. Mean trend removed. Data taken May 29, 1975.

A scattergram of standard deviation of mean velocity estimate is given in Figures 19a and b, and scattergrams of the standard deviation of width estimates is given in Figures 20a, b, and c.

All of the observed statistics agree reasonably well with theoretical predictions (Sirmans and Bumgarner, 1974, and Sirmans and Doviak, 1973).

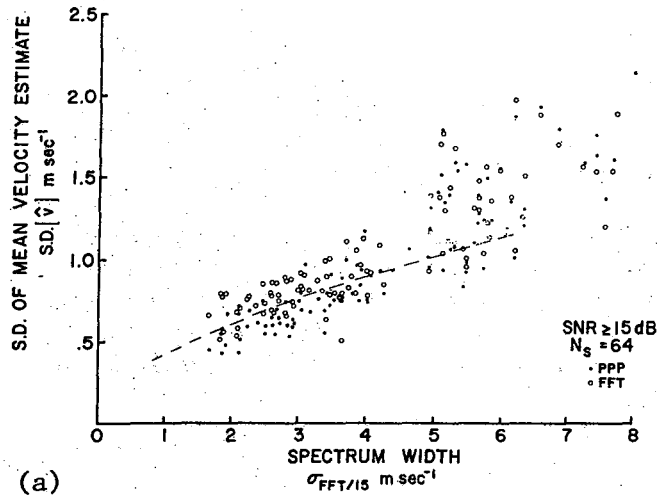

(a)

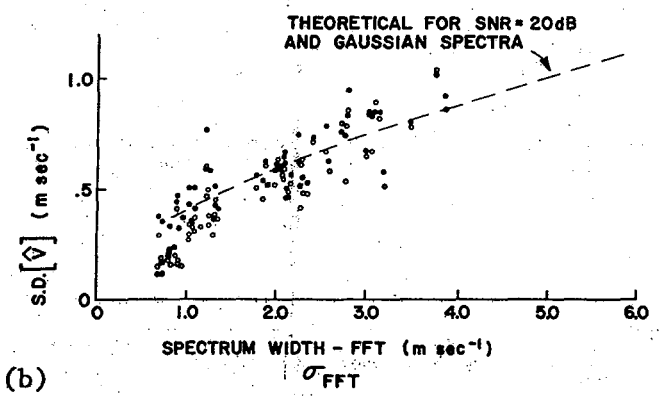

(b)

Figure 19.

(a) Scattergram of FFT and PPP mean velocity estimate standard deviation. Spectrum width estimate by the FFT with a 15 dB (below spectrum mode) threshold (FFT/15). This estimate has been adjusted for the expected bias of Gaussian spectra. Time dependent mean velocity trend was removed by least squares linear regression. Dashed curve is the theoretical standard deviation of the FFT with Gaussian spectra and SNR of 20 dB (Berger and Groginsky, 1973). Data taken April 27, 1974 with Norman Doppler.

(b) Standard deviation of mean velocity, estimate FFT=●, PPP=o. Data taken May 29, 1975. Mean trend removed by linear regression.

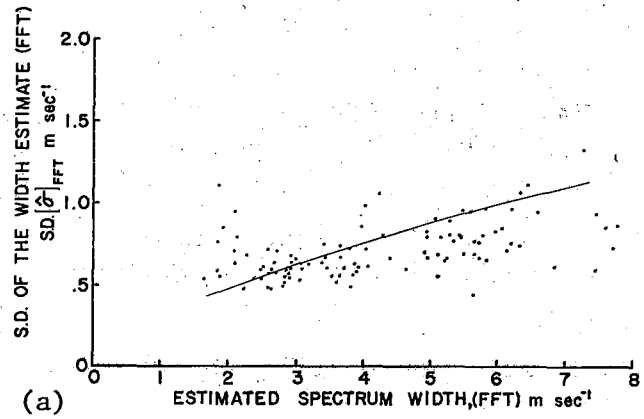

Figure 20.

(a) Scattergram of FFT width estimate standard deviation versus FFT width estimate. No adjustments for estimate bias have been made. Data set has 15 dB < SNR < 30 dB. Estimates made with 64 time samples. Trend removed by linear regression. Data taken April 27, 1974, with Norman Doppler. Solid curve is theoretical for Gaussian spectra and SNR = 15 dB (Berger and Groginsky, 1973).

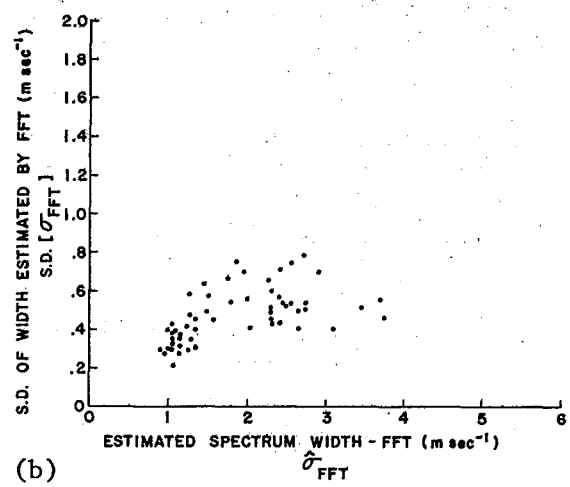

(b) Standard deviation of spectrum width estimate by FFT. Data taken May 29, 1975. SNR > 15 dB; N_S = 64. No adjustment for estimate bias. Mean trend was not removed.

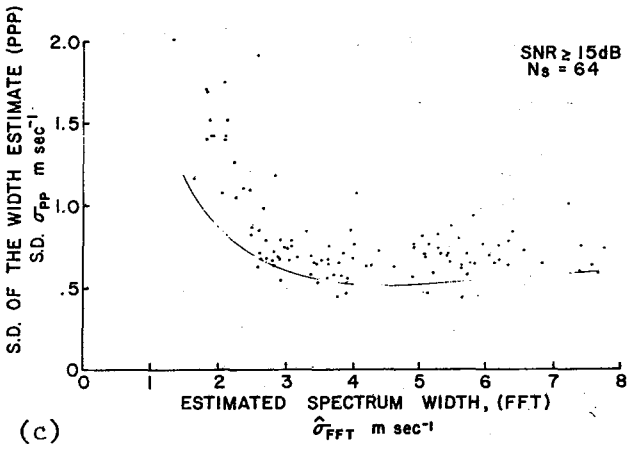

(c) Scattergram of PPP width estimate standard deviation versus width estimate by FFT/15. No adjustments for estimate bias have been made. Data set has 15 dB < SNR < 30 dB. Estimate made with 64 time samples. Data taken April 27, 1974, with Norman Doppler. Solid curve is theoretical for Gaussian spectra and SNR = 15 dB (Berger and Groginsky, 1973).

REFERENCES

Bendat, J. S., and A. G. Piersol, 1971: Random Data - Measurement and Analysis Procedures. Wiley-Interscience, New York, N. Y., 177 and 309.

Berger, T., and H. L. Groginsky, 1973: Estimation of the spectral moments of pulse train. Presented at International Conf. on Information Theory, Tel Aviv, Israel.

Brandes, E. A., 1975: Optimizing rainfall estimates with the aid of radar. J. Appl. Meteor., 14, 1339-1345.

Brigham, E. O., 1974: The Fast Fourier Transform. Prentice-Hill, Englewood Cliffs, N. J., 252.

Burlington, R. S., and D. C. May, 1958: Handbook of Probability and Statistics, with Tables. Handbook Publishers, INc., Sandusky, Ohio. 68-69.

Lee, Y. W., 1964: Statistical Theory of Communication. John Wiley and Sons, Inc., New York, N. Y., 509.

Nathanson, F. E., 1969: Radar Design Principles. McGraw-Hill Book Co., New York, N. Y.

Ruston, H., and J. Bordogna, 1966: Electric Networks: Function, Filters, Analysis. McGraw-Hill Book Co., New York, N. Y., 500-519

Sirmans, D., 1971: Quantization 'Noise'. NSSL in-house memo.

Sirmans, D., 1974a: Digital Integrator Calibration. NSSL in-house memo.

Sirmans, D., 1974b: Logarithmic Receiver Noise Power Determination. NSSL in-house memo.

Sirmans, D., 1974c: Data Acquisition Workshop Handout. NSSL in-house memo.

Sirmans, D., 1975: Doppler Radar Development. NSSL in-house memo.

Sirmans, D., and P. Barclay, 1973: Assignment of reflectivity levels to the RC 33 radar digital output. Working Paper 159, Australian Bureau of Meteorology.

Sirmans, D., and R. Doviak, 1973: Meteorological radar signal intensity estimation. NOAA Tech. Memo. ERL NSSL-64.

Sirmans, D., and W. Bumgarner, 1974: Numerical comparison of five mean frequency estimators. J. Appl. Meteor., 14, 6.

Skolnik, M. I., 1962: Introduction to Radar Systems. McGraw-Hill, New York, N. Y.

Wilson, J. H., 1970: Integration of radar and gage data for improved rainfall measurement, J. Appl. Meteor., 9, 489-497.

NATIONAL SEVERE STORMS LABORATORY

The NSSL Technical Memoranda, beginning with No. 28, continue the sequence established by the U. S. Weather Bureau National Severe Storms Project, Kansas City, Missouri. Numbers 1-22 were designated NSSP Reports. Numbers 23-27 were NSSL Reports, and 24-27 appeared as subseries of Weather Bureau Technical Notes. These reports are available from the National Technical Information Service, Operations Division, Springfield, Virginia 22151, for $3.00, and a microfiche version for $0.95. NTIS numbers are given below in parentheses.

No. 1 National Severe Storms Project Objectives and Basic Design. Staff, NSSP. March 1961. (PB-168207)

No. 2 The Development of Aircraft Investigations of Squall Lines from 1956-1960. B. B. Goddard. (PB-168208)

No. 3 Instability Lines and Their Environments as Shown by Aircraft Soundings and Quasi-Horizontal Traverses. D. T. Williams. February 1962. (PB-168209)

No. 4 On the Mechanics of the Tornado. J. R. Fulks. February 1962. (PB-168210)

No. 5 A Summary of Field Operations and Data Collection by the National Severe Storms Project in Spring 1961. J. T. Lee. March 1962. (PB-165095)

No. 6 Index to the NSSP Surface Network. T. Fujita. April 1962. (PB-168212)

No. 7 The Vertical Structure of Three Dry Lines as Revealed by Aircraft Traverses. E. L. McGuire. April 1962. (PB-168213)

No. 8 Radar Observations of a Tornado Thunderstorm in Vertical Section. Ralph J. Donaldson, Jr. April 1962. (PB-174859)

No. 9 Dynamics of Severe Convective Storms. Chester W. Newton. July 1962. (PB-163319)

No. 10 Some Measured Characteristics of Severe Storms Turbulence. Roy Steiner and Richard H. Rhyne. July 1962. (N62-16401)

No. 11 A Study of the Kinematic Properties of Certain Small-Scale Systems. D. T. Williams. October 1962. (PB-168216)

No. 12 Analysis of the Severe Weather Factor in Automatic Control of Air Route Traffic. W. Boynton Beckwith. December 1962. (PB-168217)

No. 13 500-Kc./Sec. Sferics Studies in Severe Storms. Douglas A. Kohl and John E. Miller. April 1963. (PB-168218)

No. 14 Field Operations of the National Severe Storms Project in Spring 1962. L. D. Sanders. May 1963. (PB-168219)

No. 15 Penetrations of Thunderstorms by an Aircraft Flying at Supersonic Speeds. G. P. Roys. Radar Photographs and Gust Loads in Three Storms of 1961 Rough Rider. Paul W. J. Schumacher. May 1963. (PB-168220)

No. 16 Analysis of Selected Aircraft Data from NSSP Operations, 1962. T. Fujita. May 1963. (PB-168221)

No. 17 Analysis of Methods for Small-Scale Surface Network Data. D. T. Williams. August 1963. (PB-168222)

No. 18 The Thunderstorm Wake of May 4, 1961. D. T. Williams. August 1963. (PB-168223)

No. 19 Measurements by Aircraft of Condensed Water in Great Plains Thunderstorms. George P. Roys and Edwin Kessler. July 1966. (PB-173048)

No. 20 Field Operations of the National Severe Storms Project in Spring 1963. J. T. Lee, L. D. Sanders, and D. T. Williams. January 1964. (PB-168224)

No. 21 On the Motion and Predictability of Convective Systems as Related to the Upper Winds in a Case of Small Turning of Wind with Height. James C. Fankhauser. January 1964. (PB-168225)

No. 22 Movement and Development Patterns of Convective Storms and Forecasting the Probability of Storm Passage at a Given Location. Chester W. Newton and James C. Fankhauser. January 1964. (PB-168226)

No. 23 Purposes and Programs of the National Severe Storms Laboratory, Norman, Oklahoma. Edwin Kessler. December 1964. (PB-166675)

No. 24 Papers on Weather Radar, Atmospheric Turbulence, Sferics, and Data Processing. August 1965. (AD-621586)

No. 25 A Comparison of Kinematically Computed Precipitation with Observed Convective Rainfall. James C. Fankhauser. September 1965. (PB-168445)

No. 26 Probing Air Motion by Doppler Analysis of Radar Clear Air Returns. Roger M. Lhermitte. May 1966. (PB-170636)

No. 27 Statistical Properties of Radar Echo Patterns and the Radar Echo Process. Larry Armijo. May 1966. The Role of the Kutta-Joukowski Force in Cloud Systems with Circulation. J. L. Goldman. May 1966. (PB-170756)

No. 28 Movement and Predictability of Radar Echoes. James Warren Wilson. November 1966. (PB-173972)

No. 29 Notes on Thunderstorm Motions, Heights, and Circulations. T. W. Harrold, W. T. Roach, and Kenneth E. Wilk. November 1966. (AD-644899)

No. 30 Turbulence in Clear Air Near Thunderstorms. Anne Burns, Terence W. Harrold, Jack Burnham, and Clifford S. Spavins. December 1966. (PB-173992)

No. 31 Study of a Left-Moving Thunderstorm of 23 April 1964. George R. Hammond. April 1967. (PB-174681)

No. 32 Thunderstorm Circulations and Turbulence from Aircraft and Radar Data. James C. Fankhauser and J. T. Lee. April 1967. (PB-174860)

No. 33 On the Continuity of Water Substance. Edwin Kessler. April 1967. (PB-175840)

No. 34 Note on the Probing Balloon Motion by Doppler Radar. Roger M. Lhermitte. July 1967. (PB-175930)

No. 35 A Theory for the Determination of Wind and Precipitation Velocities with Doppler Radars. Larry Armijo. August 1967. (PB-176376)

No. 36 A Preliminary Evaluation of the F-100 Rough Rider Turbulence Measurement System. U. O. Lappe. October 1967. (PB-177037)

No. 37 Preliminary Quantitative Analysis of Airborne Weather Radar. Lester P. Merritt. December 1967. (PB-177188)

No. 38 On the Source of Thunderstorm Rotation. Stanley L. Barnes. March 1968. (PB-178990)

No. 39 Thunderstorm - Environment Interactions Revealed by Chaff Trajectories in the Mid-Troposphere. James C. Fankhauser. June 1968. (PB-179659)

No. 40 Objective Detection and Correction of Errors in Radiosonde Data. Rex L. Inman. June 1968. (PB-180284)

No. 41 Structure and Movement of the Severe Thunderstorms of 3 April 1964 as Revealed from Radar and Surface Mesonetwork Data Analysis. Jess Charba and Yoshikazu Sasaki. October 1968. (PB-183310)

No. 42 A Rainfall Rate Sensor. Brian E. Morgan. November 1968. (PB-183979)

No. 43 Detection and Presentation of Severe Thunderstorms by Airborne and Ground-Based Radars: A Comparative Study. Kenneth E. Wilk, John K. Carter, and J. T. Dooley. February 1969. (PB-183572)

No. 44 A Study of a Severe Local Storm of 16 April 1967. George Thomas Haglund. May 1969. (PB-184970)

No. 45 On the Relationship Between Horizontal Moisture Convergence and Convective Cloud Formation. Horace R. Hudson. March 1970. (PB-191720)

No. 46 Severe Thunderstorm Radar Echo Motion and Related Weather Events Hazardous to Aviation Operations. Peter A. Barclay and Kenneth E. Wilk. June 1970. (PB-192498)

No. 47 Evaluation of Roughness Lengths at the NSSL-WKY Meteorological Tower. Leslie D. Sanders and Allen H, Weber. August 1970. (PB-194587)

No. 48 Behavior of Winds in the Lowest 1500 ft in Central Oklahoma: June 1966 - May 1967. Kenneth C. Crawford and Horace R. Hudson. August 1970.

No. 49 Tornado Incidence Maps. Arnold Court. August 1970. (COM-71-00019)

No. 50 The Meteorologically Instrumented WKY-TV Tower Facility. John K. Carter. September 1970. (COM-71-00108)

No. 51 Papers on Operational Objective Analysis Schemes at the National Severe Storms Forecast Center. Rex L. Inman. November 1970. (COM-71-00136)

No. 52 The Exploration of Certain Features of Tornado Dynamics Using a Laboratory Model. Neil B. Ward. November 1970. (COM-71-00139)

No. 53 Rawinsonde Observation and Processing Techniques at the National Severe Storms Laboratory. Stanley L. Barnes, James H. Henderson, and Robert J. Ketchum. April 1971. (COM-71-00707)

No. 54 Model of Precipitation and Vertical Air Currents. Edwin Kessler and William C. Bumgarner. June 1971. (COM-71-00911)

No. 55 The NSSL Surface Network and Observations of Hazardous Wind Gusts. Operations Staff. June 1971. (COM-71-00910)

No. 56 Pilot Chaff Project at the National Severe Storms Laboratory. Edward A. Jessup. November 1971. (COM-72-10106)

No. 57 Numerical Simulation of Convective Vortices. Robert P. Davies-Jones and Glenn T. Vickers. November 1971. (COM-72-10269)

No. 58 The Thermal Structure of the Lowest Half Kilometer in Central Oklahoma: December 9, 1966 - May 31, 1967. R. Craig Goff and Horace R. Hudson. July 1972. (COM-72-11281)

No. 59 Cloud-to-Ground Lightning Versus Radar Reflectivity in Oklahoma Thunderstorms. Gilbert D. Kinzer. September 1972. (COM-73-10050)

No. 60 Simulated Real Time Displays of Velocity Fields by Doppler Radar. L. D. Hennington and G. B. Walker. November 1972. (COM-73-10515)

No. 61 Gravity Current Model Applied to Analysis of Squall-Line Gust Front. Jess Charba. November 1972. (COM-73-10410)

No. 62 Mesoscale Objective Map Analysis Using Weighted Time-Series Observations. Stanley L. Barnes. March 1973. (COM-73-10781)

No. 63 Observations of Severe Storms on 26 and 28 April 1971. Charles L. Vlcek. April 1973. (COM-73-11200)

No. 64 Meteorological Radar Signal Intensity Estimation. Dale Sirmans and R. J. Doviak. September 1973. (COM-73-11923/2AS)

No. 65 Radiosonde Altitude Measurement Using Double Radiotheodolite Techniques. Stephan P. Nelson. September 1973. (COM-73-11934/9AS)

No. 66 The Motion and Morphology of the Dryline. Joseph T. Schaefer. September 1973. (COM-74-10043)

No. 67 Radar Rainfall Pattern Optimizing Technique. Edward A. Brandes. March 1974.

No. 68 The NSSL/WKY-TV Tower Data Collection Program: April - July 1972. R. Craig Goff and W. David Zittel. May 1974.

No. 69 Papers on Oklahoma Thunderstorms, April 29-30, 1970. Stanley L. Barnes, Editor. May 1974.

No. 70 Life Cycle of Florida Key's Waterspouts. Joseph H. Golden. June 1974.

No. 71 Interaction of Two Convective Scales Within a Severe Thunderstorm: A Case Study and Thunderstorm Wake Vortex Structure and Aerodynamic Origin. Leslie R. Lemon. June 1974.

No. 72 Updraft Properties Deduced from Rawinsoundings, Robert P. Davies-Jones and James H. Henderson. October 1974.

No. 73 Severe Rainstorm at Enid, Oklahoma - October 10, 1973. L. P. Merritt, K. E. Wilk, and M. L. Weible. November 1974.

No. 74 Mesonetwork Array: Its Effect on Thunderstorm Flow Resolution. Stanley L. Barnes. October 1974.

No. 75 Thunderstorm-Outflow Kinematics and Dynamics, R. Craig Goff. December 1975.

No. 76 An Analysis of Weather Spectra Variance in a Tornadic Storm. Philippe Waldteufel. May 1976.

No. 77 Normalized Indices of Destruction and Deaths by Tornadoes. Edwin Kessler and J. T. Lee. June 1976.

No. 78 Objectives and Accomplishments of the NSSL 1975 Spring Program. K. Wilk, K. Gray, C. Clark, D. Sirmans, J. Dooley, J. Carter, and W. Bumgarner. July 1976.

☆U.S. GOVERNMENT PRINTING OFFICE:1976—777-045 / 1205 REGION NO.8